Politecnico di Torino

Aerospace Engineering
A.a. 2021/2022
Graduation Session April 2022

Satellite communication channel model for rotary-wing vehicles in a mission analysis context

Relators:
Sabrina Corpino
Giuseppe Tomasicchio

Candidate:
Arsenio Maria Di Donna

Table of contents

List of figures

List of Tables

Abbreviations and Acronyms

SATCOM	Satellite communication
GEO	Geostationary Earth Orbit
LEO	Low Earth Orbit
STK	System Tool Kit
LOS	Line Of Sight
RUAS	Rotary Unmanned Air System
OPH	Optionally Piloted Helicopter
RF	Radio Frequency
AWGN	Additive White Gaussian Noise
BW	Signal beamwidth
QPSK	Quadrature Phase Shift Keying
PSK	Phase Shift Keying
BPSK	Binary phase-shift keying
ISI	Intersymbol interference
EIRP	Effective irradiated power
ITU	International Telecomunication Union
FOV	Field Of View
IN	Iridium-Next
RHC	Right Hand Circular
PSD	Power Spectrum Density
LNA	Low Noise Amplifier
BER	Bit Error Rate
LM	Link Margin
AER	Azimuth Elevation Range

Symbols and variables

D_{iam}	Antena diameter
E_b/N_0	Energy per bit
L_b	Blade width
L_r	Loss between receiver and receiving antenna
L_{tls}	Total space losses
N_b	Number of rotor blades
T_a	Antenna temperature
T_d	Blockage duration
T_p	Blockage period
T_r	Receiver noise temperature
T_s	System noise temperature
T_0	Reference temperature
V_r	Rotor angular speed
k_B	Boltzmann's constant
C/N_0	Carrier-to-noise density
D	Geometrical distance between the main rotor shaft centerline and the point of intersection between the signal and the rotor disc, projected along the direction of the helicopter noise
F	The figure of merit of the amplifier
G	Antenna gain
La	Antenna Aperture
R	Data rate
ST	Sample Time
d	Distance between the main rotor shaft centerline and the antenna
f	Signal frequency
g/T	Gain over the equivalent noise temperature

$\boldsymbol{h}$	The vertical distance between the antenna and the rotor disc
$\boldsymbol{\alpha}$	Elevation angle
$\boldsymbol{\beta}$	Azimuth angle
$\boldsymbol{\gamma}$	Blockage Ratio
$\boldsymbol{\theta}$	Signal Beamwidth
$\boldsymbol{\lambda}$	Signal wavelength

Abstract

Satellite communications are becoming increasingly important for rotary-wing vehicles applications, due to their efficiency and versatility. This work comes from the idea of allocating an antenna for satellite communication purposes on a remotely piloted helicopter and has the aim to recreate a SATCOM channel and bring it into a mission analysis context. This consideration starts with the examination of the disturbances that the rotating blades cause on satellite communication when passing above the vehicle's antenna. After succeeding in the reproduction of the results found in the literature, the disturbance phenomenon is made dependent on the frequency used for the communication. At this point, we analyzed the first mission scenario in which the helicopter communicates with a GEO satellite through Ka-band signals. This part of the work is focused on signal analysis in particular studying the power spectrum variations due to different orientations of the signal and to the rotation of the blades. Subsequently, there is an attempt to integrate the signal analysis in a mission scenario context, reproducing the L-band communications between the helicopter and the LEO Satellite constellation of Iridium Next. The global mission scenario is created in the STK environment exploiting the integration with Matlab. The goal is to obtain the highest level of automatization possible to make the scenario easily adaptable for other mission studies. Besides studying the quality of the signals through a link budget analysis, it is possible to verify the access time with every satellite according to the trajectory plan of the mission. Even if the simulation results show that constant access to the constellation is available with a good quality of the signals, for future works and iterations, it could be interesting to study how to improve communications and reduce handovers with satellites through the optimization of the flight plan of the vehicle.

1. Introduction

The purpose of this effort is to model a Satellite communication channel for rotary wings vehicles applications. Specifically, the attention is focused on the signal losses due to the rotation of the blades. This phenomenon is known as “Rotor blade signal blockage”. Conventional helicopter-satellite communications exploit landline relay stations to avoid blockage but this approach can make communications unstable because of the influence of obstacles. Nowadays, direct communications between helicopters and satellites may benefit from received signal reconstructing techniques. However, this work aims to simulate the rotor blade phenomenon through an algorithm and to introduce this disturb into a mission scenario context. At the end of this study, it is expected to be able to model different kinds of helicopter mission scenarios, in which it would be possible to know, preliminarily, the quality of the exploitable links (set the characteristics of the tools involved in the communications) and to have a visualization of the impact that the rotor blade blockage would have on satellite communications.

The first step of this process consists of a state of art study and characterization of the phenomenon followed by an attempt to replicate results found in the literature to confirm the correct modeling of the disturbance. Subsequently, changes are carried out accordingly to the model of the phenomenon found in the literature. These changes have the aim to make the rotor blade blockage dependent on the communication frequency band used during a mission introducing the signal beamwidth into the equations.

The next step is to create an algorithm for the implementation of the disturbance on a generic signal. Established that the algorithm works, it is used to disturb a Ka-band communication signal between a specific helicopter and a GEO satellite, recreated in a Simulink environment. This software it is chosen because makes it possible to change variable values while the simulation is running. That is exploited to verify if the created disturbance algorithm still works simulating a moving helicopter with respect to the satellite position.

At this point, the aim shifts to integrate the signal analysis into a mission analysis context through the aid of the System Tool Kit (STK) software. The purpose is to parameterize as much as possible the entire mission context. So, the most favorable way is to proceed with the automatization of STK through the use of Matlab scripts and plugins. This makes it easier the customization of the mission scenario, and the implementation of satellite constellations, therefore, making it possible to introduce customized disturbance sources. Now the helicopter is allocated into a mission scenario in which it has its own trajectory to follow while an entire satellite constellation is orbiting around the Earth. In this context, it is interesting to make an access analysis followed by a link margin analysis to better understand the feasibility of using an L-band satellite channel for the communications between the chosen vehicle and the satellites.

2. SATCOM channel model for rotary-wing vehicles

As known, helicopters can be exploited for several applications, including transportation of people and equipment in remote and isolated areas, find and rescue missions, relief of geographical areas that have been struck by a disaster, and more specific military applications. In many of these mission scenarios, terrestrial communication networks are often not available due to local topography (i.e the presence of mountains, valleys…) and the line of sight communications (LOS) can limit the operational flight range of the helicopter. For this reason, satellite communications are of great interest for helicopter applications. Moreover, in case of emergency, helicopter-satellite communication is an excellent alternative because it allows faster deployment than terrestrial communication networks. The recent development of the "Rotary Unmanned Air System" (RUAS) and the "Optionally Piloted Helicopter" (OPH) (which is of interest for this case of study) make it fundamental to improve the helicopter-satellite communication to guarantee the full control of the vehicle's attitude, route, and commands even when it can't be reached by a ground station. For remoted piloted helicopters, in emerging applications, the satellite system can backhaul the LOS traffic to and from the vehicle in what is known as Manned-Unmanned teaming operations. Using satellite communications, it is possible to increase the data rate of the links (very useful when there's the necessity to receive HD live videos from the vehicle that is in a monitoring mission).

2.1 Satellite constellations overview

The SATCOM solutions for helicopter applications can exploit a wide band of frequencies (from L to Ka-band) that allows communication with either LEO constellations and GEO satellites. Both solutions for SATCOM applications have their advantages and disadvantages. Operating in a closer to Earth environment LEO satellites can offer less coverage and their lifetime is shorter due to the exposure to a harsher environment (including radiation and atmospheric drag). But thanks to their closeness to the Earth, LEO satellites have a shorter communication time lag (or latency) than the GEO ones and the up and downlinks are subjected to lower path losses. Moreover, to communicate with an LEO constellation, aircraft need less transmit power and, since LEO networks are traditionally L-band, this enables to send and receive signals even in adverse weather conditions. That happens because lower frequencies suffer less from atmospheric and weather interferences than higher frequencies (such as Ku, Ka, and C). This will be explained in the next paragraph since the rotation of the rotor blades involves interferences for the helicopter signal transmitting and receiving, even the severity of this loss is related to the frequency band exploited for the communications.

In this endeavor, both of the satellite communication options will be analyzed in two different mission scenarios. In the first instance, through Simulink, it is simulated a Ka-band communication channel with a GEO satellite that can be considered static relative to the helicopter that can change its position and the orientation of the exchanged signal. Subsequently, an LEO constellation L-band link is reproduced through STK that making it easier to compute multiple satellite access and to create a more realistic mission scenario environment.

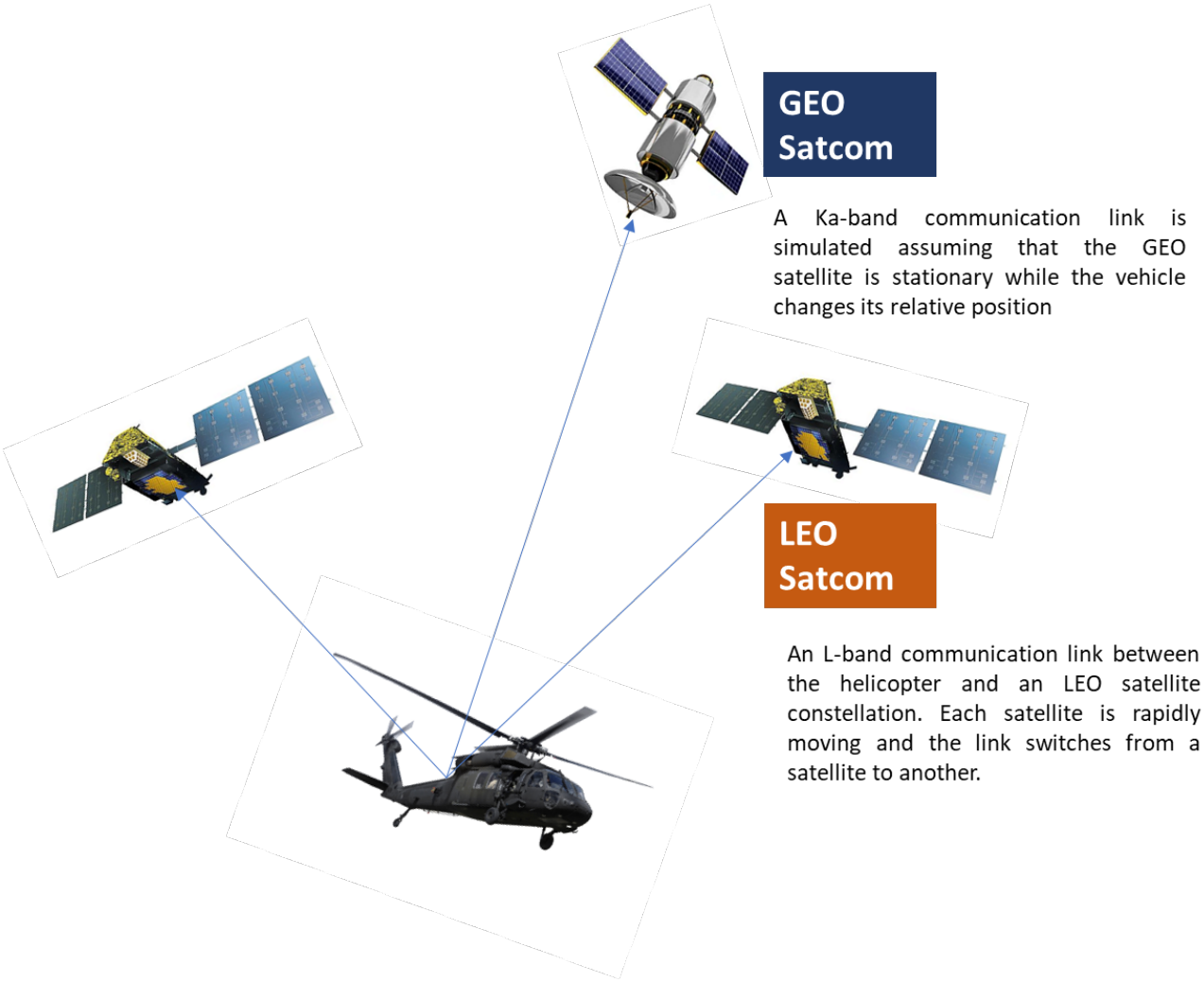

Figure 1: *Analyzed mission scenarios overview*

2.2 Rotor Blade Blockage

As the helicopter antenna sends a signal at a certain frequency, the rotation of the blades causes an attenuation every time a blade passes over the signal beam. The laboratory observations of this phenomenon date back to the development of radar in World War II. In these observations, many harmonics of sufficient amplitude are detected and analyzed in the audio spectrum [1].

It is possible to create a mathematical model in which the harmonic wave equations take into account the presence and the rotation of the blades. An example is given by De Zutter's solution, in which the faded field is evaluated analytically in the Lorenz transform frame and transformed back into the original reference frame [2].

Another method to describe the disturbance was presented by Harfoush and it is based on finite-difference time-domain methods, where elements such as the local surface speed of the object are taken into account. This approach doesn't exploit any domain transformations but

its accuracy is limited to the precision of the field interpolation on the nodes of a rectangular grid [3].

Van Badel's approach, instead, consists of considering that at discrete times, the blades are "frozen in their tracks" and, in this scenario, the electric magnetic field is calculated. The disturbances are evaluated at instants of rotation as if the scatterer were stationary. That method can be considered valid when non-relativistic speeds are reached and the rotation frequency is much smaller than the angular frequency of the electromagnetic wave [3].

Helicopter antennas can't be typically placed to eliminate the shadowing of the signal due to the blades. An exception for an antenna placement is given by the Apache Longbow, in which the hollow main rotor shaft allows the installation of the antenna in its cavity. The antenna placement is fundamental for the characterization of this phenomenon. For this study, the antenna is considered to be placed halfway between the main rotor shaft and the tail rotor shaft [4].

Preliminarily it is possible to imagine that, for a pencil beam radiation pattern, the percentage of the signal blockage will be higher if the signal is directed towards the main shaft rotor. The figure below allows visualizing this assumption.

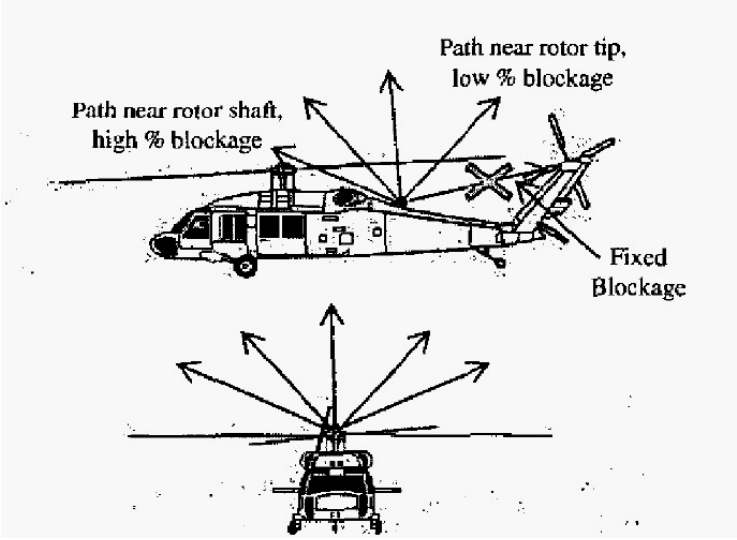

Figure 2: *Depiction of blockage for a pencil beam radiation pattern [4].*

2.2.1 Characterization of the phenomenon

When the helicopter is in hovering or in a flight, its blades will periodically pass over the antenna blocking the signal and resulting in periodical fading of the received or transmitted signal. As shown in the figure below, the fading of the signal can be modeled as a rectangular window:

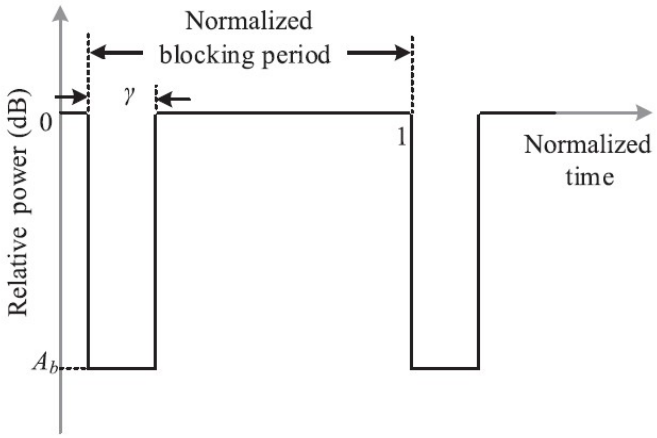

Figure 3:*Power level fading of the helicopter signal [5].*

The severity of the signal attenuation is wavelength λ dependent due to two physical phenomena. First of all, the blade material can completely block the RF energy and, consequently, diffraction is the only mechanism for energy propagation around the blade. Secondly, RF energy can pass through the blade if the blade material allows this phenomenon to happen [4].

The diffraction of a signal around any object depends on the ratio of the wavelength λ to the size of the object (the blade width in this case). When this ratio is high it means that the RF frequency readily diffracts around the blade. At short wavelengths, little diffraction occurs and the blockage becomes worse. In the figure below are reported different values of attenuation for different kinds of signals, considering the rotor blades as rectangular knife edges. As expected, it is possible to observe that for lower frequency signals (as L-band) the maximum attenuation is around -10dB. As the frequency increases to Ka-band, blockage becomes worse, generating a maximum loss of around -20dB.

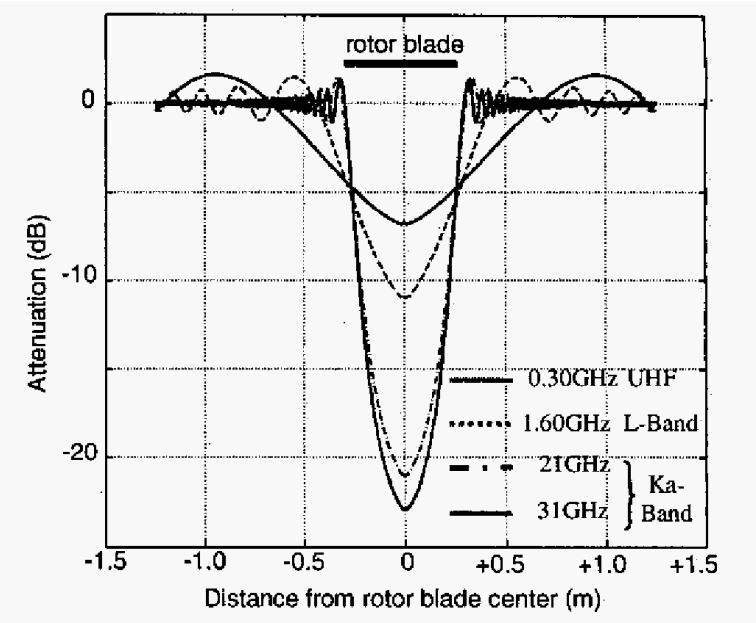

Figure 4: *Estimated rotor blade blockage at four frequencies [4].*

Helicopter rotors can also create a multi-path, Doppler-shifted signal as RF energy reflects and scatters off the rotors. An analysis of this phenomenon was conducted on the UH-60 rotor, which blades have a metallic cap on their tips. This metallic element is an excellent RF reflector and it is possible to compute the Doppler frequency seen by an isotropic antenna if the RF energy is assumed to be reflected isotropically. The combined effect of all blade tips will produce a complex signal which represents the vector sum of all radiating tips. This should not be a problem for the communication link because usually high gain Ka-Band antenna possesses off bore-sight rejection and, consequently, the amount of reflected energy will be small. Moreover, the wavelength of high-frequency signals is smaller than the reflecting surfaces and this gives rise to complex scattering patterns as opposed to simple specular reflection. Finally, if the considered data rate is greater than Doppler frequency, the Doppler effect is negligible [4]. For these reasons in this analysis, the attention is focused only on the RF blockage effect.

Between two instants in which two blades sweep over the antenna, there is a time interval that can be called: the blockage period (T_p).

The blockage period is inversely proportional to the product of the number of the blades that constitute the main shaft, and the rotor angular speed V_r [5]:

$$T_p = \frac{1}{V_r N_b}$$

(2. 1)

For a generic helicopter, assuming that its rotor angular speed remains constant, it's possible to assert that the blockage period is constant.

The other fundamental element for this analysis is the blockage duration period T_d. This value represents the period that the blade needs to pass over the antenna during its rotation. The blockage duration period varies with the contribution of the Elevation angle of the signal beam α, and the Azimuth angle, intended as the orientation of the signal relating to the helicopter nose direction β [5]:

$$T_d = \frac{L_a + L_b \sin(\alpha)}{V_r 2\pi D} \tag{2. 2}$$

$L_a$and L_b represent the antenna aperture and the width of the blade, respectively.

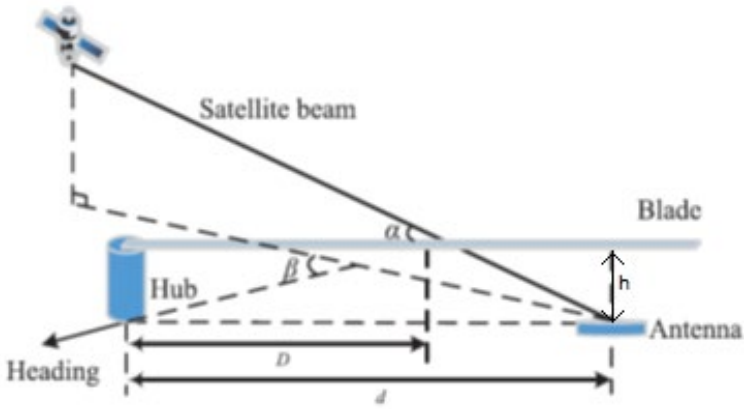

Figure 5: *Geometric representation of the rotor blade blockage [5].*

As shown in the figure above, D represents the geometrical distance between the main rotor shaft centerline and the point of intersection between the signal and the rotor disc, projected along the direction of the helicopter nose. For this reason, calling with an h the vertical distance between the antenna and the rotor disc, and with a d the distance between the main rotor shaft centerline and the antenna, it is possible to determine D as:

$$D = d - \frac{h}{\sin(\alpha)} \cos(\alpha) \cos(\beta) \tag{2. 3}$$

2.2.2 Blockage Ratio

The severity of the phenomenon can be represented by the Blockage Ratio [5]:

$$\gamma = \frac{T_d}{T_p}$$

(2. 4)

According to the previous paragraph, this value depends on the geometric characteristics of the helicopter and the signal beam orientation. The number of the rotor blades itself influences this parameter. Helicopters with smaller blade pieces generally exhibit lower blockage ratios than those with larger blade pieces. In literature, it is possible to find a graphic that shows how the blockage ratio varies depending on the azimuth and elevation angles (for a fixed helicopter model). The picture below shows the blockage ratio trend for a four blades rotor helicopter.

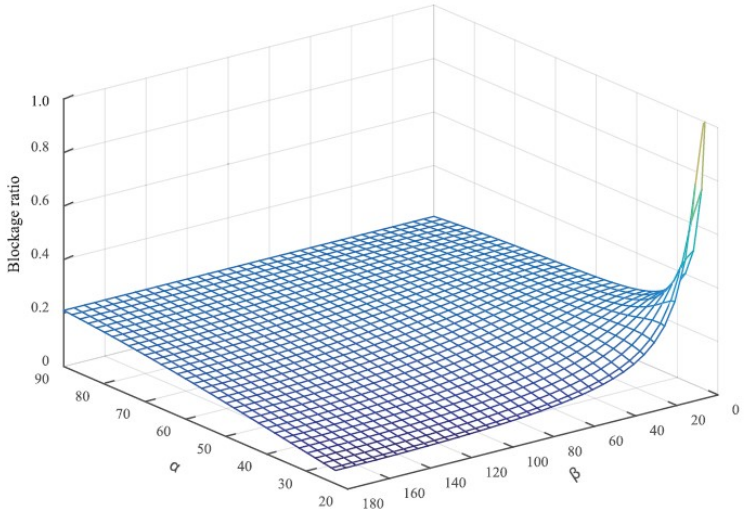

Figure 6: *Blockage ratio trend for a four-blade helicopter [5].*

The blockage ratio varies from 0 to 1 and it is mostly lower than 0.25 in this specific case. As mentioned in the previous paragraph, γ is higher for low azimuth and elevation angles. That's a situation in which the signal beam is directed towards the main shaft and, consequently, the blockage duration is higher.

The received signal r from the helicopter can be calculated as [5]:

$$r = h \cdot s + n$$

(2.5)

Where s is the transmitted signal, h is the blockage fading and n is the AWGN.

This is the starting point for the subsequent analysis, in which there is an attempt to recreate these results and to bind this phenomenon to the communication band chosen.

2.2.3 Simulation of the phenomenon

As the first step for the analysis, it is necessary to choose a helicopter model and, therefore, the geometric parameters for the definition of the blockage period. For this specific case of study, a three-blade main rotor helicopter is chosen. In the table below are reported the main geometrical and performance parameters used for the analysis. The calculations are not specific for a single helicopter model, so changing a parameter will modify the obtained results.

Number of blades ($\boldsymbol{N_b}$)	3
Rotor Speed (V_r)	48 rad/s
Antenna Aperture (L_a)	0.30 m
Height between the antenna and the rotor blade (h)	0.8 m
Distance between the hub and the antenna (d)	2.3 m
Blade width (L_b)	0.32 m

Table 2. 1: *helicopter parameters used for the case of study*

These parameters are necessary to calculate the blockage period and duration. However, to recreate the same result reported in Figure 6, it is necessary to add two more parameters: elevation and azimuth angle. As for the literature case, α varies from 20° to 90° and β varies from 0° to 180°. The azimuth angle variation from 0° to 180° is justified by the fact that for symmetry reasons, it is possible to obtain the same results from angles in a range between 180° and 360°.

At this point, it is possible to create two arrays containing 50 elements each that represent the attitude angle variation. Then, with a "for" cycle, it is possible to evaluate the geometric parameter D (discussed previously) and the blockage duration T_d. The blockage duration is represented by a 50x50 matrix in which every row contains a different elevation angle and every column an azimuth angle. Now it is possible to calculate the blockage period and to obtain the same graph reported in Figure 6.

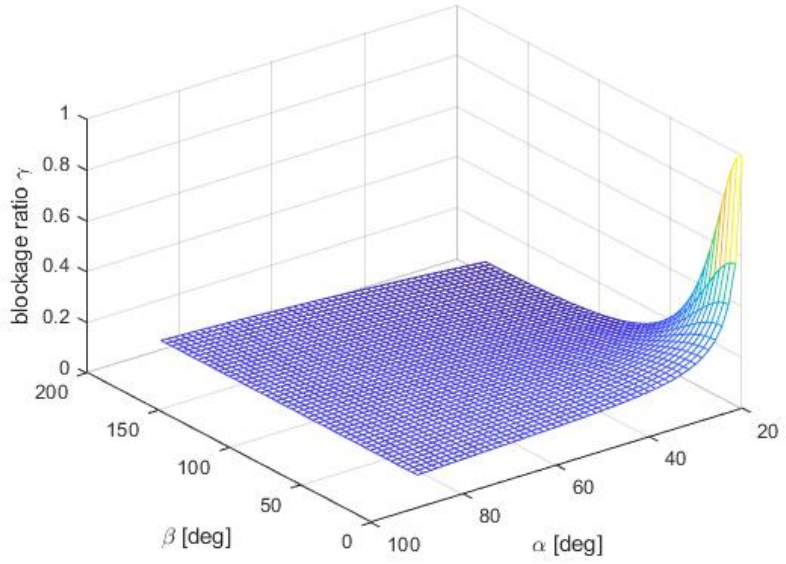

Figure 7: *Blockage ratio obtained in Matlab environment.*

Unlike the literature plot, in this case, the blockage ratio is mostly under 20%. Unfortunately, it wasn't possible to find information about the geometry parameter used for the case described in the literature. That would have allowed making a better comparison with the results obtained in Matlab. Anyway, even if the obtained results aren't the same as the ones in Figure 5, it is possible to observe the same trend in γ variation with the angles. Even in this case, the blockage ratio reaches high values for very small attitude angles. In particular, it reaches 100%, when $\alpha = 20°$ and $\beta = 0°$. With a blockage ratio of 100 %, the signal can be considered always attenuated by the rotation of the blades. Moreover, the blockage ratio doesn't vary with the azimuth angle when the elevation angle reaches 90°.

2.2.4 The first application of the signal blockage algorithm

The results showed before are the demonstration that the blockage duration is correctly calculated. At this point, it is possible to try to implement the RF blockage to an arbitrary sinusoidal signal. For this example, it is taken into account a signal with the following characteristics:

Frequency (f_s)	4000 Hz
Sample frequency (F_s)	10000 Hz
Sample time (t)	$0: 1/F_s : 1 - 1/F_s$
Signal equation (x)	$x = \cos(2\pi f_s t)$

Table 2. 2: *Signal characteristics.*

Thanks to the" Matlab Signal Analyzer" it is immediately able to represent the time-dependent signal trend, the power spectrum, and the Spectrogram.

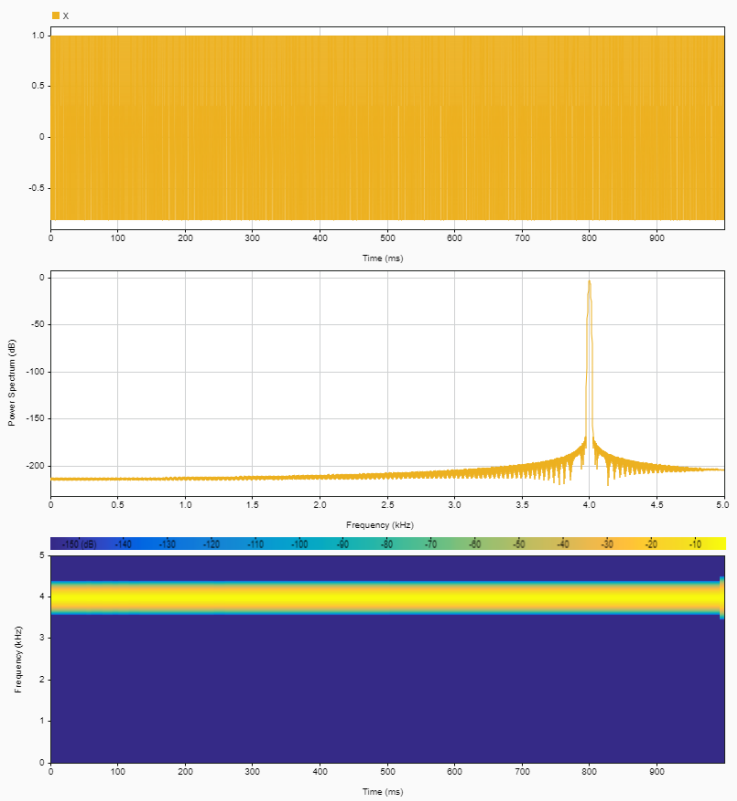

Figure 8: *Continous sinusoidal signal, power spectrum in the frequency domain, and signal spectrogram in the time domain.*

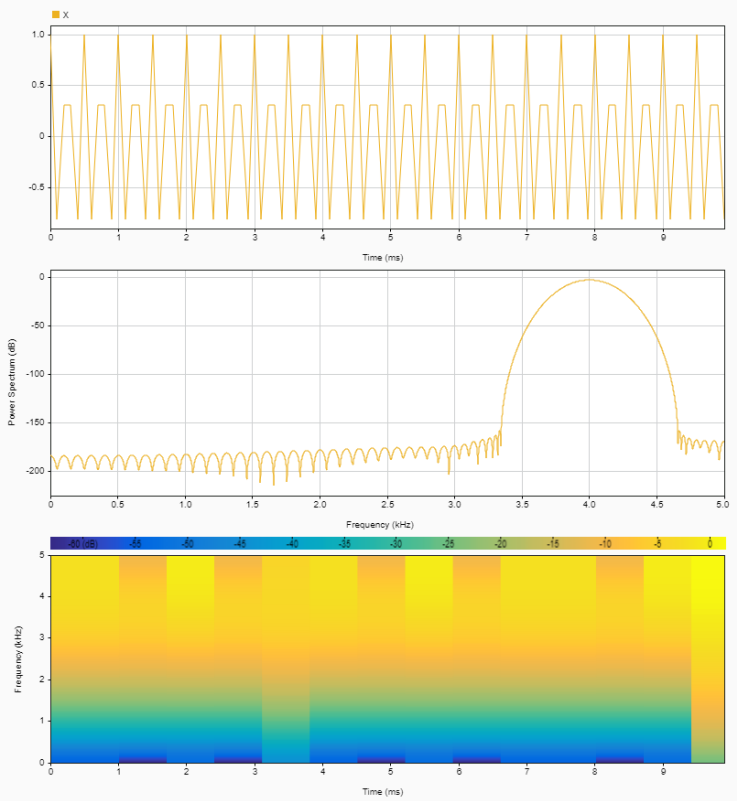

Figure 9: *Continuous sinusoidal signal in a 0.01s time interval.*

As can be observed, the signal has a continuous trend without any kind of interference or attenuation. The signal power has a peak at around 4kHz.

The rotor blade blockage algorithm consists of a "for" cycle in which it is made a check on the time variable. The assumption is that at instant t=0s the rotor blade (which is considered as a rectangular plate) is already over the helicopter antenna attenuating the signal. In this case, the sinusoidal wave equation is multiplied by an attenuation factor. Assuming that the signal will be attenuated of $Loss = 25dB$, the attenuation factor is given by the following formula:

$$l = \frac{1}{10^{\frac{Loss}{20}}} \tag{2.6}$$

The attenuation is produced when the time instant is bigger than the blockage period T_d multiplied by a counter (m) and the sum between the blockage duration T_d and $m \cdot T_p$. Initially, m is set to 0, so the condition for the attenuation is satisfied and the signal power will be reduced for the duration of the blockage phenomenon. From the beginning of attenuation having passed an equal amount of time as the blockage duration, the counter is increased by one. Therefore, until the next blade will pass over the antenna (it means until the blockage period will be passed) the signal isn't attenuated. As for the previous case, it is possible to exploit the Signal Analyzer to verify if the blockage algorithm works. The following image shows the signal attenuated for an azimuth angle of $\beta = 10°$ and an elevation angle of $\alpha = 45°$.

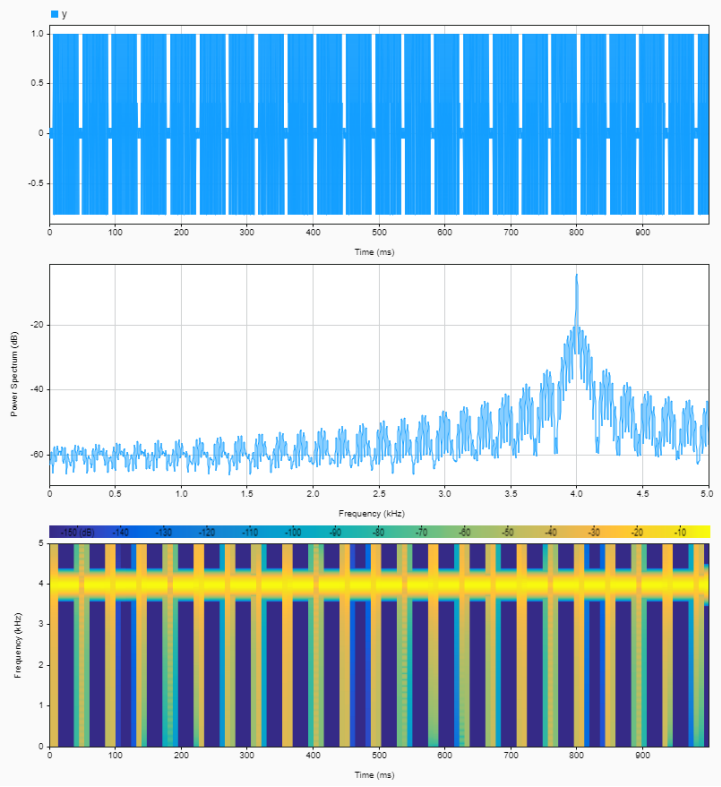

***Figure 10**: Sinusoidal signal periodically attenuated by the rotation of the blades for $\alpha = 45°$ and $\beta = 10°$.*

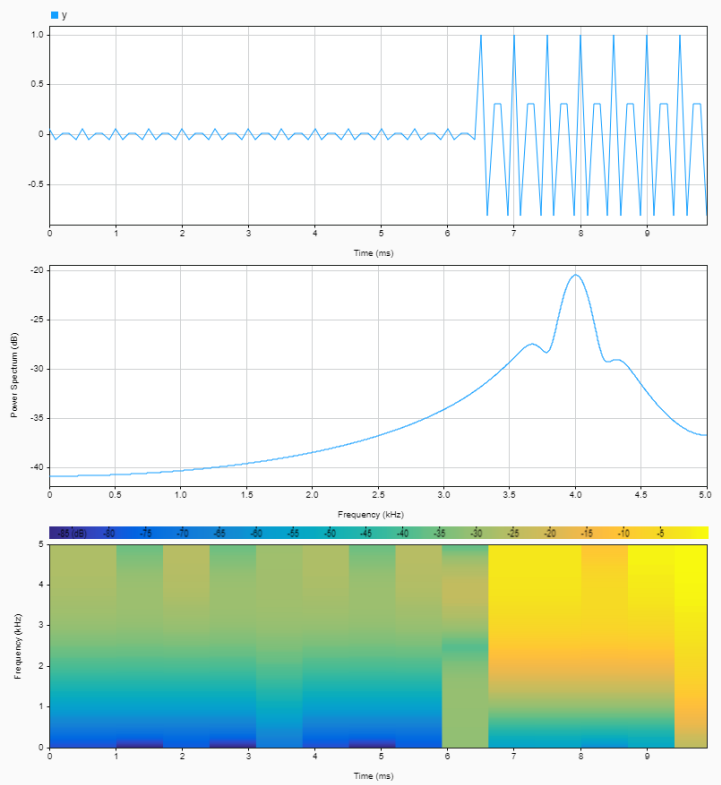

***Figure 11**: Sinusoidal signal periodically attenuated in a 0.01s time interval.*

As it is possible to observe, every time a blade passes over the antenna, the signal is reduced by the chosen attenuation factor. In the spectrogram, it is possible to visualize vertical strips spaced by the blockage period, that represent the power decrease in the received or transmitted signal. In this case, the power peak at 4kHz is lower, demonstrating that the signal suffers from power loss.

2.2.5 Including the signal frequency into the disturbance phenomenon

The treatment of the rotor blade blockage found in the literature just considered the antenna diameter as the distance that the rotor blade has to cross to induce the signal attenuation. However, this doesn't take into account the signal beamwidth, which could be smaller or larger than the antenna diameter at the heigh where takes place the intersection with the rotor blades. For this reason, an attempt to include the beamwidth and, consequently, the signal frequency into the rotor blade blockage algorithm is carried out. The beamwidth of the major lobe of a signal is the point at which the signal power drops below 3dB the peak value (that is equivalent to the loss of 50% of the signal power). There are several formulas to evaluate the beamwidth of a signal, depending on the antenna type. For this case of study, it is assumed that the helicopter is equipped with a parabolic antenna. For this reason, the beamwidth can be calculated as:

$$\theta = \frac{21}{f_{GHz} D_{iam}} \tag{2.7}$$

Where f_{GHz} is the signal frequency expressed in GHz and D_{iam} is the plate diameter in m. It is assumed that the major lobe of the signal is included in a cone with a semi-aperture angle equal to $BW/2$.

2.2.6 Ka-band Signal

As the first attempt of inclusion of the beamwidth in the calculations, it is taken into account a Ka-Band signal with a frequency of $f = 29.96\,GHz$ and emitted from an antenna with a diameter of $D_{iam} = 0.31m$. With these parameters, the resulting beamwidth is $\theta = 2.2611°$. It is possible to visualize the beam as a cone with a semi-aperture angle equal to the beamwidth.

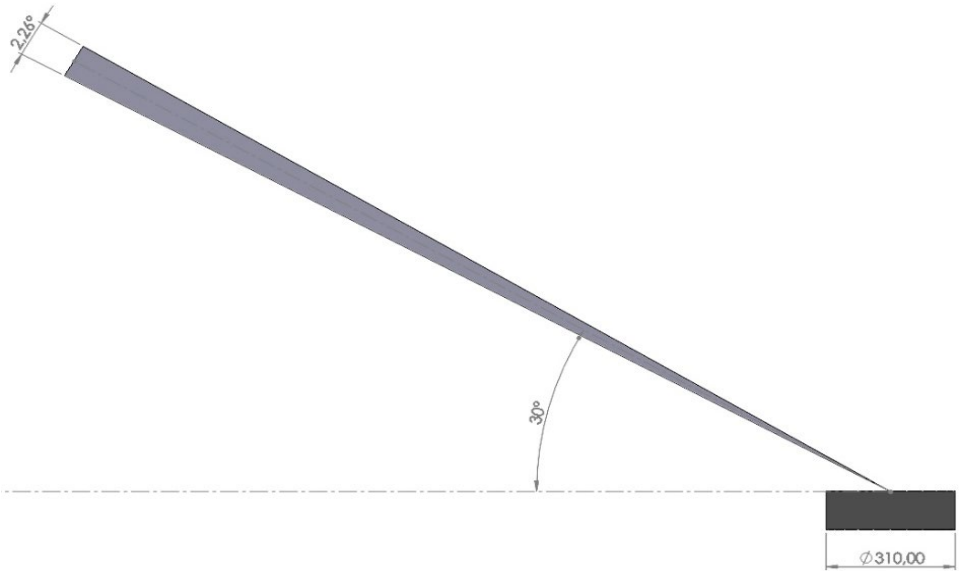

Figure 12: *Visualization of the beamwidth of a 29.96GHz signal, with an $\alpha = 30°$ and $\beta = 0°$.*

The vertical distance between the rotor blade and the antenna is given by $h = 0.8m$. At this height, the rotor blade cuts the signal beam, and an ellipse it's created by this intersection. To replace the antenna diameter into the blockage duration formula, it is necessary to calculate the distance, perpendicular to the helicopter nose direction, covered by the rotor blade. In the specific case under assessment, the azimuth angle is null, so the distance covered by the blade is equal to the minor axis of the ellipse.

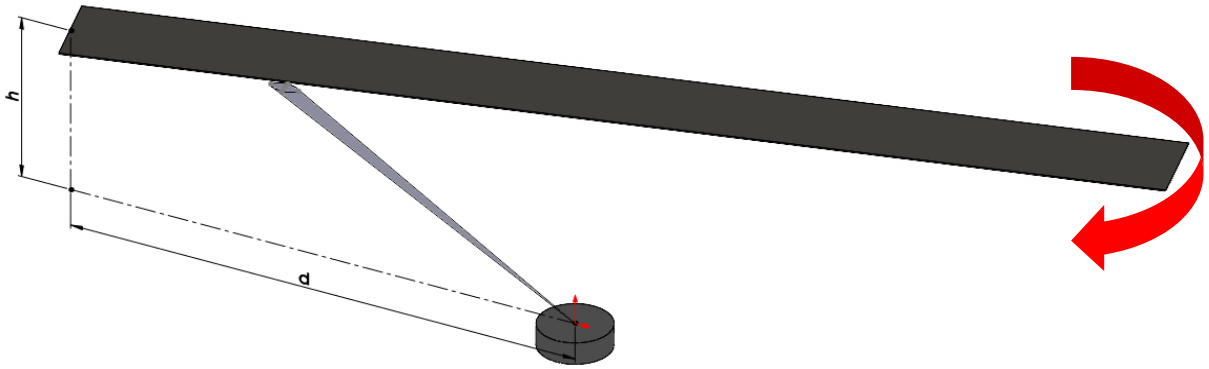

Figure 13: *3D Model of a rotating blade cutting the Ka-band signal beam.*

Figure 14: *View from above of the blade crossing the elliptic section of the beam.*

But it is necessary to obtain a generic formulation for this problem. The figure below shows the geometric elements necessary to obtain the distance covered by the blade.

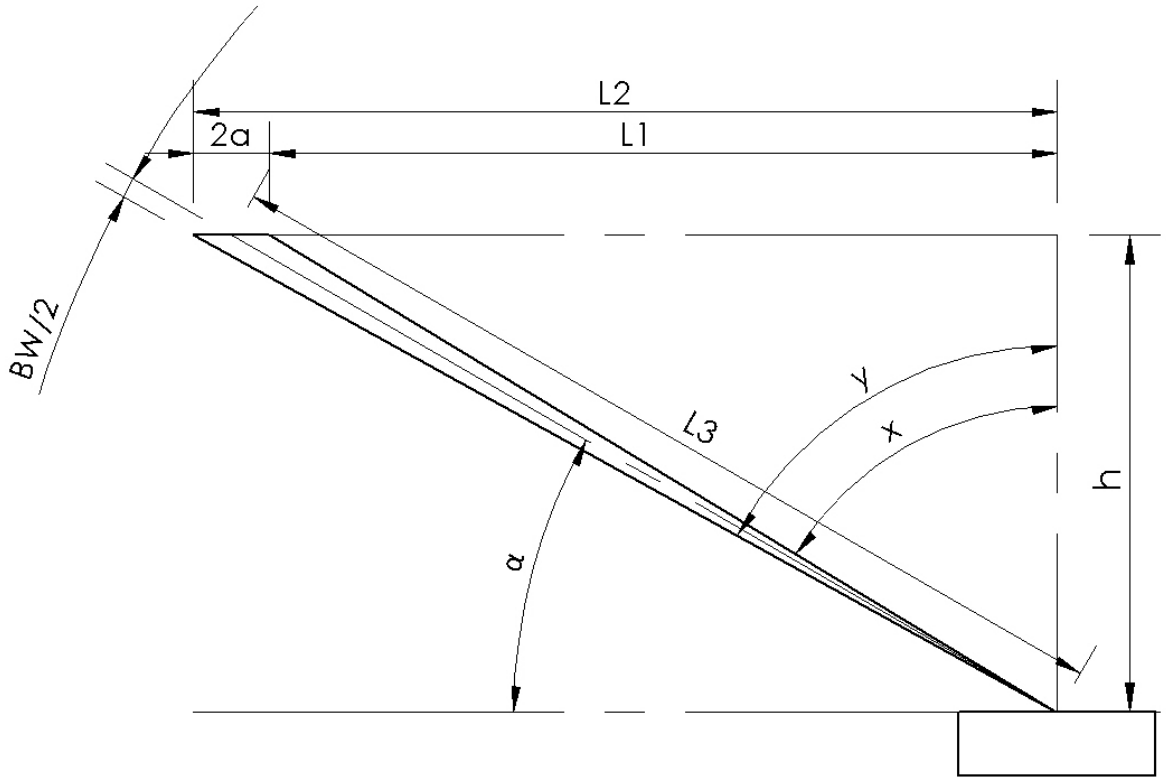

Figure 15: *Drafting of the cut signal beam.*

The only parameters required for the next calculations are the distance between the antenna and the blade h, the elevation angle α, and the beamwidth (BW).

The first step for finding L_a is the calculation of L_1 and L_2:

$$x = 90 - \alpha - \frac{BW}{2}$$

(2.8)

$$y = 90 - \alpha + \frac{BW}{2}$$

(2.9)

$$L_1 = \frac{\sin(x)}{\cos(x)} \cdot h$$

(2.10)

$$L_2 = \frac{\sin(y)}{\cos(y)} \cdot h$$

(2.11)

Now that L_1 and L_2 are available, it is possible to obtain the major axis of the ellipse:

$$a = \frac{L_2 - L_1}{2}$$

(2.12)

Although L_3 may seem the centerline of the cone, it is not. L_3 is the distance between the top of the cone and the intersection between the major and minor axes of the ellipse. So it can be calculated as:

$$L_3 = \sqrt{h^2 + (a + L_1)^2}$$

(2.13)

At this point it is possible to obtain the semiminor axis of the ellipse:

$$b = L_3 \cdot \frac{\sin\left(\frac{BW}{2}\right)}{\cos\left(\frac{BW}{2}\right)}$$

(2.14)

The angle used for the calculation of the semiminor axis is half of the beamwidth, but the real angle that should be used is a little bit smaller. For a Ka-band signal, this difference is fully negligible. For an L-band signal, the beamwidth increases and so does the difference between $BW/2$ and the real angle. But even in the worst case, the difference is less than 1°, so for sake of simplicity, half of the beamwidth can be used in this formulation.

The case taken into account is the simplest one. The beam is directed in the same direction as the helicopter nose, indeed. But, as mentioned before, the signal beam can rotate to keep the link with the satellite. For this reason, the distance that the blade has to cross, to attenuate the signal changes with the helicopter attitude relative to the signal beam direction. To have a better understanding of the described scenario, it can be useful to observe the figures below:

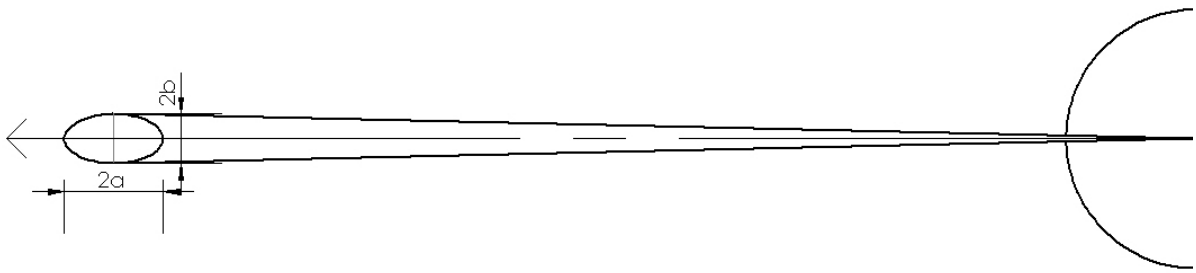

Figure 16: *Ka-band signal beam with $\beta = 0°$.*

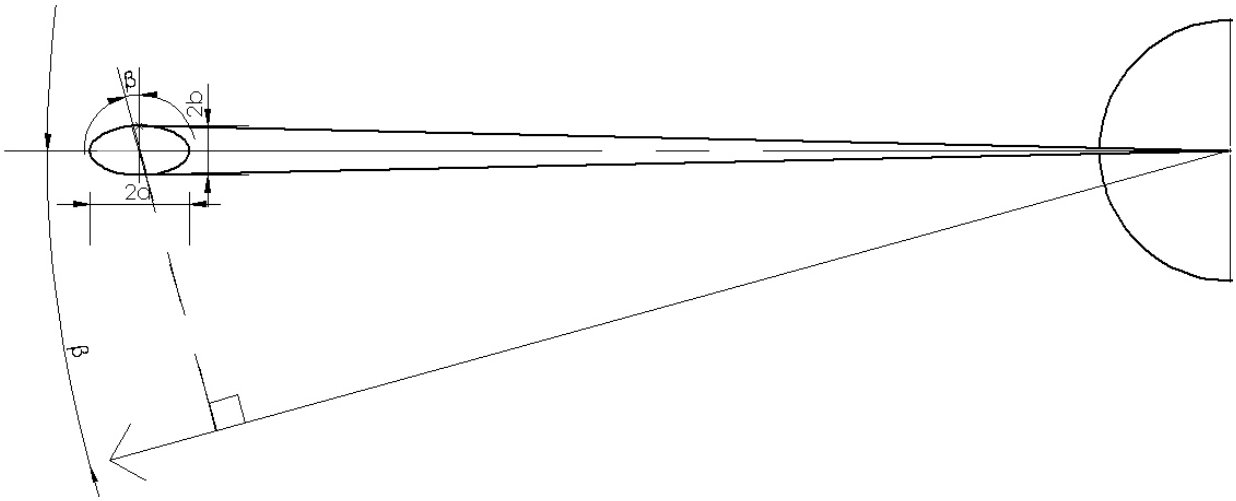

Figure 17: *Ka-band signal beam with $\beta \neq 0°$.*

As stated before, when $\beta = 0°$, the distance L_a to be used in the blockage duration formula is equal to 2b. When the signal has an azimuth angle not equal to 0°, it is necessary to exploit the ellipse equation to calculate the position of a point rotated by β from the minor axis.

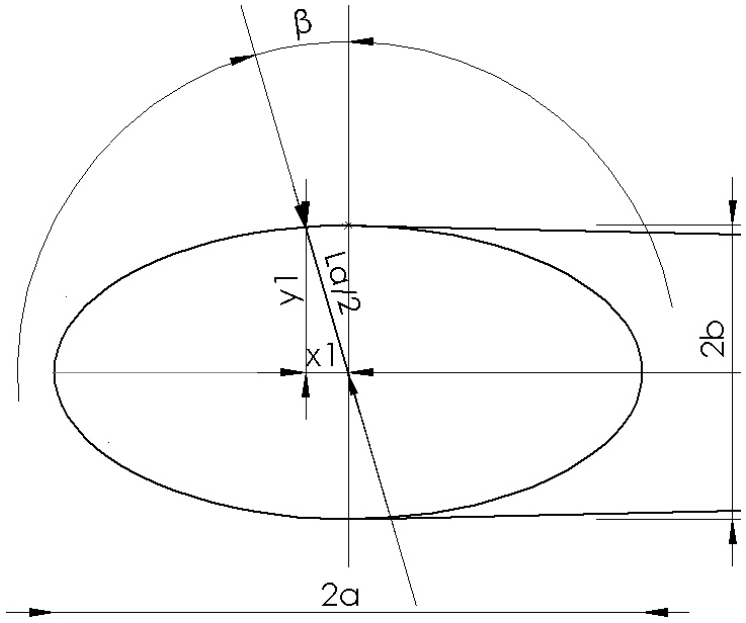

Figure 18: *Detailed view of the geometric elements necessary to calculate L_a.*

It can be observed that:

$$x_1 = \left(\frac{L_a}{2}\right) \cdot \sin(\beta) \tag{2.15}$$

$$y_1 = \left(\frac{L_a}{2}\right) \cdot \cos(\beta) \tag{2.16}$$

And knowing that the ellipse equation is:

$$\frac{x_1^2}{a^2} + \frac{y_1^2}{b^2} = 1 \tag{2.17}$$

It is possible, now, to state that:

$$L_a = \sqrt{\frac{1}{\frac{\sin^2(\beta)}{a^2} + \frac{\cos^2(\beta)}{b^2}}} \tag{2.18}$$

At this point, it is possible to use L_a to calculate T_d for several azimuth and elevation angles and then, to plot the 3D graph of the blockage ratio:

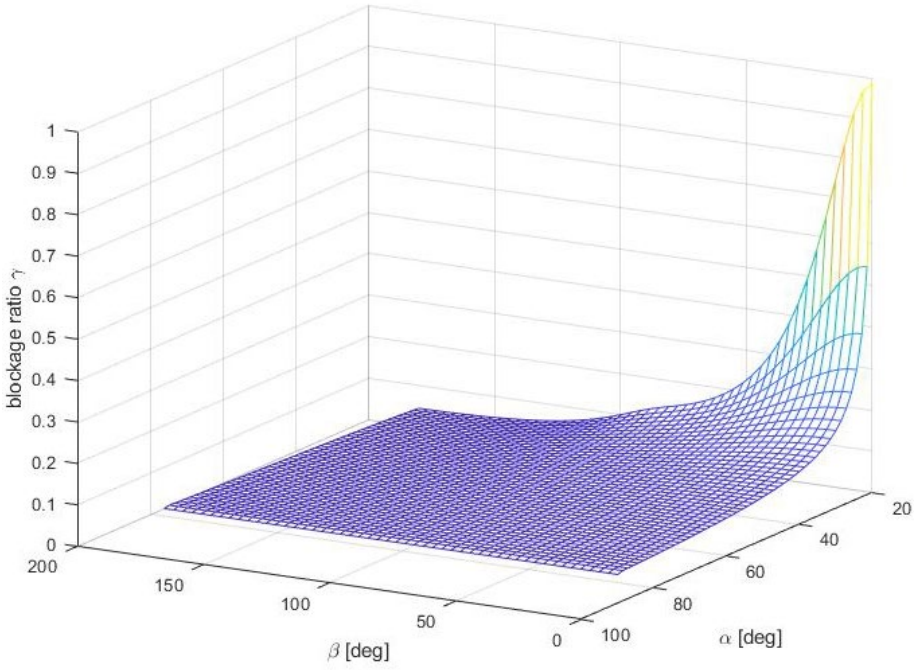

Figure 19: *Blockage ratio obtained taking into account the signal beam.*

Now it is possible to make a comparison between this result and the one presented in the 2.3 Section:

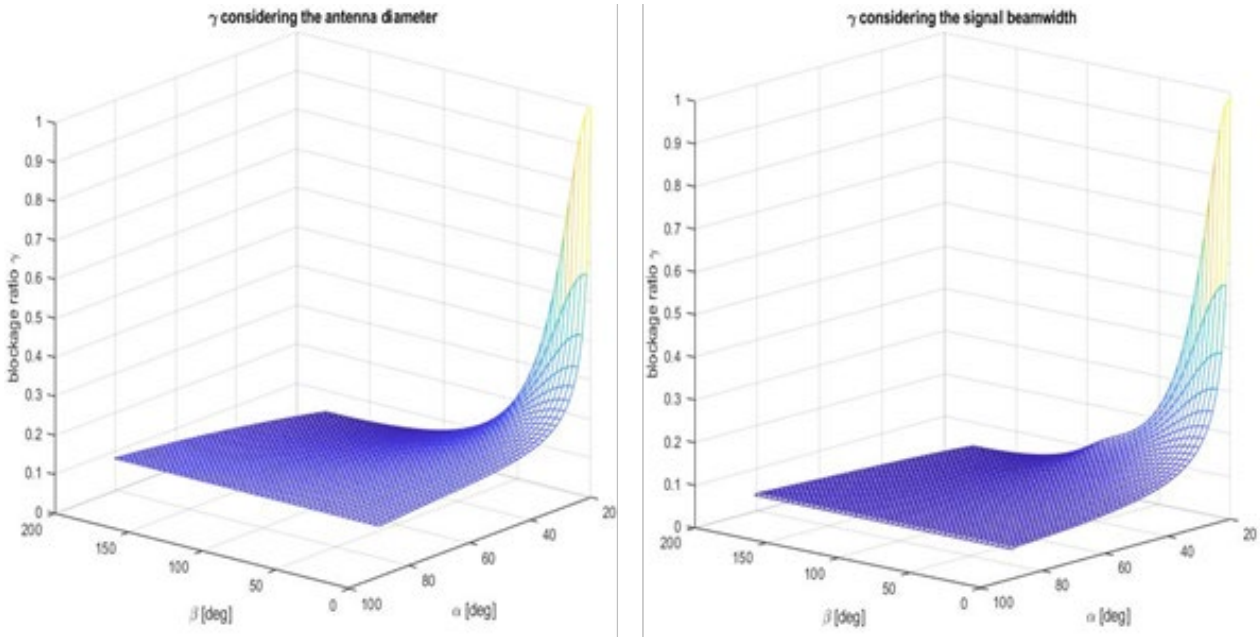

Figure 20: *Comparison between the "classic" blockage ratio trend and the modified one.*

As it can be observed the new blockage ratio is mostly smaller than the one found in the literature. That can be explained by the fact that in the Ka-band case, the beam is smaller than the antenna diameter, so the blockage duration is tendentially shorter. In the new blockage ratio mesh, it is possible to observe a little "hump" when $\alpha \cong 20°$ and $50° \leq \beta \leq 100°$. That may be justified by the fact that for a very small elevation angle the blockage duration tends to become very high. Moreover, when the azimuth angle comes closer to 90°, the signal beam is in a position such that L_a tends to the value of the major axis length of the ellipses. So even if D is increasing (in the interval in which $50° < \beta < 100°$), L_a grows faster and this produces a rapid increase of the blockage ratio. When β becomes lower than 50°, L_a decreasing is overcome by D, so it is possible to observe a little decrease in the blockage ratio. For lower values of the azimuth angle and elevation angle, it is possible to visualize the same γ trend found in the literature.

At this point, it is possible to test the new blockage algorithm on a signal. As the first example, the algorithm could be tested on a Ka-Band signal. This can be useful to demonstrate that for attitude angle values very far from the critic values, the new blockage duration is smaller.

Here is a table with the specification of the used signal:

Frequency (f_s)	29.96 GHz
Sample frequency (F_s)	10^8
Sample time (t)	$0: 1/F_s : 0.3 - 1/F_s$
Signal equation (x)	$x = \cos(2\pi f_s t)$
Beam Width (BW)	2.3364°
Elevation angle (α)	45°
Azimuth angle (β)	10°

Table 2. 3: *Test signal characteristics.*

As can be seen, for a higher frequency it is necessary to use a higher sample frequency. For this reason, it is not possible to plot a one-second-long signal. This could create memory problems. For this reason, the time interval is reduced to 0.3s. Even if it's a small-time interval, it is sufficient to observe the blockage phenomenon. Through the original algorithm it is possible to obtain the following result:

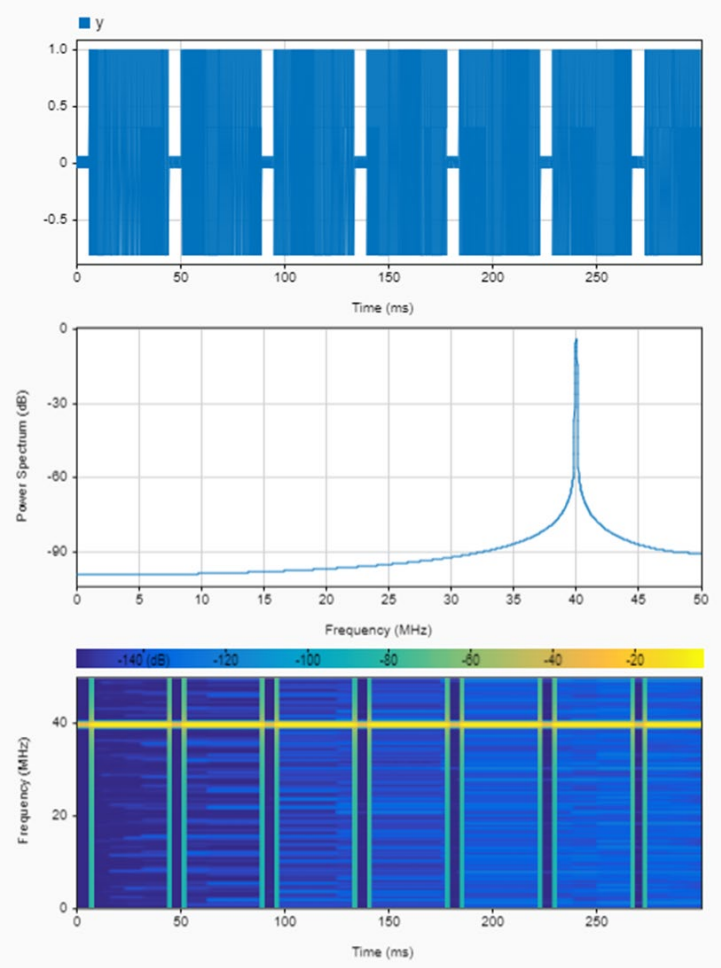

Figure 21: *"Classic" blockage algorithm applied to a Ka-band Signal.*

Then, the same signal is disrupted by the modified Blockage algorithm:

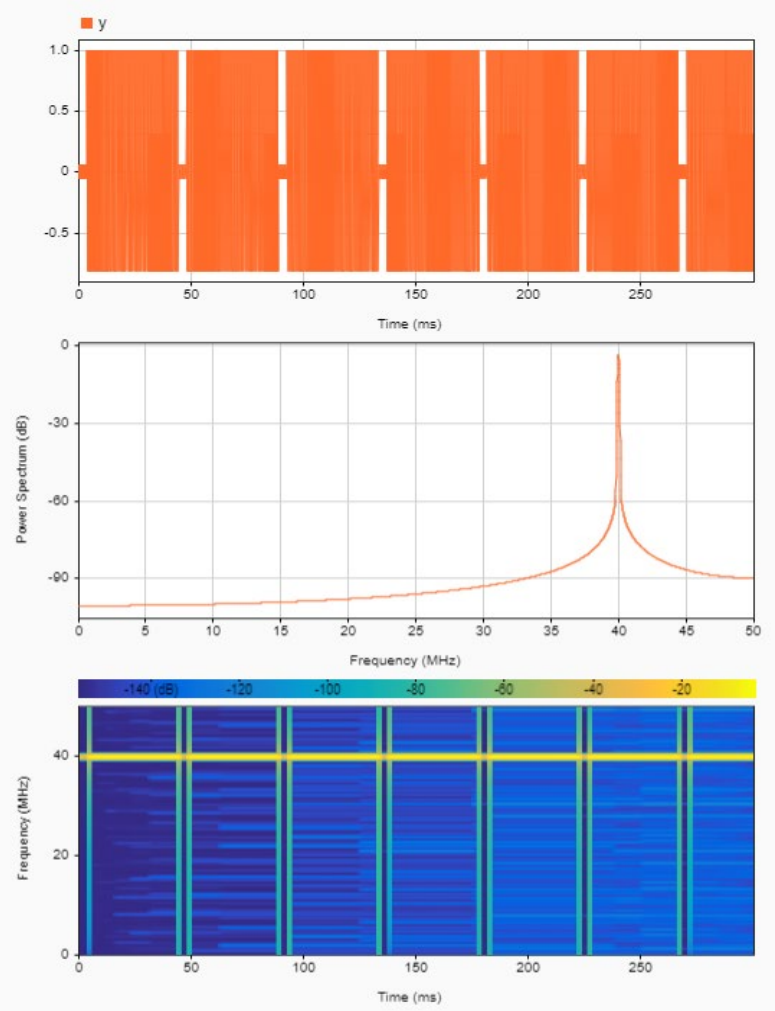

Figure 22: *Modified Blockage algorithm applied to a Ka-band signal.*

In the figure below a comparison between the two cases is reported. As expected, with the new blockage algorithm, the blockage duration is shorter. By the calculations, it is possible to obtain that with the "classic" blockage algorithm $T_d = 0.0074s$ while with the new one $T_d = 0.0051s$. Graphically it is possible to observe that the vertical white stripes in the signal trend graph, have a smaller width in the second case than in the first one. Moreover, it is possible to see the same detail in the spectrogram graph. This graphical evidence, confirms that the new algorithm works and has the advantage to take into account the type of signal that is transmitted or received.

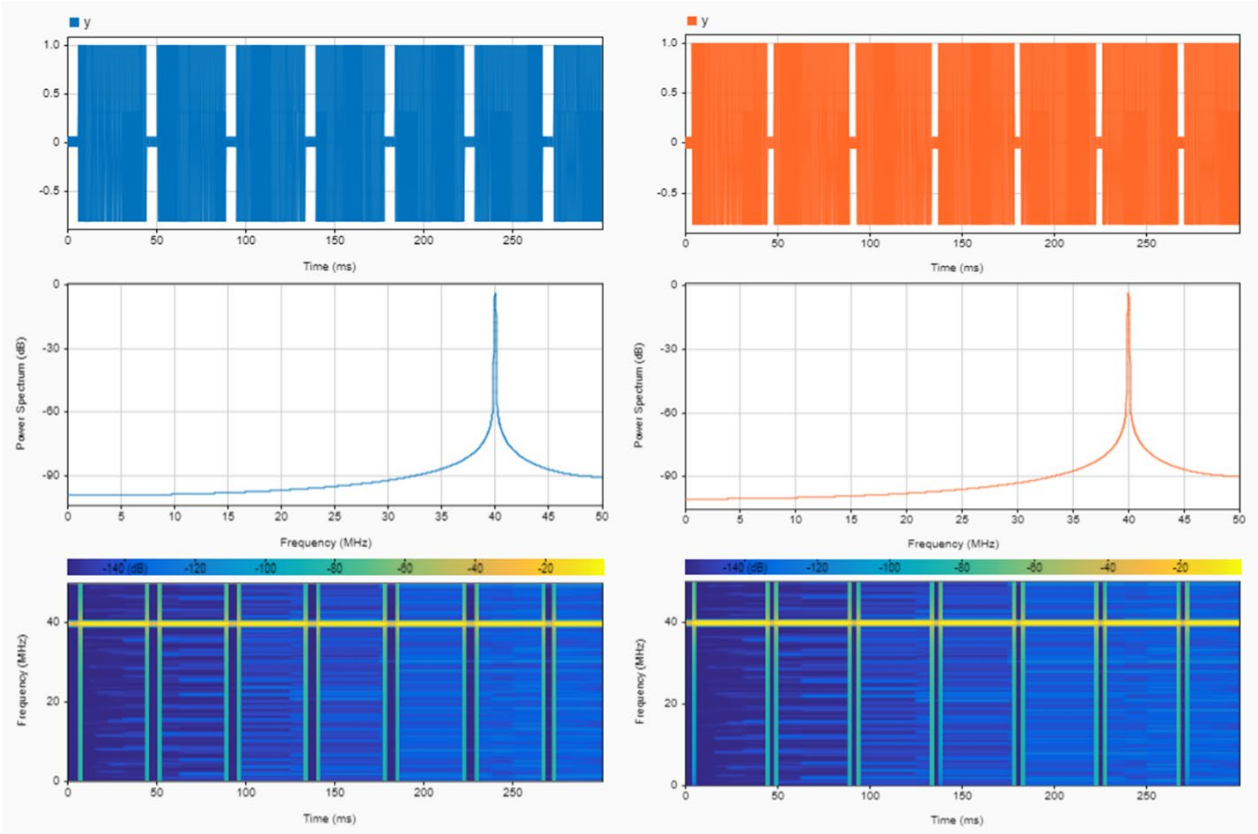

***Figure 23**: Comparison between the effect of the two different algorithms on the same signal.*

2.2.7 L-band Signal

In the Ka-band signal case, the beamwidth makes the L_a that the rotor blade has to overcome smaller than the antenna diameter. It is known that reducing the signal frequency makes the beamwidth increase. The L-band includes frequencies between 1GHz and 2GHz. With this kind of frequency, it is expected that the beam has a width bigger than the antenna diameter and the helicopter rotor blade. For this reason, it is necessary to modify the blockage algorithm to make it work even when the signal beam width is bigger than the antenna diameter.

The table below contains the characteristic of the signal used for the improvement of the blockage algorithm:

Frequency (f_s)	1.616 GHz
Sample frequency (F_s)	10^8
Sample time (t)	$0: 1/F_s : 0.3 - 1/F_s$
Signal equation (x)	$x = \cos(2\pi f_s t)$
Beam Width (BW)	43.3168°
Elevation angle (α)	45°
Azimuth angle (β)	10°

Table 2. 4: *L-band signal characteristics.*

The figure below allows us to observe the changes in the dimensions of the main lobe of the signal.

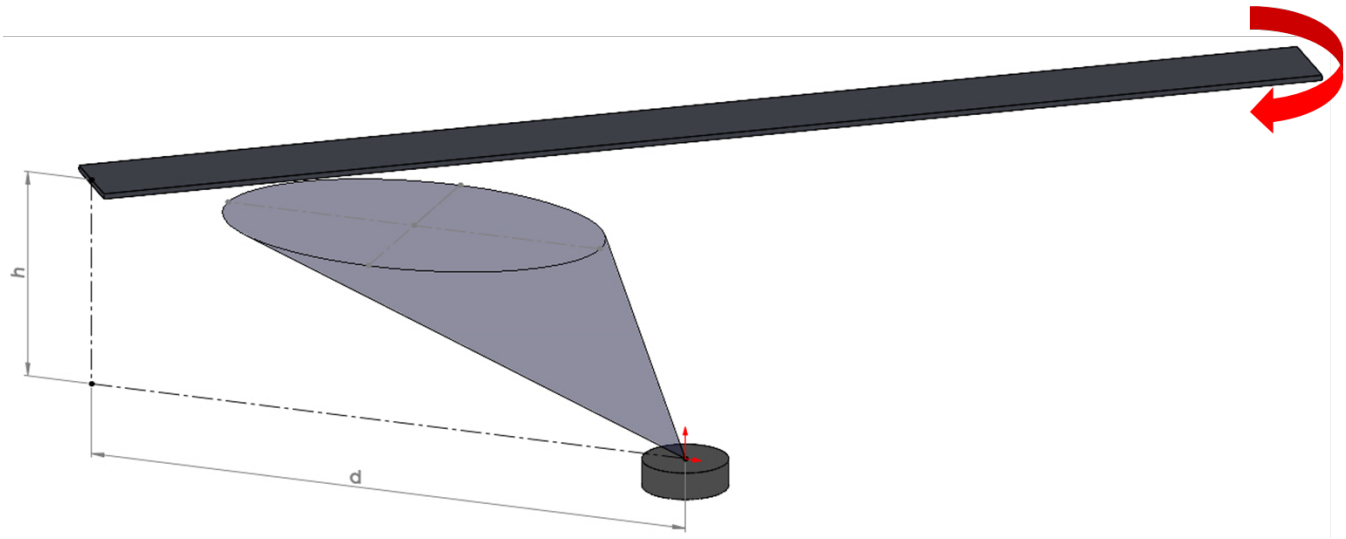

Figure 24: *3D Model of a rotating blade cutting the L-band signal beam.*

In this new condition, the signal main lobe is mostly larger than the antenna diameter and the blade width. For this reason, the new algorithm takes into account this situation, and when the condition $L_a > D_{iam}$ is satisfied L_a is calculated by the following formula:

$$L_a = \frac{h}{\sin(\alpha)} \cdot \tan\left(\frac{BW}{2}\right)$$

(2.18)

This modification is necessary because if the rotor blade is excessively smaller than the L_a, the signal would be attenuated for an excessively high amount of time. This would be an excessive oversizing of the blockage phenomenon. For this reason, this modification reduces the length of the distance that the blade has to travel to produce the attenuation. Most of the signal power is focused in a smaller region than the entire size of the ellipse obtained from the intersection between the blade and the cone.

Repeating the same calculations made in the 2.5.1 section, it is possible to obtain the blockage ratio graph for an L-band signal.

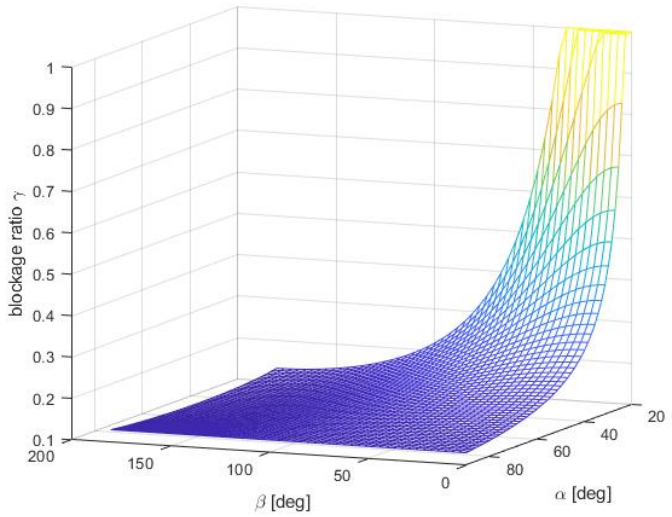

Figure 25: *Blockage ratio for an L-band signal.*

At this point, it is possible to make a comparison between this new γ plot and the blockage ratio diagram for a Ka-band signal. This can be useful to predict which impact the rotor blade blockage would have on an L-band Signal.

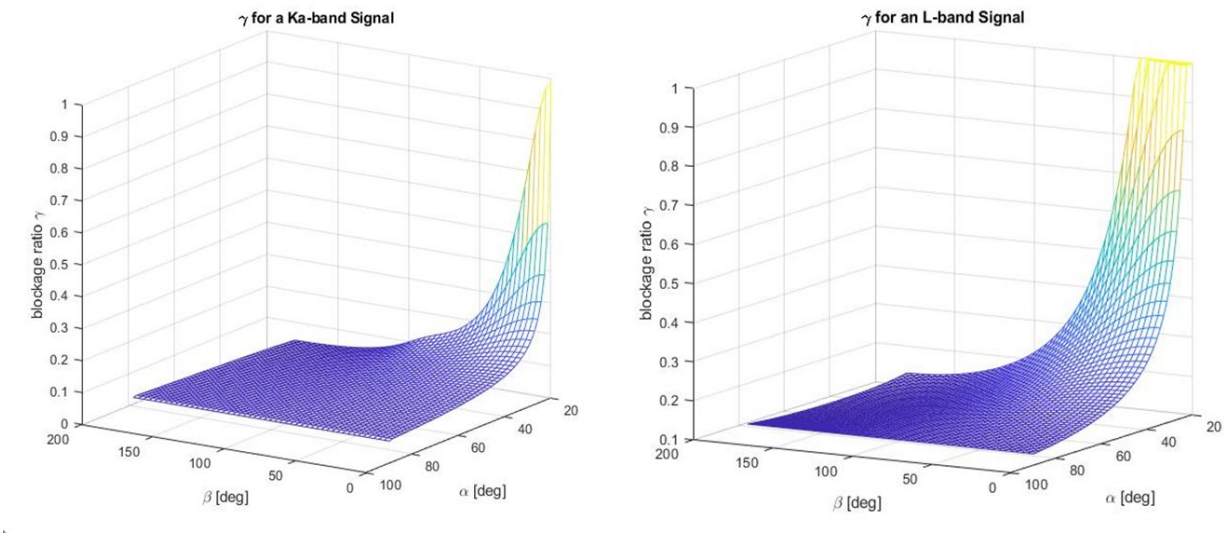

Figure 26: *Comparison between blockage ratio diagrams for Ka-band and L-band signal.*

The blockage ratio for the L-band signal is always higher than 10% and starts its rapid ascension for α and β angles higher than the Ka-band case of study. Moreover, it is possible to see that for critical values of azimuth and elevation angles, the blockage ratio is cut at $\gamma = 1$. That happens because, due to the signal beams' bigger dimensions, the blockage duration can, mathematically, become higher than the blockage period, not relating any practical sense and indicates a situation in which the signal is constantly attenuated by the passage of the blades.

As the final step, the new blockage algorithm is tested on the signal which characteristics are reported in Table 2.5. Differently from the Ka-band signal case, the blockage period now is visibly longer. That could make the signal quality considerably worse.

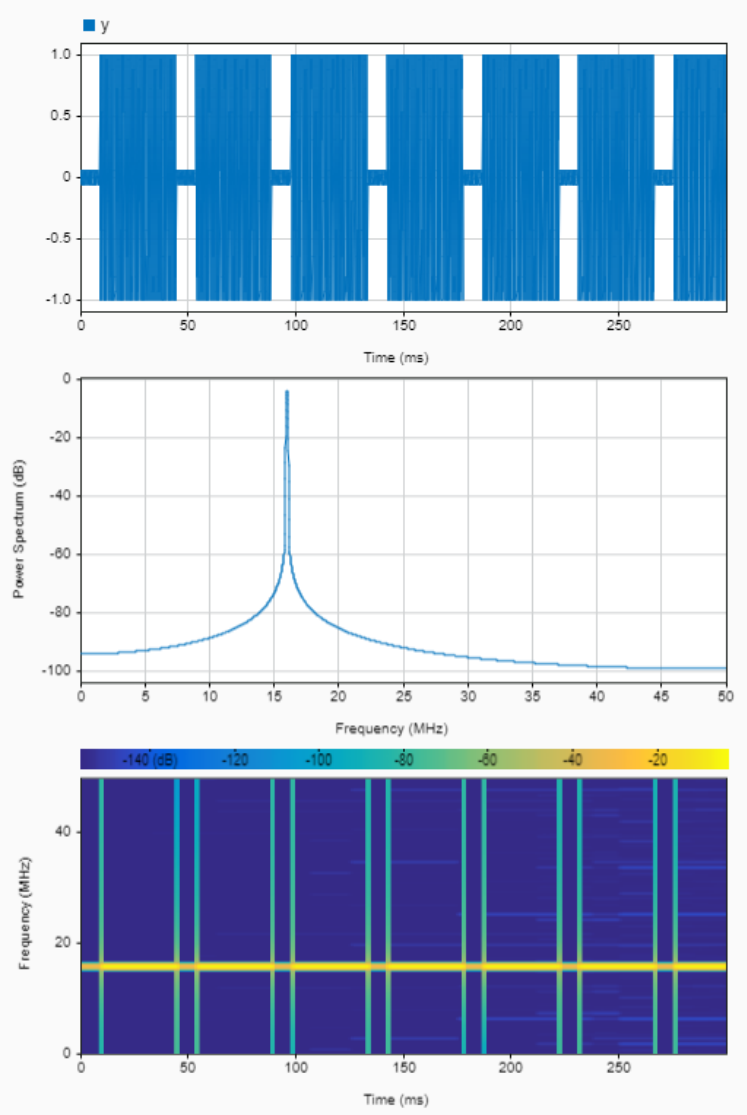

Figure 27:*L-band signal attenuated by the rotor blade blockage.*

3. Integration of the rotor blade blockage into a Ka-band satellite link

The previous analysis was made on a continuous wave signal, without any evolution in time in terms of signal orientation. To overcome this limitation, in this section it's reported an attempt to recreate a satellite link between a helicopter and a ground station, exploiting a geostationary satellite. The aim is to observe the effect that the changes in the beam orientation have on the signal attenuation and, consequently, verify if the algorithm can work in a time-evolving simulation.

3.1 Uplink simulation

The first scenario analyzed provides that the helicopter transmits the signal to the GEO satellite. To recreate the satellite link and make a time-evolving situation, the Matlab Simulink environment is exploited. This software is useful for this purpose because it allows changing the analysis parameters while the simulation is running.

The information between the helicopter and the ground station is in the form of a digital signal, and the carrier of the link is in Ka-band, to reconnect this analysis with the first part of the study presented.

The model consists of a "Helicopter transmitter", a "transmission channel", a "Satellite transponder" and a "Ground receiver". Every Simulink block is chosen and set to recreate a plausible Ka-band satellite link. In the figure below is reported the complete satellite channel modeled on Simulink:

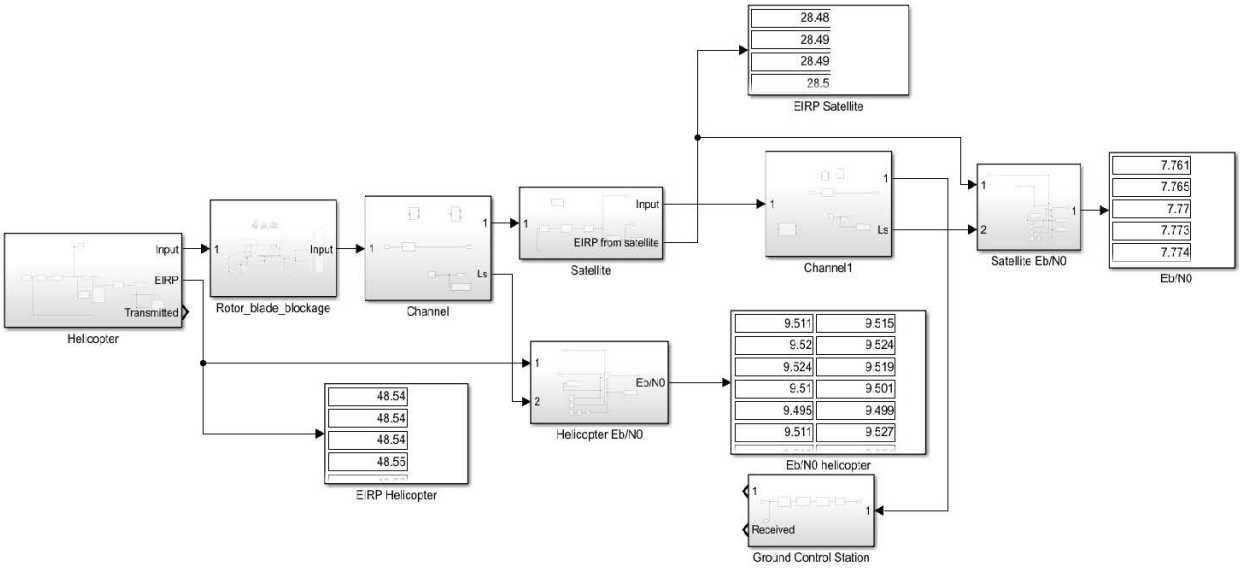

Figure 28:*Simulink satellite channel model used to simulate an uplink between the helicopter and the ground station.*

3.1.1 Helicopter transmitter block

The "helicopter transmitter" consists, primarily, of a Bernoulli Binary generator block. This block generates random binary numbers using a Bernoulli distribution (discrete probability distribution of a random variable which takes the value 1 with probability p and the value 0 with probability q=1-p). The Bernoulli Binary is used to generate random data bits to simulate digital communication systems. The output of the block is set on "double" and the probability of zero is set on 0.5, but it is not relevant for the purposes of this study. Other settable parameters are the "Sample time" and the "Sample per frame". The sample time is strictly

related to the bandwidth of the signal. In particular, the relationship between these two parameters is given by the equation:

$$ST = \frac{1}{2 \cdot BW}$$

(3. 1)

where ST is the sample time and BW is the bandwidth. The time between output updates, instead, is given by the product of the Sample per frame and the Sample time. The Sample per frame, moreover, defines the number of the Bernoulli Binary block output columns. So, if the Sample time is fixed, every $(Sample\ time \cdot Sample\ per\ Frame) seconds$ the b lock generates a $Sample\ per\ Frame - by - 1$ vector.

The following block is the QPSK Modulator Baseband. In the quadrature phase-shift keying modulation, two bits are modulated at once. The phase shift chosen for this case of study is $\pi/4$. QPSK allows the signal to carry twice as much information as ordinary PSK using the same bandwidth. The input type parameter is set to “Bit” (relating to the previous block that generates a binary sequence of numbers) and the constellation ordering is set to “gray”. For this reason, the block uses the following signal constellation:

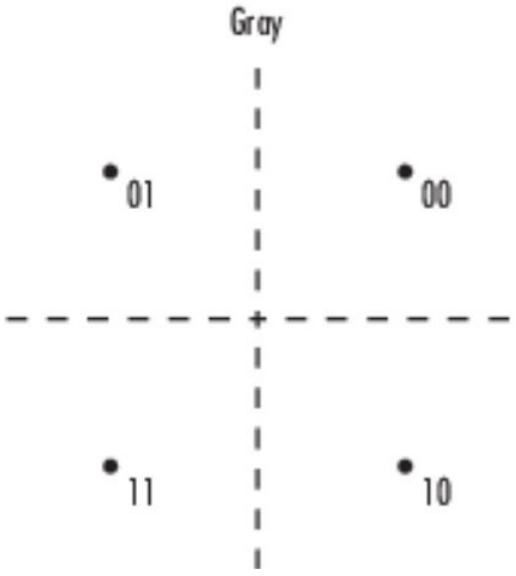

Figure 29: *Gray Mapping [6].*

To reduce the intersymbol interference (ISI) a raised cosine filter is added. The ISI is a phenomenon that affects signals and consists of interference between subsequent symbols. This has a similar effect as noise and makes the communication link less reliable. The raised-cosine filter belongs to the Nyquist filter family, so its impulse response is null for time instants multiple of the time symbol. It's called like that because the non-zero portion of its spectrum is a cosine function, “raised” above the frequency axis. Its spectrum manifests an odd symmetry about $1/2T$, where T is the symbol-period of the communication system. In the Helicopter transmitter, the raised cosine filter is set with a square root shape and with a roll-

off factor of 20%. A roll-off factor is a real number between 0 and 1 that determines the excess bandwidth of the filter. A 20% roll-off factor means that the bandwidth of the filter is 1.2 times the input sampling frequency. The filter span in symbols, instead, specifies the number of the symbol at which the block truncates the impulse response [7]. This parameter and the output samples per symbol, determine the length of the filter's impulse response. Moreover, it is possible to set a linear amplitude filter gain, which is used to scale the filter coefficients.

As the last block for the helicopter transmitter, there is a dB Gain block that is used to simulate the parabolic antenna gain at the specified signal frequency. That is given by the formula:

$$G = 20.4 + 20 \cdot \log_{10}(D_{iam}) + 20 \cdot \log_{10}(f_{GH_z})$$

(3. 2)

Here is reported a table that resumes the most important parameters used in this block

Carrier frequency (f)	29.96 GHz
Bandwidth (BW)	6.744 MHz
Samples per frames	5120
Rolloff factor	0.2
Filter Span	6
Samples per symbol	8
Linear amplitude filter gain	12 dB
Antenna Gain $(T_x Gain)$	36 dB

Table3. 1: *Parameters used in the helicopter block.*

Below it is possible to observe the constituents blocks of the Helicopter transmitter:

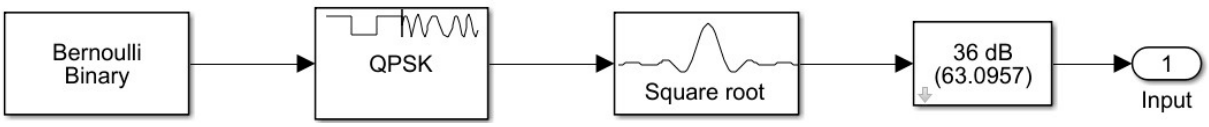

Figure 30: *Internal elements of the "Helicopter transmitter" block.*

3.1.2 Rotor Blade Blockage Block

The rotor blade blockage block wasn't already implemented in Simulink, so it is built from the ground. It is composed of several subsections with different functions.

The higher level of the block consists of the time check on the signal to reduce its power every time that the blade passes over the beam. Most of the blocks that compose this section are

if-action blocks that reproduce the same logic process described in section 2.4. Here is the scheme of this first section of the block:

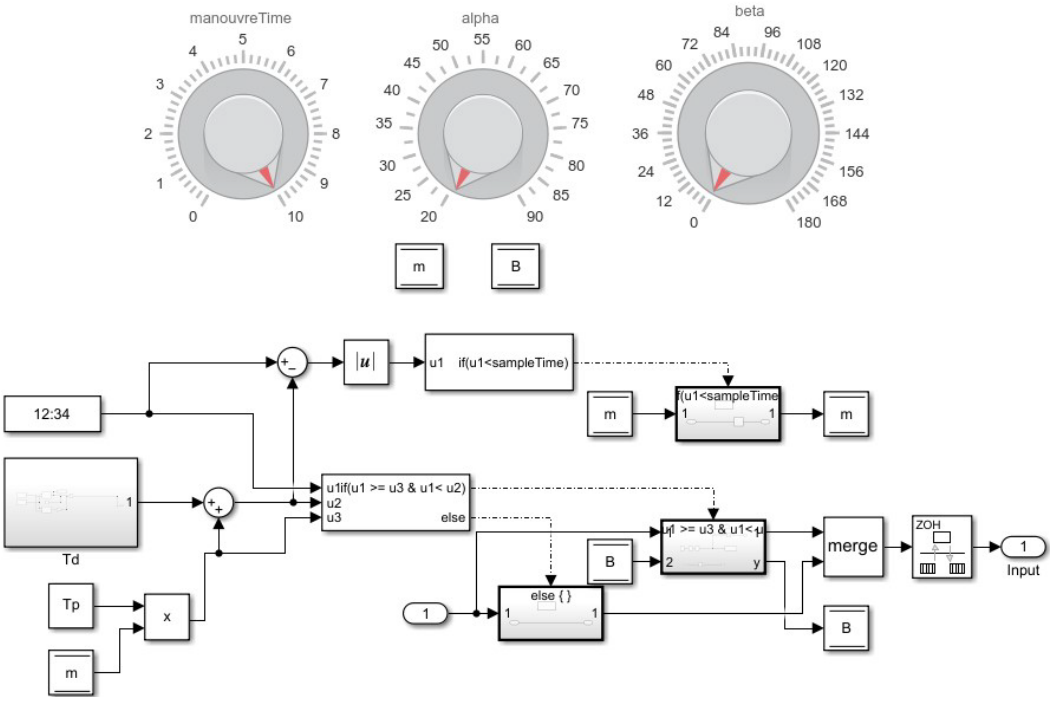

Figure 31: *First section of the "Rotor lade Blockage" block.*

As can be seen, above the blocks there are three knobs. These knobs are useful to change the attitude angles of the signal during the simulation with an editable speed. The parameters controlled by the knobs are grouped into a subsection of the "T_d" block:

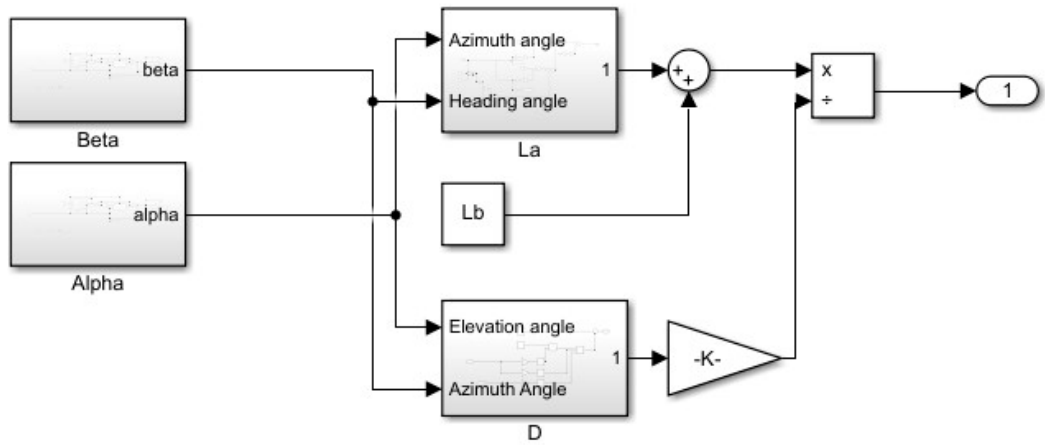

Figure 32: *T_d block section*

In the T_d block it is possible to find several subsections in which are calculated important parameters such as α, β, L_a and D. The formulas used for the calculation of L_a and D have already been discussed in the previous sections.

It is necessary a special acknowledgment for the α and β blocks that are essential to change the signal attitude while the simulation is running. This is one of the principal advantages of moving the analysis to Simulink. In this way, it is possible to verify if the algorithm still works when the attitude angles change as they do in a real mission scenario. For the sake of simplicity, the variation of the attitude angles is simulated as linear maneuvers. Through the "maneuver time" block, it is possible to set the amount of time necessary to change attitude angles, and with the α and β knob, it is possible to set the new attitude angle as a target that has to be reached in the defined maneuver time. The attitude angle knob controls a "constant" block. When the knob rotates the constant block changes its value and becomes the target value. Through a linear function block, every step time the actual attitude angle approaches the target, the new attitude angle value is saved into a "Data Store Memory" block.

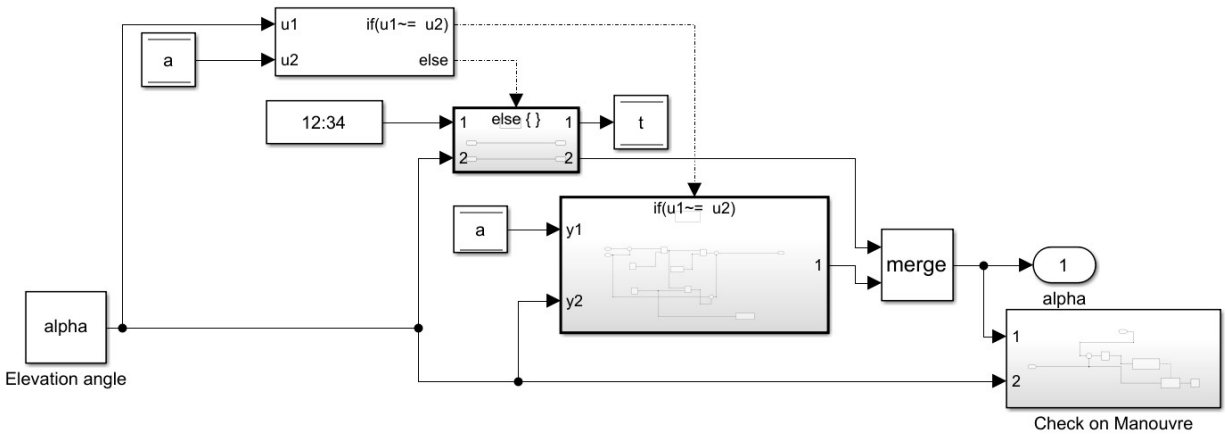

Figure 33: *Elevation angle control block*

In the figure below, it is possible to observe an example of the time variation of the elevation angle obtained by this block. Fixing the maneuver time at 10 seconds and the azimuth angle to 0°, the elevation angle varies from 20° to 45°, then from 45° to 70° and, in the end, from 70° to 90°. In a hypothetical mission scenario, it is possible to imagine that the helicopter is pointing and moving toward the satellite; so $\beta = 0°$ and the elevation angle tends to increase. Sometimes the helicopter stops and passes in hovering flight, for this reason, the elevation angle stops varying with time. Then the helicopter restarts moving and the elevation angle increases until it reaches the value of $\alpha = 90°$, which represents the situation in which the helicopter is perfectly under the satellite.

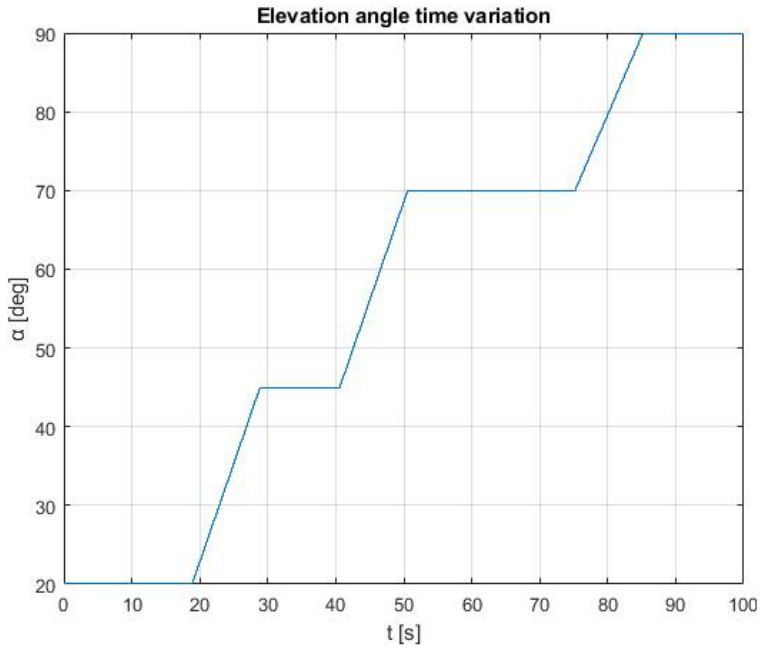

Figure 34: *α time variation.*

3.1.3 Channel block

The channel block has the purpose to simulate the transmission medium of the signal. In this first iteration of the simulation, only the free space path loss is taken into account. For this reason, the channel block simulates the loss of signal power due to the distance between the transmitter and the receiver. The scheme below can be useful to better understand the geometrical parameters involved in the free space path loss.

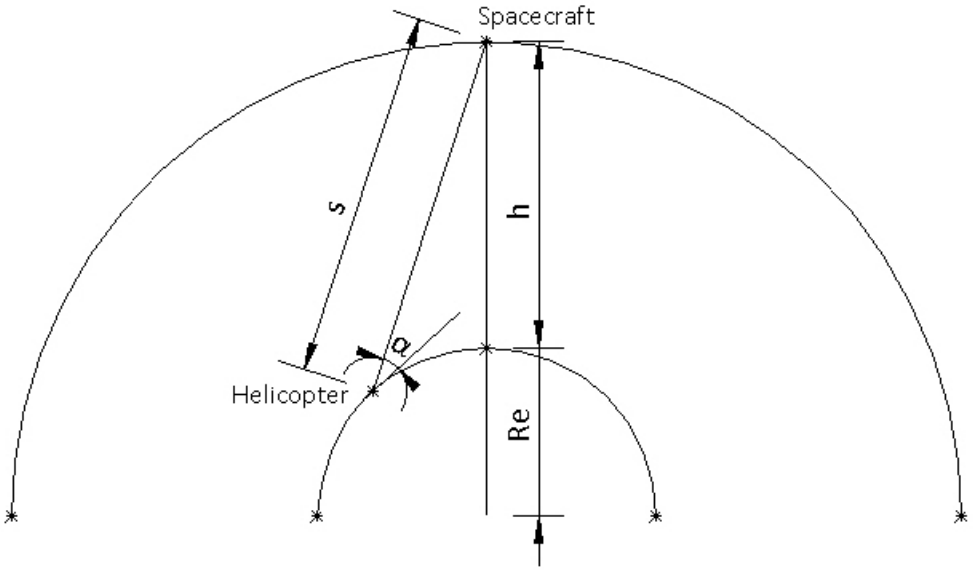

Figure 35: *Free space loss.*

In the previous figure, h is the satellite mean height above the surface, R_e is the Earth radius and S is the slant range. With these geometric parameters, it is possible to calculate the free space loss as:

$$L_s = 22 + 20 \cdot \log_{10}\left(\frac{S}{\lambda}\right) \tag{3. 3}$$

Where λ is the wavelength of the signal and S is given by the equation:

$$S = R_e \cdot \left[\sqrt{\frac{r^2}{R_e^2} - \cos^2(\alpha)} - \sin(\alpha)\right] \tag{3. 4}$$

In the last equation, r is given by the sum of the Earth radius and the mean height of the satellite.

So, in this study, the variation of the elevation angle provokes the variation of the free space path loss. In this particular scenario, considering a GEO satellite ($h \cong 35786$km), that communicates in Ka-band ($\lambda = 0.01\ m$), the average free-space path loss is $L_s = 214\ dB$. The helicopter flight altitude can be neglected in this calculation, because of the very high altitude of the satellite.

3.1.4 Satellite block

In this scenario, the satellite is used to make the helicopter communicate with a ground station. For this reason, the satellite is simulated as a transponder that receives, amplifies, and retransmits the signal. The satellite block is composed of two "dB gain" blocks that simulate a gain of 42dB for the satellite antenna, and an amplifier block.

The amplifier block generates a complex baseband model of an amplifier with thermal noise. For this study, it was chosen the cubic polynomial model for the amplifier block. This model uses linear power gain to calculate the linear coefficient of a third-order polynomial. Moreover, the nonlinearity type of the block is set to "Input third-order intercept point" (IIP3), which influences the magnitude of the output signal.

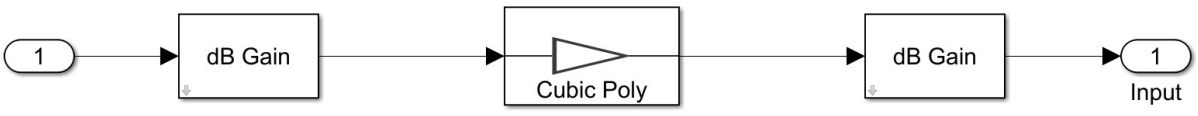

Figure 36: *Satellite transponder.*

As mentioned above, the goal of this part of the study is to verify if the disturbance algorithm works for attitude angles that vary with time. For this reason, in the satellite block (and even in the channel block) elements are missing such as cable loss, noise temperature, atmospheric absorption. All these elements will be taken into account in the next part of the analysis that will involve STK.

3.1.5 Ground Station block

In this first scenario, the ground station receives, amplifies, and demodulates the signal. For this reason, the first block in this section is a dB gain block that simulates a parabolic antenna of 1.8m in diameter (so 49.3 dB). The subsequent block is a cubic polynomial amplifier, that has the same characteristics as the satellite amplifier.

The "raised cosine receive filter" block is placed behind the demodulator block. The characteristics of this filter are the same as in the "raised cosine transmit filter" block. So, for this reason, the parameters used in this block are the same as the ones used for the transmitter.

At the end of the Ground Station block, there is the "QPSK Demodulator" block. As for the filter case, even the demodulator is using the same parameters that are set in the transmitter. The only difference is that for the demodulator it is possible to choose the "Decision type" that in this case is set to "Hard decision".

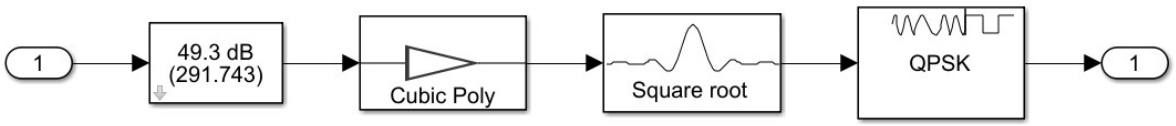

Figure 37: *Ground Station block.*

3.1.6 Uplink simulation results

Now that all the blocks have been described, it is possible to observe some results that demonstrate that the disturbance algorithm works. To visualize the results, exploited tools such as the Simulink spectrum analyzer and the MatLab spectrum analyzer, import the results from Simulink.

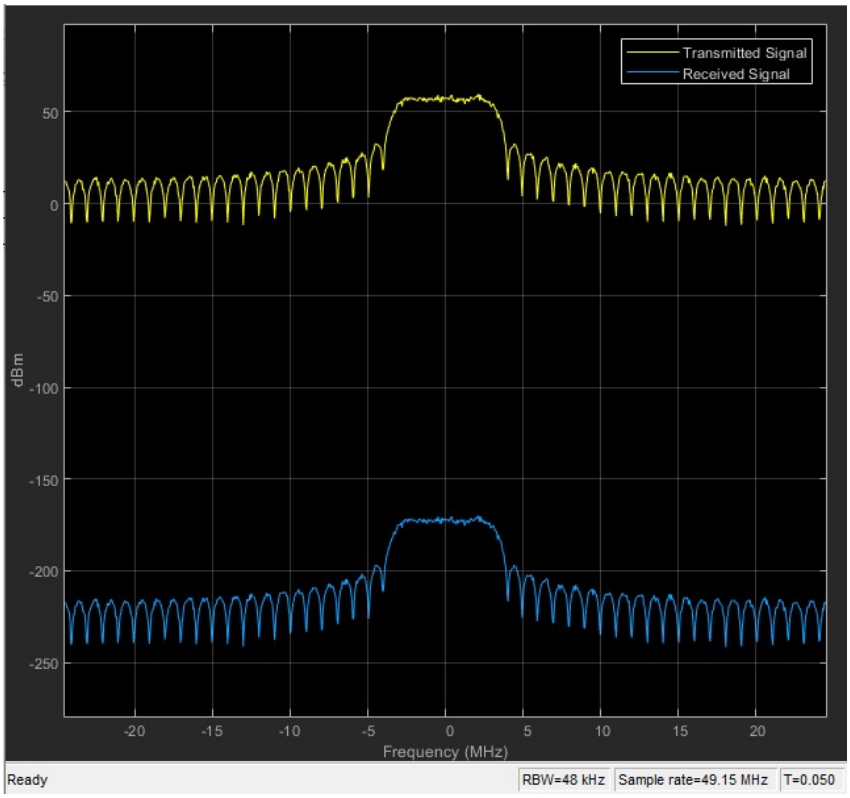

Figure 38: *Transmitted and Received Signal without blade disturbance in an uplink scenario.*

This first result is the visualization of the signals power spectrum from the Simulink Spectrum Analyzer, without the implementation of the rotor blade blockage. The next results will be focused on the transmitted signal. The figure below shows the power spectrum and spectrogram obtained from the transmitted signal and registered just before the signal enters the channel block.

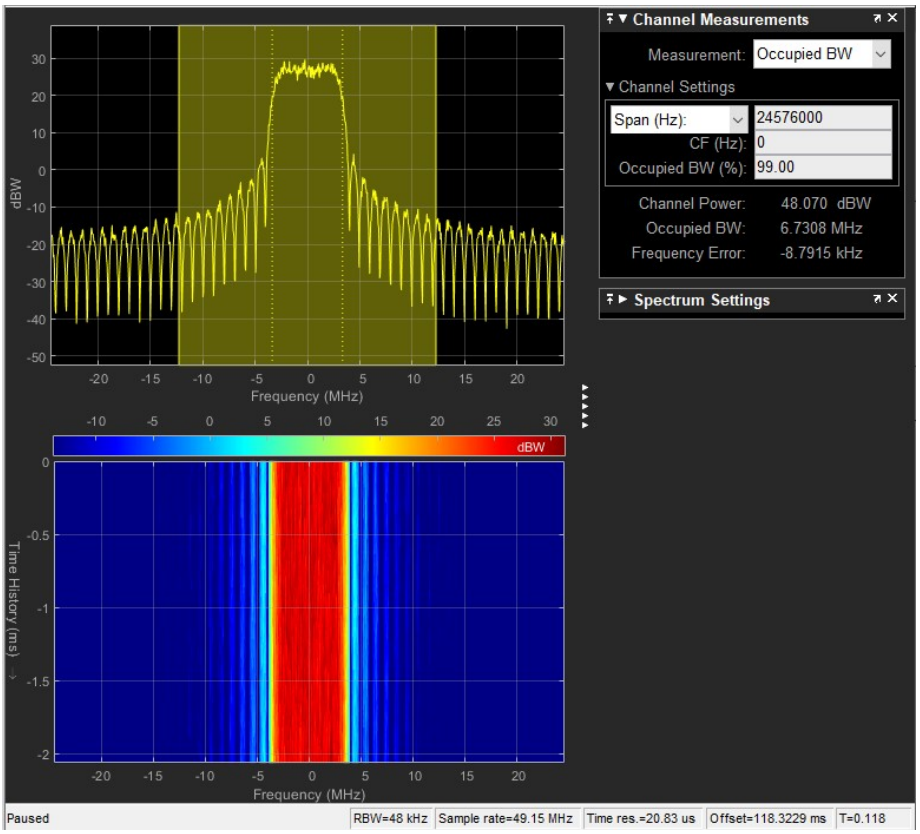

Figure 39: *Transmitted signal power spectrum and spectrogram.*

As can be observed, the transmitted signal occupied bandwidth is about 6.7 MHz as expected. For occupied beamwidth, it can be considered the bandwidth that contains 99% of the total integrated power of the signal, centered on the assigned channel frequency. The Channel Power detected from the spectrum analyzer is about 48dBW. In that specific bandwidth, this value can be considered as the effective irradiated power (EIRP) of the transmitter, which is coherent with the values presented in table 3.1.

In the first case for the application of the rotor blade blockage algorithm, the most critical one is chosen. The first analysis is run, with a $\alpha = 20°$ and $\beta = 0°$. As discussed in the previous sections, in this condition the signal is always attenuated by the rotation of the blades. For this reason, it is expected a reduction of 25dB in the channel power (with a fixed “Occupied Bandwidth”).

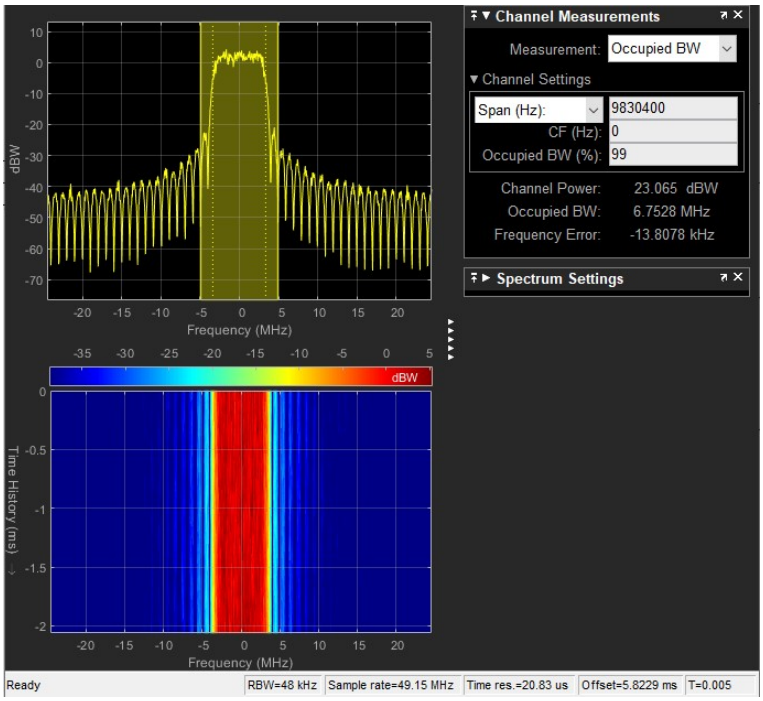

Figure 40: *Transmitted signal attenuated for $\alpha = 20°$ and $\beta = 0°$.*

The next test simulates a condition in which $\alpha° = 45°$ and $\beta = 30°$. According to the formulas analyzed previously, for this attitude and the signal taken into account, the expected attenuation period is $T_d = 0.0048s$. The time attenuation of the signal is visible through the spectrum analyzer while the simulation is running. Here are reported screenshots of the instant in which the attenuation is starting.

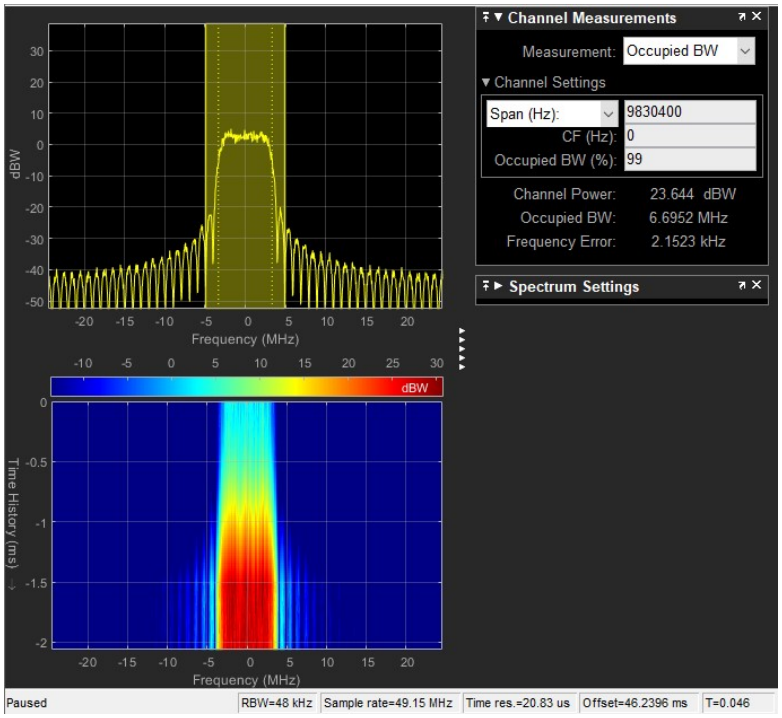

Figure 41: *Transmitted signal attenuated for $\alpha = 45°$ and $\beta = 30°$.*

As it can be seen, when the blade starts to pass over the signal beam, the channel power decreases. This phenomenon can be observed in the power spectrum diagram and the spectrogram. To compare this analysis to the preliminary one, it is possible to import the signal data on MatLab (through a "To Workspace" block) and use the Signal Analyzer tool to observe the signal attenuation during a short period.

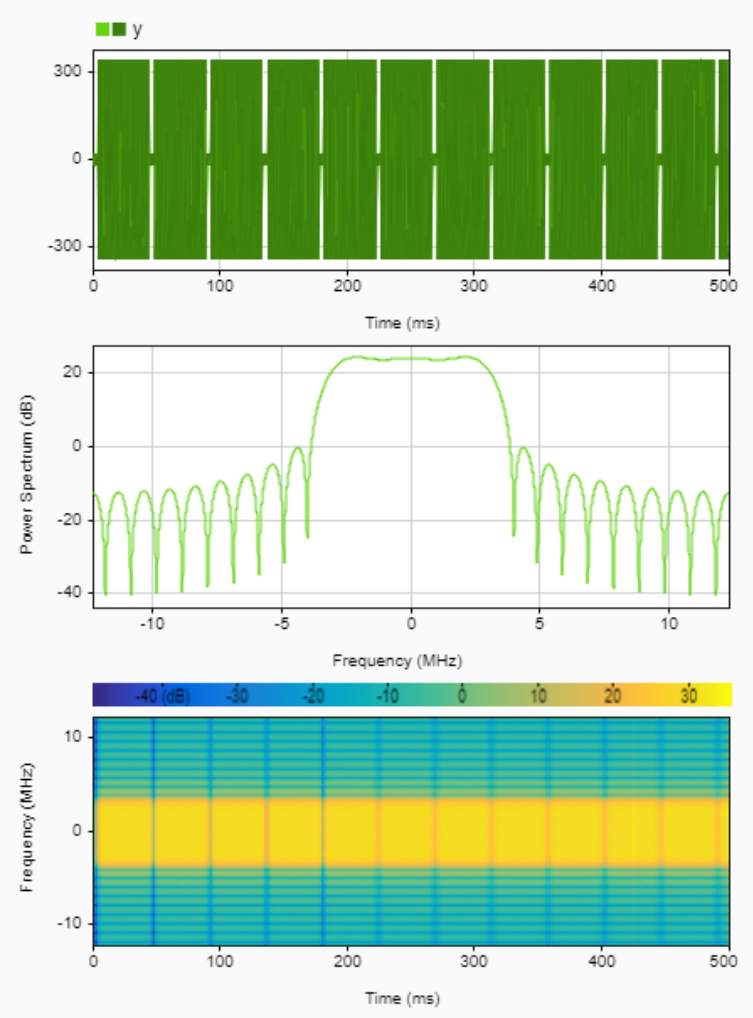

Figure 42: *Transmitted signal for $\alpha = 45°$ and $\beta = 30°$.*

The power spectrum is coherent with the one shown in the spectrum analyzer. The advantage, in this visualization of the results, is that it is possible to observe the signal attenuation in several instances. The sample time used for the "To Workspace" block is very short ($0.00042s$), for this reason, the number of elements of the array imported to Matlab could be too high to allow visualization in the Signal analyzer. So, the simulation is stopped at 0.5s.

It is now possible to change the elevation angle of the signal, to visualize the variation in the blockage duration T_d.

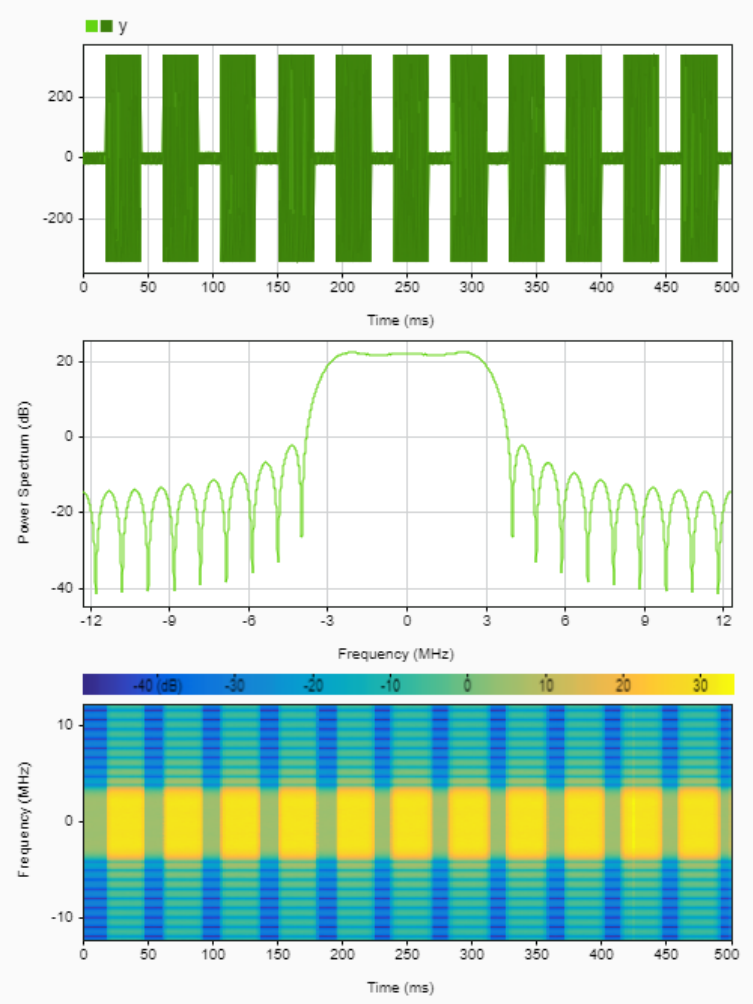

Figure 43: *Transmitted signal for $\alpha = 20°$ and $\beta = 30°$.*

As discussed before, for smaller elevation and azimuth angles, a longer blockage duration is expected. Figure 42 confirms these expectations. As can be seen, the light blue stripes in the spectrogram representing the power attenuation, have bigger widths than the ones in the previous case. The purpose of this Simulink analysis, however, is to verify that the disturbance algorithm works even when the attitude angles change while the simulation is running. For this reason, in the next figure, it is possible to observe the variation in the signal attenuation caused by the increase of the elevation angle from 20° to 45°. In this analysis, the azimuth angle is fixed at 30°, and it is possible to imagine that the helicopter is moving toward the satellite without making any turn maneuver.

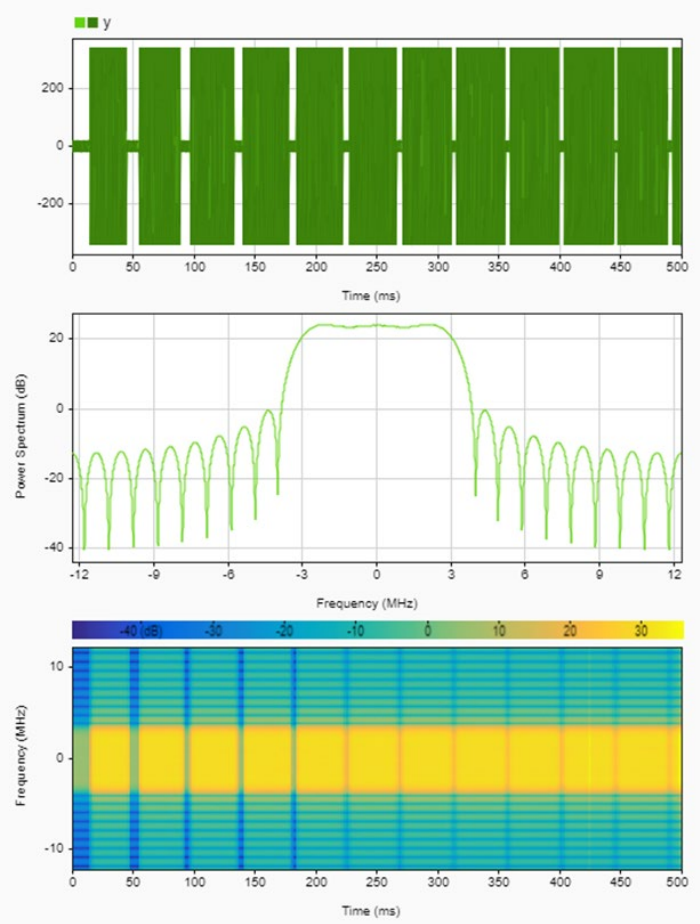

Figure 44: *Transmitted signal while α is increasing from 20° to 45° and $\beta = 30°$.*

As expected, the power attenuation stripes become smaller while the elevation angle becomes bigger. The signal is still measured in a small time interval (0.5s). That means that the elevation angle varies in a very short amount of time and that would never happen in a real mission scenario. As explained before, that's a problem related to the maximum quantity of array elements that Matlab can handle. But, since the purpose of this simulation, is to verify that the attenuation block can handle attitude angle variations, these results can be considered satisfactory.

3.2 Downlink Simulation

In this second scenario, recreated in Simulink, the helicopter receives a signal sent from the same ground station of the previous analysis. As for the previous case, the signal is received and retransmitted from the same GEO satellite. For this reason, the Satellite and channel block, are the same as discussed before. There are some differences in the "Transmitter" and "Receiver" blocks and, the "Rotor blade blockage" block is now right before the "Receiver" block.

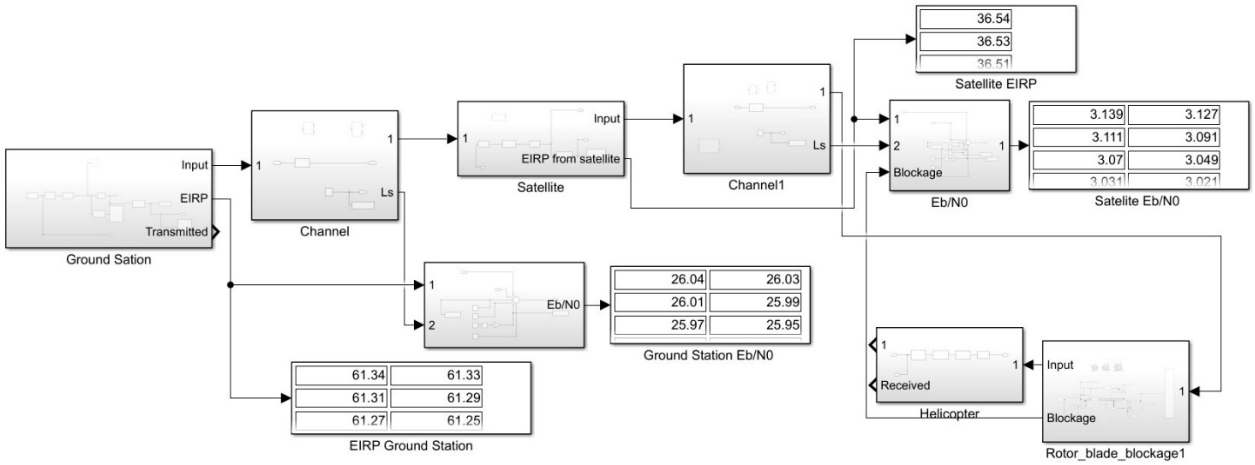

Figure 45: *Simulink satellite channel model used to simulate downlink between the ground station and the helicopter.*

The "Ground station" block is now modeled as the "Helicopter" block in the previous case, and vice-versa. However, the parameter used to generate the transmitted signal and to simulate the receiver are different.

Carrier frequency (f)	29.96 GHz
Bandwidth (BW)	3.4 MHz
Samples per frames	2560
Rolloff factor	0.2
Filter Span	6
Samples per symbol	8
Linear amplitude filter gain	7.5 dB
Antenna Gain $(T_x Gain)$	52.9 dB

Table3. 2: *Parameters used in the "Ground Station" block.*

As can be observed, the occupied bandwidth, in this case, is smaller than in the previous one. Moreover, because of the bigger antenna diameter (1.8m in this case), the antenna gain reaches about 53 dB. There aren't other important changes in the communication channel model so, as for the previous case, it is now possible to visualize the results.

3.2.1 Downlink Simulation Results

Even in this case, it is possible to visualize the transmitted and received signal through the spectrum analyzer block.

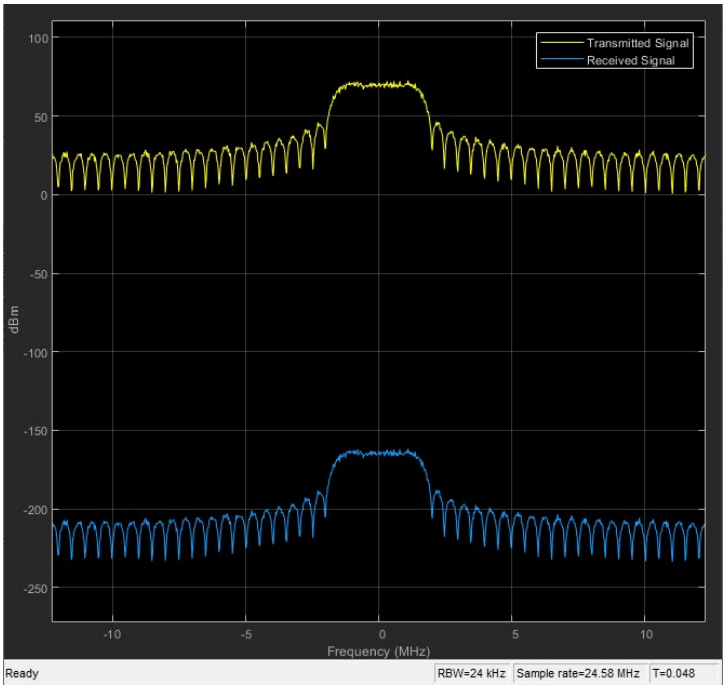

Figure 46: *Transmitted and Received Signal without blade disturbance in a downlink scenario*

It's already possible to see that the transmitted signal reaches higher values of power than in the previous case. Taking a look at the power spectrum and spectrogram of the transmitted signal can allow us to better observe this increment in power.

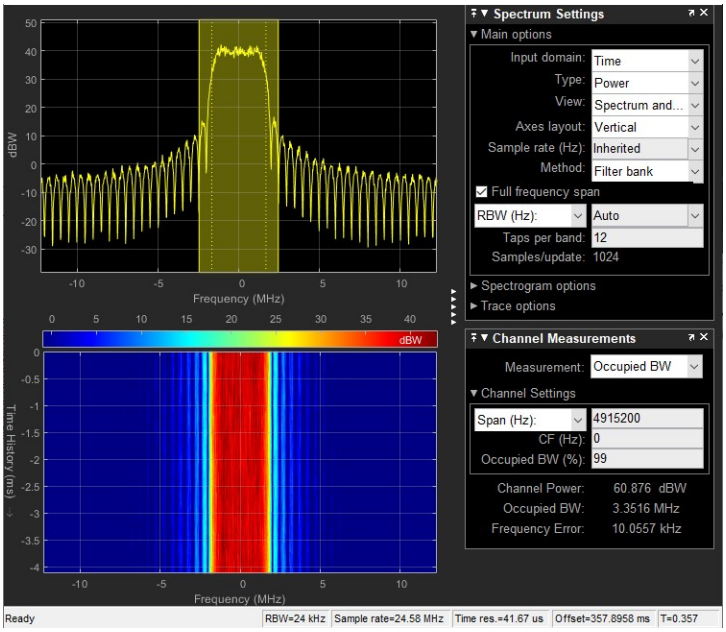

Figure 47: *Transmitted signal power spectrum and spectrogram in a downlink scenario*

In this case, the EIRP of the ground station is about 61dBW, with smaller occupied bandwidth. As for the previous case, it is now possible to verify if the “Rotor blade blockage” block works when the helicopter receives the signal.

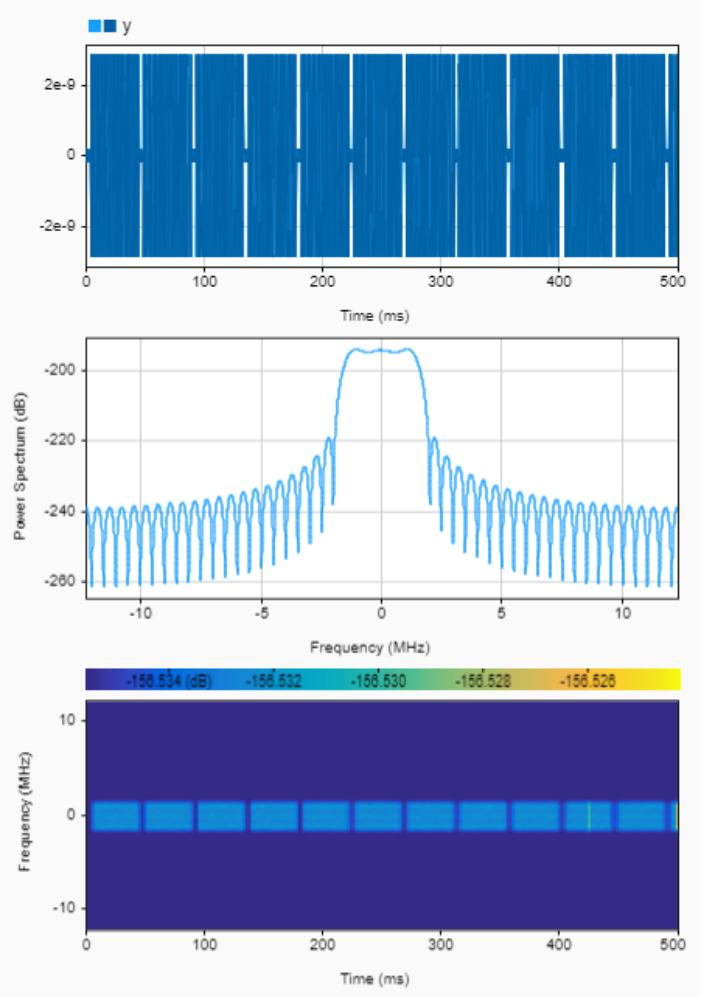

Figure 48: *Received signal for $\alpha = 45°$ and $\beta = 30°$.*

Even in this case, it is possible to observe the periodical attenuation caused by the rotation of the blades. The signal power is lower than in the previous case. The signal spectrum shows darker colors and now, the attenuations, are represented as dark blue vertical lines. The reduction of the signal power is justified by the fact that this is the signal received by the helicopter that has been attenuated by the “Channel” block and the “Rotor blade blockage” block.

It is now possible to visualize the received signal for $\alpha = 20°$ and $\beta = 30°$ and the received signal for an elevation angle variation from 20° to 45°.

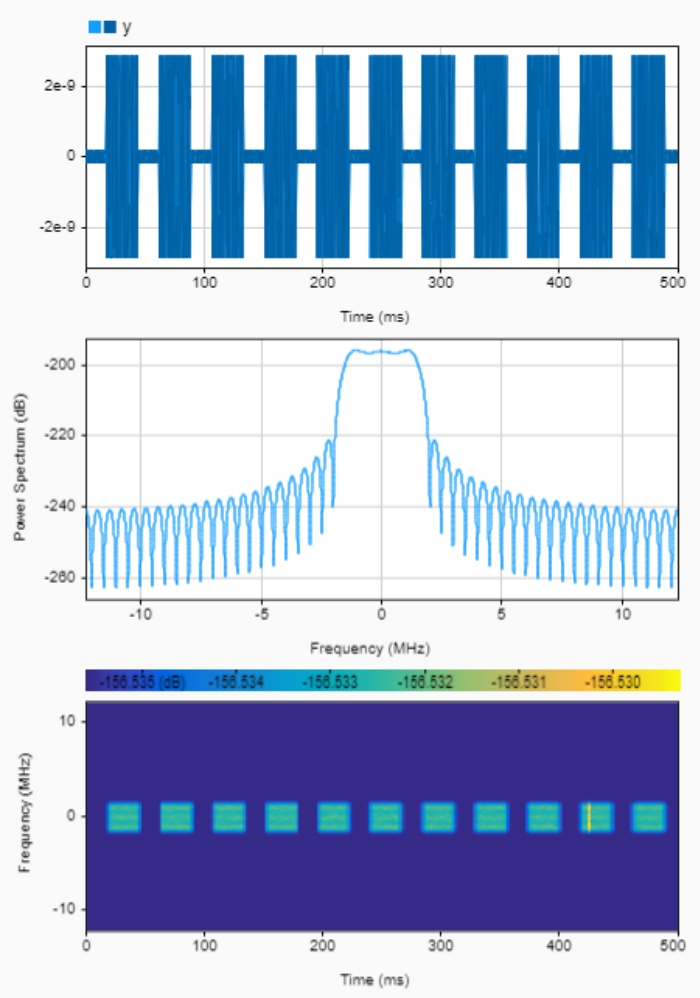

Figure 49: *Received signal for $\alpha = 20°$ and $\beta = 30°$*

Like the uplink case, the increment of the blockage duration is visible in the signal spectrum.

The same results obtained in the uplink case, are obtained in the downlink scenario in which the elevation angle varies. As for the previous case, in the figure below, it is observed a reduction of the blockage duration while the elevation angle increases.

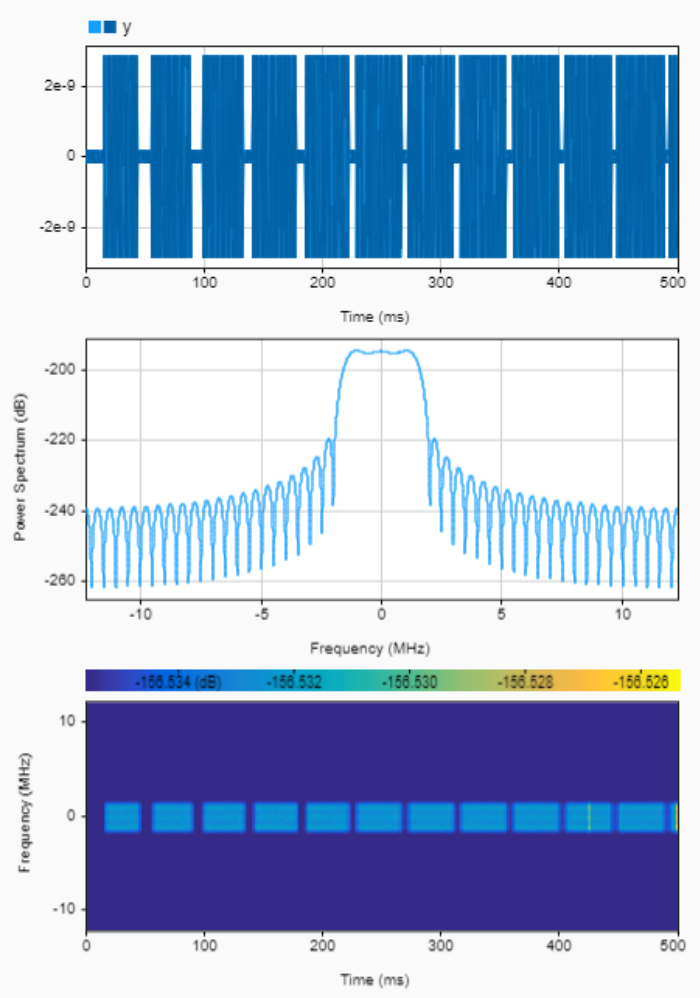

Figure 50:*Received signal while α is increasing from 20° to 45° and $\beta = 30°$*

In conclusion, the creation of this Simulink communication channel has been useful to test and verify the proper functioning of the blockage algorithm. Now that the simulation is completed and the errors in the algorithm have been fixed, it is possible to move on to the second part of this study.

4. Signal analysis integration in a mission scenario context

As mentioned before, this second part of the study is focused on an attempt to integrate the signal analysis stated in the first part of this study, in a mission scenario context. In particular, the System Tool Kit (STK) is exploited to create a mission scenario for the helicopter taken into account in the previous analysis and to collect data related to its communication with a satellite constellation. So, in this context, the helicopter will not be a static object communicating with a single satellite but will be brought in a mission scenario in which it is possible to modify its path, its velocity, its attitude, and its communication channel according to the user's preferences and necessities.

Therefore, another goal of this work is to parameterize as much as possible the scenario. That would make the mission elements easier and faster to be modified by the user. To achieve this purpose, the connectivity between Matlab and STK is exploited. Through specific code lines, it is possible to send commands from MatLab to STK to create scenarios, add elements, model transmitters, receivers, and communication channels. Moreover, the rotor blade disturbance is not implemented in STK but this problem can be overcome through the MatLab Plugin script.

A Plugin script provides a method for incorporating customer-specific modeling into STK analysis. Basically, it is a Matlab function that is read by STK while the simulation is running. Through a MatLab Plugin, it is possible to customize several STK objects including transmitters and receivers, in which it will be possible to include the rotor blade blockage as signal loss.

4.1 STK scenario

The first step is to create a scenario that defines the context in which the properties and the behavior of the mission objects are defined. In the scenario creation, it is possible to set the simulation start time and stop time and set the environmental characteristics.

The scenario start time and stop time, influence the position of the satellites in their orbit at the beginning of the simulation. In this case study, the start period is:

$$19\ Nov\ 2021\ 10{:}38{:}40.000, +3h$$

Where "+3h" means that the simulation stop time is set three hours later than the start time. The next step is to define the scenario "RF environment" properties.

4.1.1 Rain, clouds & fog

In this section of the RF environment properties, it is possible to set the "Rain", "Clouds and fog" model. These models are not mutually exclusive, so it is possible to set both models for the same simulation. For example, it is possible to model rain and cloud & fog loss when there is another layer of clouds above the rain.

When enabled, STK uses the rain model to calculate the amount of signal degradation caused by the rain. The attenuation is principally caused by the absorption from the water molecules

and is a function of the elevation angle of the signal and its frequency. The rain loss increases if the signal frequency increases thereby increasing with the decreasing of the elevation angle due to a greater distance in which the signal has to travel through the atmosphere portion where the rain is falling. Rain produces a rise in the antenna noise temperature as well.

It is possible to choose a default Rain model from STK or to create a script plugin to customize the loss according to the user's necessities. For this case, it was set an STK rain global annual statistical model. For this case, it was set an STK rain global annual statistical model. This model divides the world into different rain regions and for each region, it associates with rainfall rates and probabilities which are determined from historical measurements. Between the available STK rain models, is set the "ITU-R P618-12" which is based on the most recent revision of ITU recommendation ITU-R P618. This model calculates the probability of non-zero rain attenuation for a slant-path length variation in a defined period. Moreover, STK allows enabling the cross-polarization loss of the signal, i.e the depolarization of the communication link due to rain [8].

Even for the "Clouds and Fog" a default STK model is set, i.e the ITU-R P840-7. Generally, cloud attenuation becomes more relevant if the signal frequency is high (above 10GHz). For clouds or fog consisting of small droplets, generally less than 0.01cm, the model exploits a mathematical model based on Rayleigh scattering to calculate the value of the attenuation for frequencies up to 200GHz [9]. Even in this case, the attenuation is dependent on the slant-path length of the signal. It is also possible, to set some parameters that STK uses to compute the signal attenuation such as "Cloud Ceiling" (i.e the height of the cloud layer above the ground), the "Cloud Layer Thickness, the "Cloud Temperature" and the "Liquid Water Content Density Value" (i.e the amount of water content within the clouds and fog layer). For this study, the parameters chosen for the "Clouds and Fog" model are:

Cloud Ceiling	3 km
Cloud Layer Thickness	0.8 km
Cloud Temperature	258.1500 K (-15°C)
Liquid Water Content Density Value	0.35 g/m^3

Table 4. 1: Parameters set for the STK "Clouds and Fog" model.

Each type of cloud has specific characteristics. The parameters chosen for this scenario, according to literature references, are typical of Cumulus clouds.

4.1.2 Atmospheric absorption

The electromagnetic waves are absorbed in the atmosphere according to their wavelength. This phenomenon is mainly caused by the presence of oxygen and water vapor. STK provides a series of atmospheric absorption models that can be selected for the mission scenario. In this case, it was decided the ITU-R P676-9 Atmospheric Absorption Model that performs a ray tracing on a propagation path. The atmosphere is divided into concentric shells and computes line segments within each shell along the propagation path. The signal attenuation along each segment is computed and multiplied by the length of the segment. Finally, all the attenuations or each segment are added to arrive at an overall attenuation [10]. STK allows setting two attenuation calculations.

For this case of study, the selected atmospheric absorption model exploits a "Fast. Approx Method" for the calculations. This is an empirical curve-fit model that can be used for a frequency range between 1-350 GHz. This method is an alternative to the line-by-line calculations, that are more accurate, but the absolute difference between the results of these methods is less than 0.1dB/km. The "Fast. Approx Method" calculates a "specific attenuation" due to the dry air and the water vapor at a certain altitude and a "zenith attenuation" which is calculated along the slant paths through the Earth's atmosphere.

4.1.3 Tropospheric scintillation

This part of the ITU-R P618 already introduced in section 4.1.1 takes into account rapid fluctuations of the signal due to tropospheric scintillation fade. The tropospheric scintillation is caused by a rapid variation of the refractive index along the path (due to atmospheric phenomenons such as turbulence) and consists of a fluctuation (called scintillations) of the signal level received. The scintillations are generally constant around the mean signal level and are influenced by the season and the weather. The amplitude of the fluctuation increases with the reduction of the signal wavelength, with the path length (i.e with a low elevation angle) and small receiving antenna, and decreases if the antenna beamwidth decreases (keeping the same aperture). It is also possible to find a correlation between the signal fluctuations and the radio refractivity, which depends on the water vapor content of the atmosphere [8].

So, once the model for the Tropospheric scintillation is selected, STK allows setting some parameters that influence this phenomenon such as the "Surface Temperature" (i.e the average surface ambient temperature for one month or more), the "Tropo Fade Outrage" (that is used to compute loss in dB that occurs in the percentage time not exceeding the specific limit) and the "Percent Time Refractivity Gradient < -100 N" (i.e the amount of time, in percentage, in which the refractivity gradient in the lowest 100m of the atmosphere is less than -100N units/km). For the last parameter listed, when more reliable local data are not available, it is possible to exploit charts that give statistics for the World which were derived from a 5-year data set. Observing the chart below, it is possible to choose a 10% time gradient for the month and the geographical area chosen for this particular study.

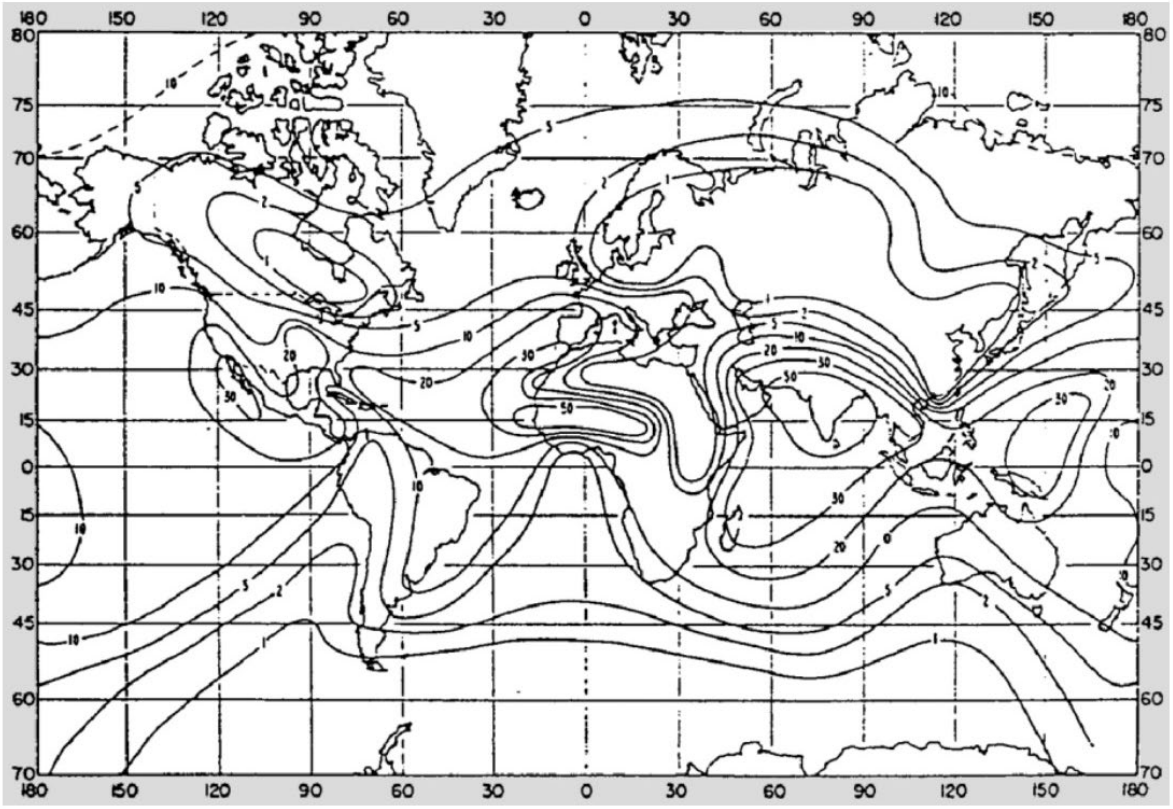

Figure 51:*Percentage of time gradient ≤-100 (N-units/km) for November [11].*

For the “Surface Temperature”, instead, it is possible to use the seasonal average value for a specific geographic area obtained from weather information for the site of interest. The values set for the listed parameters are reported in the table below.

Surface Temperature	18 °
Tropo Fade Outage	0.1%
Percent Time Refractivity Gradient	10%

Table 4. 2: *Tropo Scintillation model parameters.*

4.1.4 Iono Fading

While the signal is traveling through the ionosphere many effects can take place. The interaction between the electromagnetic wave and the total electron content of the ionosphere can generate a rotation of the polarization, also known as “Faraday rotation”, a time delay of the signal and a change in the apparent direction of the arrival due to refraction. The small-scale irregular structures in the ionosphere can produce a rapid variation of the signal amplitude and phase and random rotations that can be described in stochastic terms. Furthermore, these irregularities act like divergent and convergent lenses that defocus and

focus the signal waves affecting the amplitude, the phase, and the angle of arrival of the signal. Lastly, time delays and non-linear polarization rotations can generate Doppler effects [12].

Due to the complex nature of the phenomenons related to the ionosphere, it's not always possible to exploit simple analytic formulas to describe the "Iono Fading". That's the reason why STK relies on the "ITU-R P531-13" model, which is a method for evaluating ionospheric propagation effects in different geographical areas and seasons based on the use of parameters obtained by experimental measurements. In this model, the total electron content of the ionosphere is estimated by the use of the International Reference Ionosphere model, considering the actual path through the ionospheric layer that the signal has to travel.

4.2 STK Satellite Constellation

As mentioned before, in this part of the study there's the interest in simulating the link between the helicopter used in the previous analysis and a satellite constellation. In particular, it would be interesting to study a satellite link in L-band with a LEO constellation. Recreating this link in STK would allow studying the quality of the communication in a more realistic mission scenario context and, thanks to the automatization and customization reached by using Matlab scripts, it would be easier to study different combinations of helicopter trajectories, satellite constellations, and signal bands. For this first iteration, the attention is focused on the recreation, in STK, of the Iridium Next constellation.

4.2.1 Iridium Next

Iridium-Next is the new generation of satellites that in January 2017 has started to replace the old Iridium generation. It consists of 66 operating orbiting units, 9 on-orbit spares, and 6 ground spares for a total of 81 satellites. For the sake of simplicity, in the presented scenario the constellation contains only the 66 operating satellites divided into 6 orbital planes containing 11 units each. Every unit follows a polar circular orbit at an altitude of 780km with an inclination of 86.4° and a period of 101 minutes per orbit. Thanks to the geometry of its orbit this constellation can provide 24/7 real-time visibility over the entire Earth's surface.

Usually, in STK it is possible to insert new satellites from the "Standard object database" but, in this case, to allow the integration with Matlab and the parametrization of the mission scenario a TLE file is exploited to create the constellation. The TLE file (in .txt format) is read by Matlab and, through a "for cycle", every orbital element is sent to STK that, exploiting a "Two Body" propagator, creates the orbit of each satellite. STK gives a wide choice of satellite propagators and a "Two Body" one, for sure, is not an accurate model of a vehicle's actual force environment (because that takes into account only the effect of the body viewed as a point mass). However, being the aim of this study the analysis of the communication links, in this first iteration this propagator can be considered suitable for the simulation. The figures below are useful for a comparison between the actual Iridium Next constellation and the one recreated in STK.

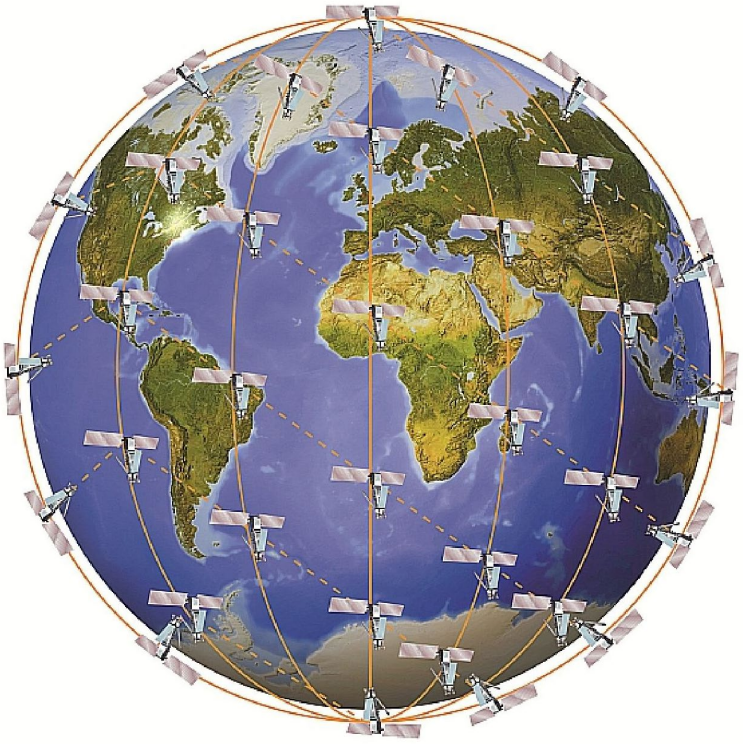

***Figure 52**: Actual orbital coverage of the Iridium NEXT constellation of 66 spacecraft [13].*

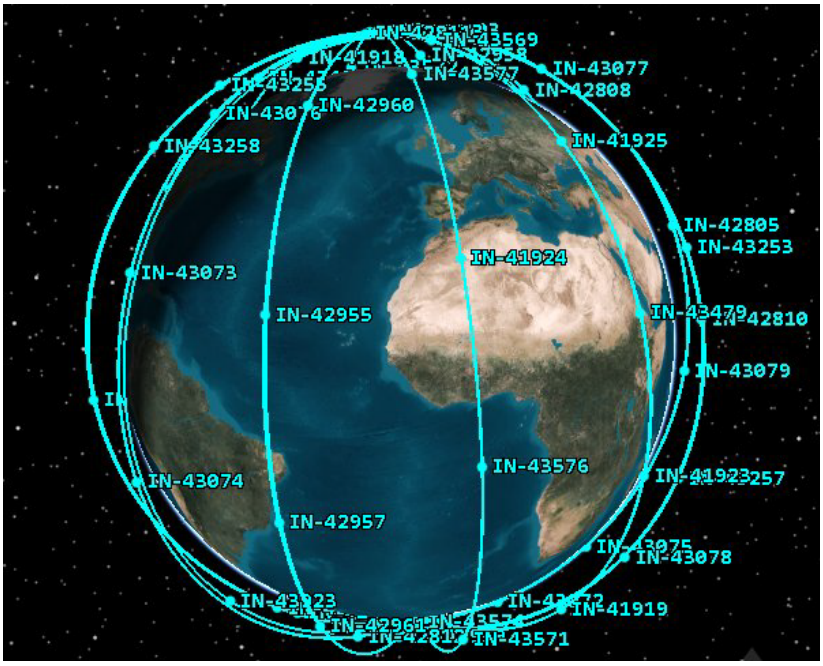

***Figure 53:** Iridium NEXT constellation of 66 spacecraft recreated in STK.*

4.2.2 Satellite constellation transmitters

Now that all the satellites are initialized and saved in a constellation, it is possible to add transmitters as objects associated with the spacecraft. Before introducing any transmitter, however, it is recommended to add a sensor to each satellite and then to associate the transmitter to the sensor itself. This process is followed because in this way the transmitter can be moved following the sensor pattern. According to the Iridium-NEXT datasheet, each satellite has a 75° half-angle nadir FOV [13]. For this reason in the STK simulation, each satellite is equipped with a "Simple Conic" sensor with a 75° cone half-angle and a fixed nadir pointing type (that is obtained setting a 0° azimuth angle and a 90° elevation angle). With this cone aperture, it is expected that each satellite has a wide coverage on Earth. That can be observed in the figure below.

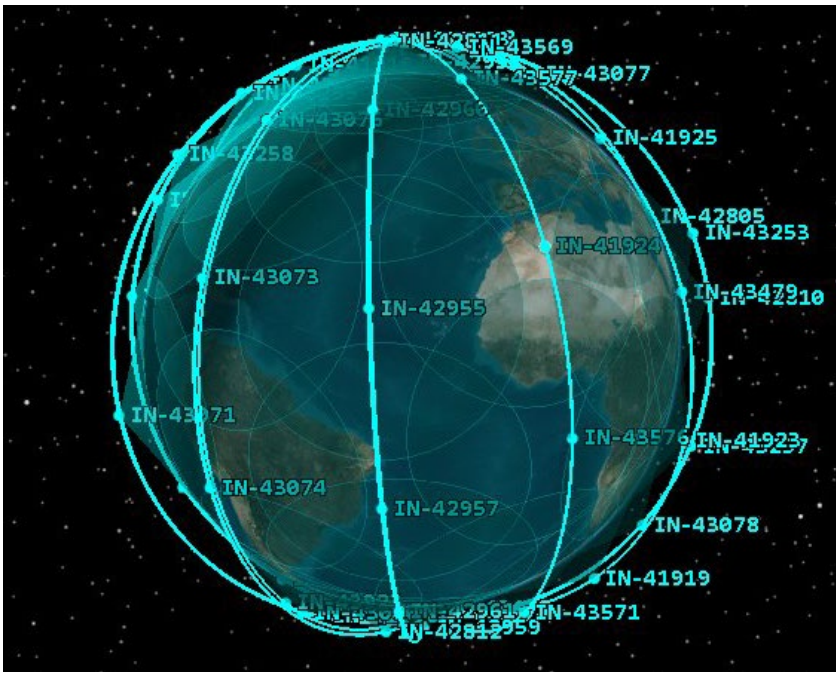

Figure 54: *Iridium NEXT field of view.*

The main element of the Iridium Next communication system is an L-Band phased array antenna positioned in the Earth-facing panel and generating 48 transmit beams for communication with user terminals [13]. The communication with the terminals is organized in a Time-Division Duplex (TDD) architecture which divides the downlink from the uplink exploiting different time slots in the same frequency band. This kind of antenna creates more than 5000 km of footprint area on Earth. It is possible to select in STK the phased array antenna model in the transmitter properties. In this section, it is possible to choose the beam configuration for the antenna. The "Designer" section of the antenna allows choosing the

number of elements and their disposition. The parameters set for the antenna are listed in the following table.

Type	Polygon
Number of sides	6
Lattice Structure	Rectangular
Number of elements along X	8
Number of elements along Y	8
Number of elements	48
Polarization	Right-hand circular

Table 4. 3:*Phased array antenna design parameters.*

This parameter setting allows to obtain a 48 Elements phased array antenna, that is in line with the Iridium NEXT L-band antenna properties mentioned before. Through the STK viewport, it is possible to have a look at the layout of the configured elements.

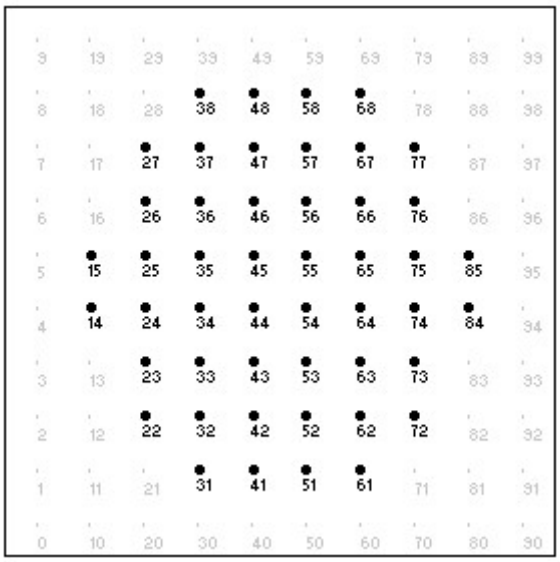

Table 4. 4*: Phased array antenna elements configuration.*

For L-band communications, a link between Iridium Next and a user typically operates at 64kbps. Moreover, the L-Band up and downlinks of this constellation operate from 1616MHz to 1626.5MHz using a QPSK modulation with an occupied bandwidth of 31.5kHz [14]. Each channel is spaced 41.667 kHz from the other and this is the minimum bandwidth needed for receivers to correctly receive the signals from one satellite of this constellation [15]- [16]. For the downlink as for the uplink, the polarization exploited from Iridium is the "Right Hand Circular"(RHC) [16]. Unfortunately, it isn't possible to find all the needed data on the Iridium Next datasheet but, consulting Iridium Next link budgets available online, some of the missing

parameters can be obtained [17]. For example, a typical value for the Iridium transmitter power is about 5dBW (which is used in this case study). The next table sums up all the parameters described up to now.

Frequency	1.6265 GHz
Power	5 dBW
Data Rate	0.050 Mb/sec
Modulation	QPSK
Signal Bandwidth	0.0315 MHz

Table 4. 5: *Iridium Next transmitter parameters.*

The last step is to add a filter to the transmitter that will allow adjusting the bandwidth of the signal. Iridium Next satellites are equipped with root-raised cosine filters with a 40% Roll-off factor and 25kbs symbol rate [18]- [19]. These parameters can be used to model the filter in STK after having enabled the power spectrum density (PSD) for each satellite.

Type	Root Raised Cosine
Upper Bandwidth Limit	0.01575 MHz
Lower Bandwidth Limit	-0.01575 MHz
Roll-off factor	40%
Symbol Rate	0.025 Mb/sec

Table 4. 6*: Iridium Next satellite transmitter filter parameters.*

The chart below allows us to visualize the spectrum magnitude of the unfiltered signal, the filtered signal spectrum, and the filter magnitude.

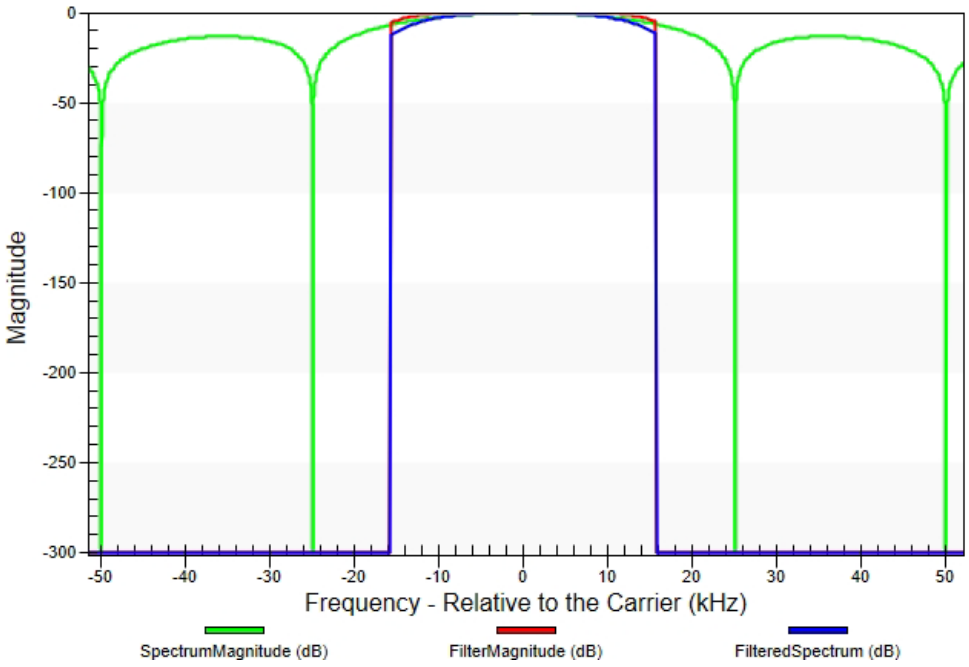

***Figure 55**: Filtered signal transmitted from a satellite of Iridium-Next constellation.*

4.2.3 Satellite constellation receivers

As for the transmitters, the Iridium Next receivers are equipped with a phased array antenna constituted by 48 elements. The antennas' physical characteristics can be considered the same used for the transmitter modeling. In the receiver modeling, it is possible to introduce new parameters related to the low noise amplifier (LNA) and the system temperature. The LNA has its own gain and losses related to the cable between the antenna and the amplifier, and between the amplifier and the receiver. It is possible to assume that each Iridium Next satellite is equipped with 2 meter long coaxial cables, with a loss of 0.08 dB/m. Thus making the antenna to LNA and the LNA to receiver line losses equal to 0.16dB. Another important value introduced in the receiver is the system noise temperature (T_s). The system noise temperature can be set as a constant entering the value directly or can be calculated by STK introducing other parameters (such as the LNA Noise figure, Antenna to LNA transmission line temperature, and the antenna noise). For lack of these precise values, it was decided to consider the T_s as a constant and to calculate this parameter using the method illustrated in the 4.3.1 section. The receiver system noise used to calculate the figure of merit of the LNA is taken from the following figure.

Noise Temperature	Frequency (GHz)					
	Downlink			Crosslink	Uplink	
	0.2	2–12	20	60	0.2–20	40
Antenna Noise (K)	150	25	100	20	290	290
Line Loss (dB)	0.5	0.5	0.5	0.5	0.5	0.5
Line Loss Noise (K)	35	35	35	35	35	35
Receiver Noise Figure (dB)	0.5	1.0	3.0	5.0	3.0	4.0
Receiver Noise (K)	36	75	289	627	289	438
System Noise (K)	221	135	424	682	614	763
System Noise (dB-K)	23.4	21.3	26.3	28.3	27.9	28.8

***Figure 56**: Typical system noise temperatures in satellite communication links in clear weather [20].*

For an uplink signal frequency between 0.2 and 20 GHz the expected receiver noise temperature is around 289K. So, according to the 4.2 formula, the LNA figure of merit is equal to F=1.996. The receiver frequency, in addition, is set on "auto track" that allows the receiver to track and lock onto the transmitter's carrier frequency with which it is currently linking. The same principle is valid for setting the auto-selection of the demodulator. The satellite receivers' main characteristics are resumed in the table below.

LNA gain	2 dB
Antenna to LNA line loss	0.12 dB
LNA to receiver line loss	0.12 dB
Polarization type	Right-hand circular
System Noise Temperature	600.7290 K (27.7868 dB)
Demodulator	QPSK
Antenna Type	Phased array

***Table 4. 7:** Satellite receiver parameters.*

The receiver is equipped with a Root-cosine filter with the same Roll-off factor and symbol rate as the transmitter. The bandwidth is slightly larger than the one used for the transmission. That is done to ensure the complete capture of the transmitted signals' bandwidth and to ensure a high bandwidth overlap.

Type	Root Raised Cosine
Upper Bandwidth Limit	0.0205 MHz
Lower Bandwidth Limit	-0.0205 MHz
Roll-off factor	40%
Symbol Rate	0.025 Mb/sec

***Table 4. 8:** Iridium Next satellite receiver filter parameters.*

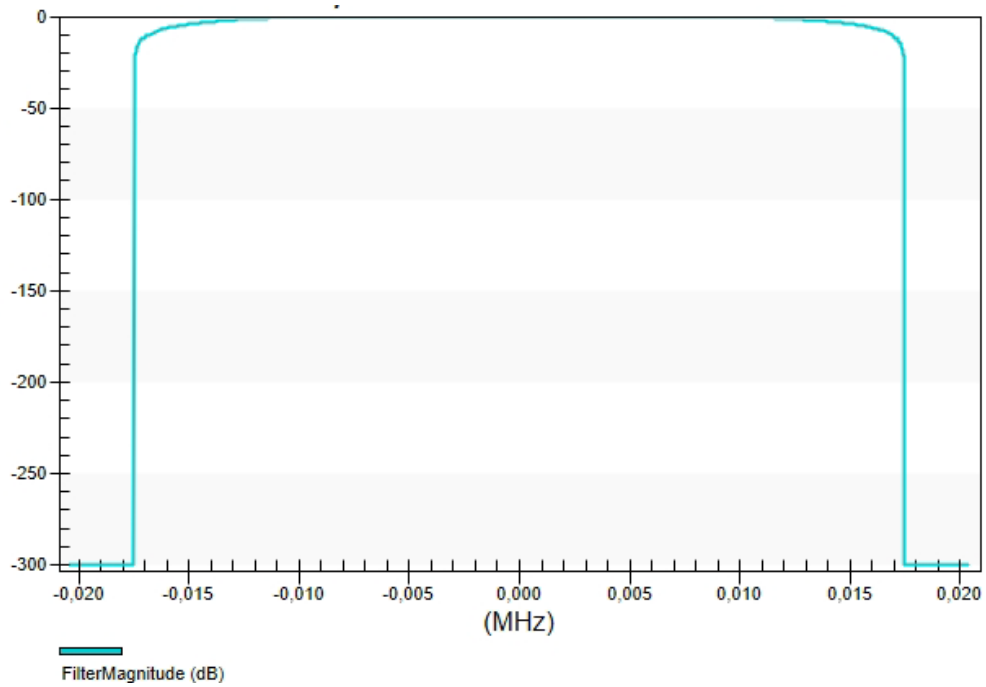

Figure 57: *Filter magnitude of the satellite receiver*

4.3 STK helicopter model

As for the satellite constellation, even, in this case, it is possible to exploit Matlab for the automatization of the STK scenario creation. The helicopter is introduced as a common aircraft and its trajectory path is read from a .txt file, by the STK "Great Arc" propagator. This propagator defines the route of an aircraft combining the waypoints (that are expressed in terms of latitude and longitude), altitude, speed, and turn radius. This last parameter represents the radius of the circle that describes the turn of the vehicle. Moreover, it is possible to reference the aircraft altitude from mean sea level, terrain data, or WGS84 (i.e the central body's reference ellipsoid). In this analysis, the altitude of the helicopter references the mean sea level. As the first iteration of this study, it is assumed a route divided into a climb, cruise, and descent for a total of 70 min of flight. During this trajectory, it will be fundamental for the analysis to collect data about azimuth, and elevation angles of the signal that will be used for the implementation of the rotor blade blockage. Moreover, this trajectory can be modified in future iterations to optimize the communication links with the satellite constellation. The parameters used to set the helicopter route are listed in the next table:

Latitude [deg]	Longitude [deg]	Altitude [km]	Speed [km/sec]	Trurn Radius [km]
40.98737	17.2429	0.05	0.01389	0
4.99179	17.23986	0.25	0.01389	1
40.99789	17.23568	0.5	0.01389	0
41.27283	16.97389	0.750	0.0306	1
41.45585	16.50866	0.65	0.04	0
41.72205	16.05261	0.5	0.045	1

Table 4. 9: *Helicopter route parameters.*

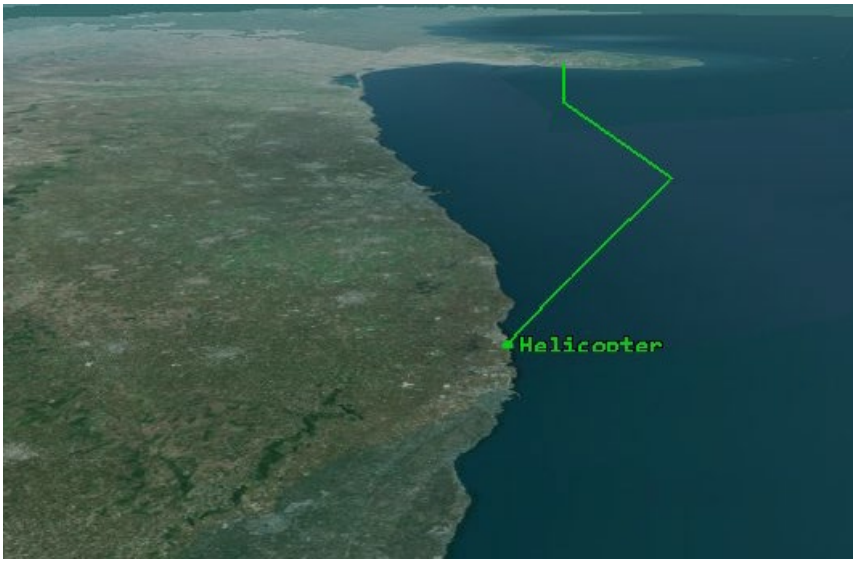

Figure 58: *Helicopter route visualization.*

4.3.1 STK helicopter receiver model

Since one of the aims of this part of the study is to integrate the Matlab modeled blade disturbance in STK, it is not possible to use an STK default receiver type as the starting point to model the same receiver used for the previous analysis. The solution, as mentioned before, is to exploit the opportunity to select the "Script Plugin receiver model" type and customize its properties directly in Matlab. The plugin script works as a Matlab function and, every time step of the simulation is polled by STK to obtain the output values useful for the calculations. The receiver model, moreover, can receive input from the STK simulation. In particular, it is possible to receive from STK the simulation time, the azimuth, and the elevation angles measured from the antenna boresight in the antenna coordinate system (they represent the direction of the communication link).

To properly calculate the blockage duration and the instant in which the phenomenon occurs, it is necessary to check, instant by instant, the simulation time. Unfortunately, it is not possible to save the simulation time variable in the plugin script while the simulation is running. To

overcome this problem it was decided to run two analyses. The first analysis is run with a very small step time (about 0.001s) to collect very precise data about the simulation time instants, the range of the signal, and the related attitude angles. The rotor blade blockage algorithm is applied by reading the acquired data and calculating the instant in which the disturbance starts and its duration according to the formulas discussed before. In the end, all the data are stored in a matrix whose last column (dedicated to the losses) contains a 0 when the disturbance doesn't happen, and the value of the loss when there's the attenuation (for an L-band signal the blockage loss is about 10dB).

The second analysis is run to obtain results about the communication links. The matrix containing the time, the attitude angles, and the attenuations is saved in a .txt file. In addition, using the same time interval of the previous analysis would be excessive for a link budget analysis in a mission scenario context. So, the step time is increased to 0.07s and the matrix loses all the lines that don't correspond to a step time multiple. That would make the analysis faster and allow us to observe the attenuation phenomenon on a larger time scale. While the simulation is running the .txt file containing the attenuation matrix is read by the plugin scripts that check the loss value in the current time instant. The value of the loss (that can be 0dB or 10dB in this case) is stored in the "Pre Receive Loss" output variable and then sent to STK.

The other output parameters are set to be compliant with the helicopter communication system modeled in the first part of this study. The plugin script doesn't allow to choose an antenna model but it's possible to set its gain. The antenna gain is calculated using the 3.2 formula for the expected received signal frequency. The table below contains the parameter used to model the "Script Plugin, receiver model".

Frequency	1.6265 GHz
Bandwidth	41.667 KHz
Antenna Type	Parabolic
Antenna Diameter	0.3 m
Antena efficiency	55%
Antenna Gain	11.577 dB
Pre-receive loss	0/10dB
Polarization type	Right-hand circular
System Noise Temperature	115.7 K (20.6348 dB)
Receiver Noise Figure	1 dB
Demodulator	QPSK

Table 4. 10: *Script plugin receiver model parameters*

The system noise temperature depends on three parameters: the antenna noise T_a (i.e the interference given by other noise sources around the receiver), the line losses between the antenna and the low noise amplifier L_r (which are proportional to cable length and cable

type), and the figure of merit of the amplifier F (which is an indicator of the performance of a device). The formula used to calculate the system noise temperature is:

$$T_s = T_{ant} + \left(\frac{T_0(1 - L_r)}{L_r}\right) + \left(\frac{T_0(F - 1)}{L_r}\right)$$

(4. 1)

where T_0 is the reference temperature equal to 290 K. The antenna noise can be assumed from specific tables and diagrams. In particular, since the helicopter in this mission scenario is in a low altitude operation, it is possible to consult the ground station antenna noise diagram for the worse propagation case (5° elevation angle) [21].

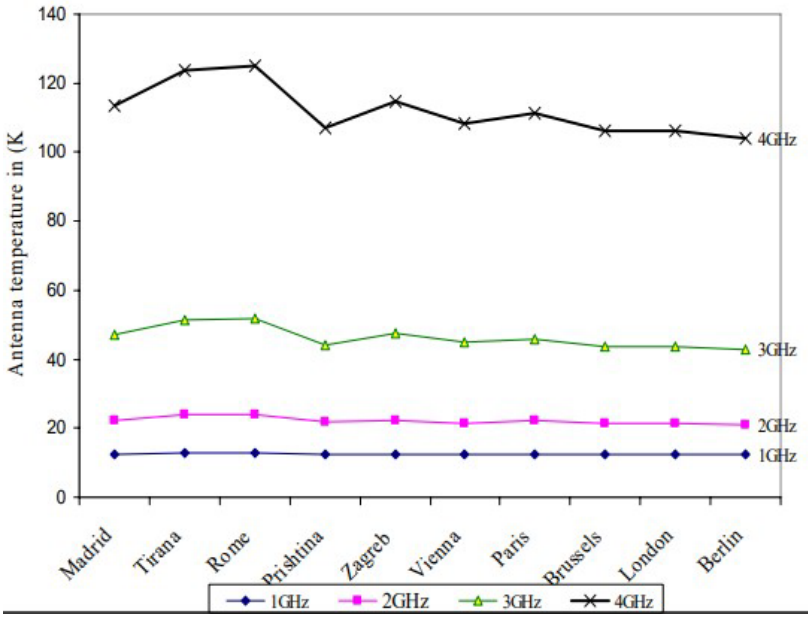

Figure 59: *Antenna temperature in the worse propagation case [21].*

Consulting the antenna noise diagram, for this study, it is set a 15K antenna temperature. The line losses are calculated, considering the loss/m attributed to the cable and the cable length. Assuming to have a 4m long coaxial cable with a 0.06 dB/m loss, L_r is equal to 0.24 dB. For these preliminary calculations, it is possible to assume that the receiver noise temperature T_r is around 75 K. That makes it possible to calculate the figure of merit of the helicopter receiver, using the following formula:

$$F = 1 + \frac{T_r}{T_0}$$

(4. 2)

Using the listed formulas, it is possible to obtain the system noise temperature value reported in Table 4.7 which is equivalent to a 20.63 dB loss.

Even in this case, the helicopter sensor is assigned to a sensor that is targeted to the Satellite constellation. This allows computing the link budgets and a visualization of the link direction during the simulation.

Figure 60: *STK helicopter visualization.*

4.3.2 STK helicopter transmitter model

As for the receiver, in this case, it is possible to set a "Script Plugin transmitter model" for the helicopter. This allows introducing the signal blockage loss as "post transmit loss" output. The transmitter is modeled trying to be compliant with the parameters already used in the Simulink analysis. The helicopter antenna is assumed to have a parabolic reflector and a diameter of 0.3m. It is also assumed that the helicopter transmits a signal at a quite lower frequency than the one transmitted by the satellite ($f = 1.616\, GH_z$) to test the lower frequency limit for the Iridium Next constellation. The output carrier power is set to 16W according to the previous simulations. The data rate and the signal bandwidth are set according to the Iridium Next properties mentioned in 4.2.3. The modulation chosen for the transmitter is the QPSK and the polarization is an RHC. The link budget analysis follows the same procedure described in the previous paragraph. All the transmitter parameters are resumed in the next table.

Frequency	1.616 GHz
Power	10 dB
Antena Type	Parabolic
Antenna Diameter	0.3 m
Antenna Efficiency	55%
Gain	11.5315 dB
Post transmit loss	0/10 dB
Data rate	0.035 Mb/sec
Signal Bandwidth	0.0315 MHz
Modulation	QPSK
Polarization Type	RHC

Table 4. 11: *Helicopter transmitter parameters.*

4.4 Coverage and access analysis

Before proceeding with the link budget analysis, it can be useful to analyze the coverage of the mission area guaranteed by the constellation in terms of the revisit time of the satellites and the access between the helicopter and the Iridium-Next units.

For the first step, it is necessary to introduce an area target that is as near as possible to the helicopter's trajectory. In this case, even if the vehicle flies over the sea for most of the mission time, the nearest geographic area target is Italy. The coverage is guaranteed when one of the Iridium-Next FOV cones contains the area target. At this point, it is possible to insert a Coverage Definition and assign to it the area of interest as a custom region. This allows STK to create a grid on the target area to properly determine the coverage. The grid can be made denser modifying the point granularity in terms of area. For this specific case, it is set a 5000 km^2 area that allows obtaining the following grid for the selected geographic area.

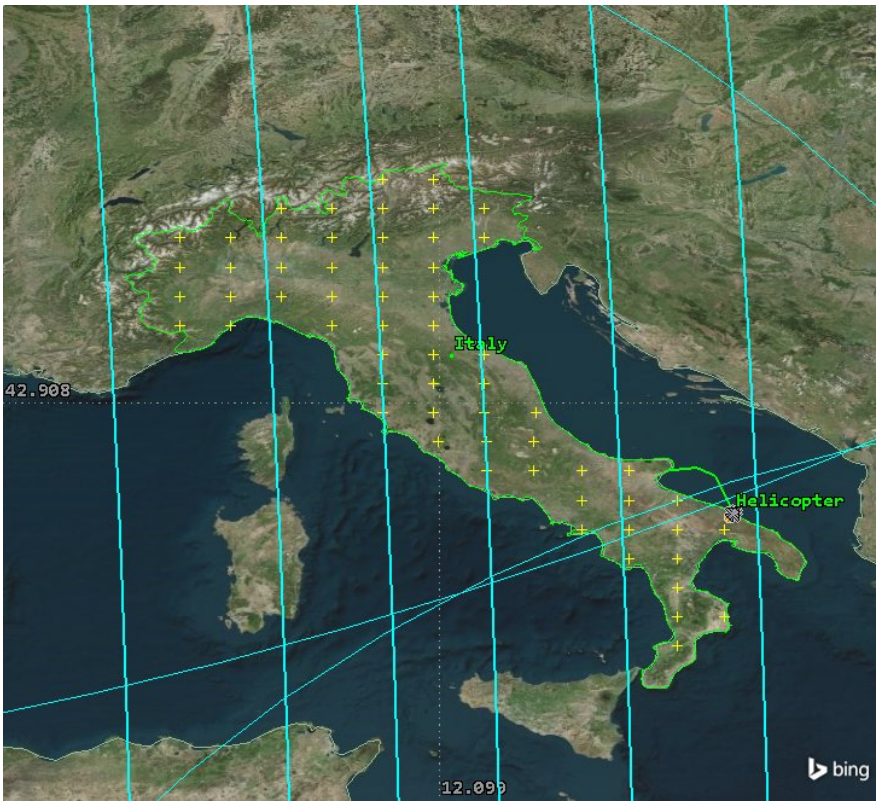

***Figure 61**: Coverage grid for the selected target area.*

Choosing a smaller area for the point granularity would make the grid denser, increasing the time required for the calculations. Since the satellite FOV cone angle can cover big geographic areas, it is not necessary to use denser grids. At this point, it is necessary to assign the constellation satellite as objects included in the coverage definition.

The next step is to insert a “Figure of Merit” that allows specifying the method by which the quality of coverage is measured. This analysis is focused on the maximum revisit time of each satellite of the constellation, to verify if the target area is always covered for communications. Then it is necessary to enable the satisfaction and impose that the figure of merit is satisfied when the maximum revisit time is greater than 0 s (that allows to visualize all the revisit times). In the figure below, it is possible to observe that for the entire duration of the mission (70 min) the target area is always covered by a satellite.

Figure 62: *Iridium-Next maximum revisit time.*

The maximum revisit time is calculated for 70 minutes with a step time of 10 minutes. According to the legend, the maximum revisit time is around 0 seconds. This guarantees that the chosen geographic area is always covered. It is also possible to study the revisit time of a single satellite above the same area. For the coverage study, it is set the first satellite that has access to the target area when the mission starts: IN-41925. Measuring the maximum revisit time for this satellite in 180 minutes with a time step of 10 minutes, according to the legend, it is possible to notice that the interval between two consecutive passages is between 80 and 90 minutes. Inspecting the coverage grid, directly from STK it is possible to verify that the maximum Revisit time, in 180 minutes, is equal to 86 minutes.

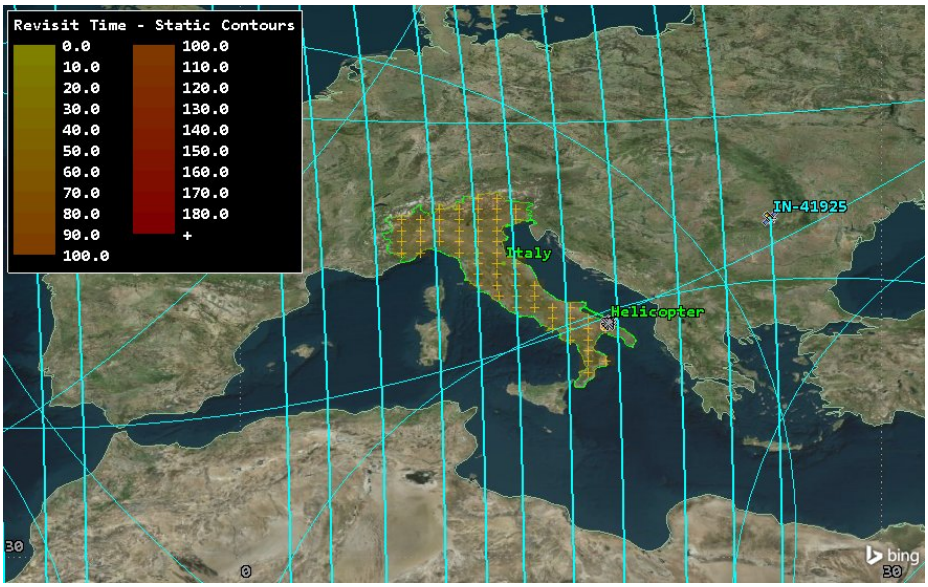

Figure 63: *Maximum revisit time for a single satellite in 180 minutes.*

It would be interesting to extend the maximum revisit time analysis for a larger period, to calculate how much time the same satellite of the previous analysis needs to come back over the same target area. The analysis is extended for 48h with a time step of 60 minutes and allows us to know that the maximum Revisit time measured for IN-41925 is about 564 minutes (9.4 h) according to the coverage grid. It is possible to notice that, in the figure below, the Revisit time legend reaches up to 1440 minutes (24 h). The legend was reduced to make it more readable but it has been verified that the maximum revisit time is the same for a 48 h long mission scenario.

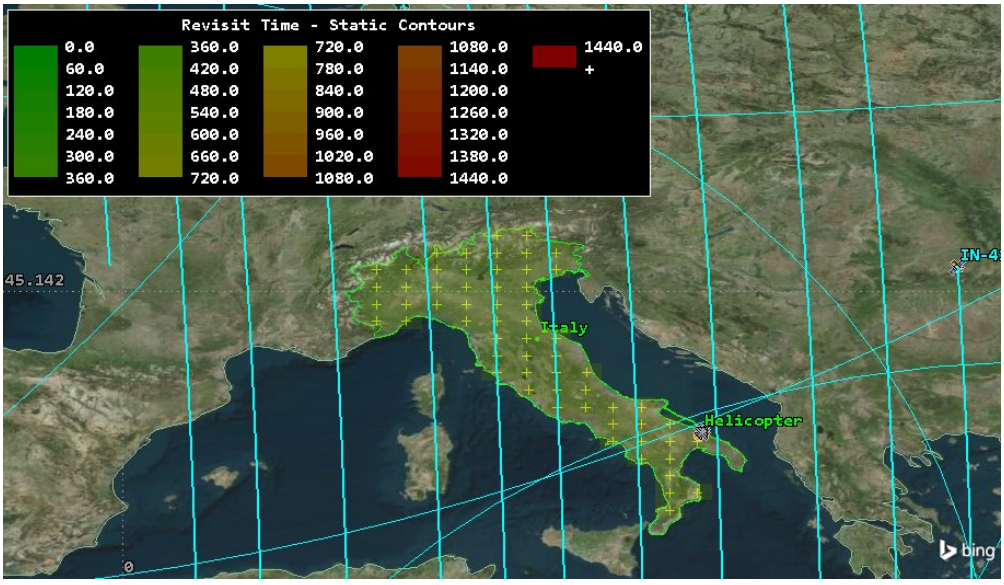

Figure 64: Maximum revisit time for a single satellite in 48h.

At this point, it is possible to run an access analysis. This STK tool allows verifying, for the entire duration of the mission, when it is possible to create a communication link between the vehicle and the constellation and for how long each link is available. In a mission scenario in which the vehicle is remotely piloted exploiting its SATCOM channel, it is important to guarantee a constant connection with the constellation. For this reason, before evaluating the quality of the signal, it is important to verify if there will be any lack of signal during the mission.

The chart below is obtained by calculating the access between the helicopter receiver and every satellite of the constellation. It shows every access available and its duration. The legend below the chart identifies the satellite involved in the access through different colors. The access is available when the signal elevation angle ranges from 10° to 90°. When the elevation angle required goes below 10°, the access ends. It is possible to observe that in several instants during the mission multiple accesses are available. This is caused by the wide field of views of the satellites that overlap in several regions. In this case, the signal with the higher quality will be exploited.

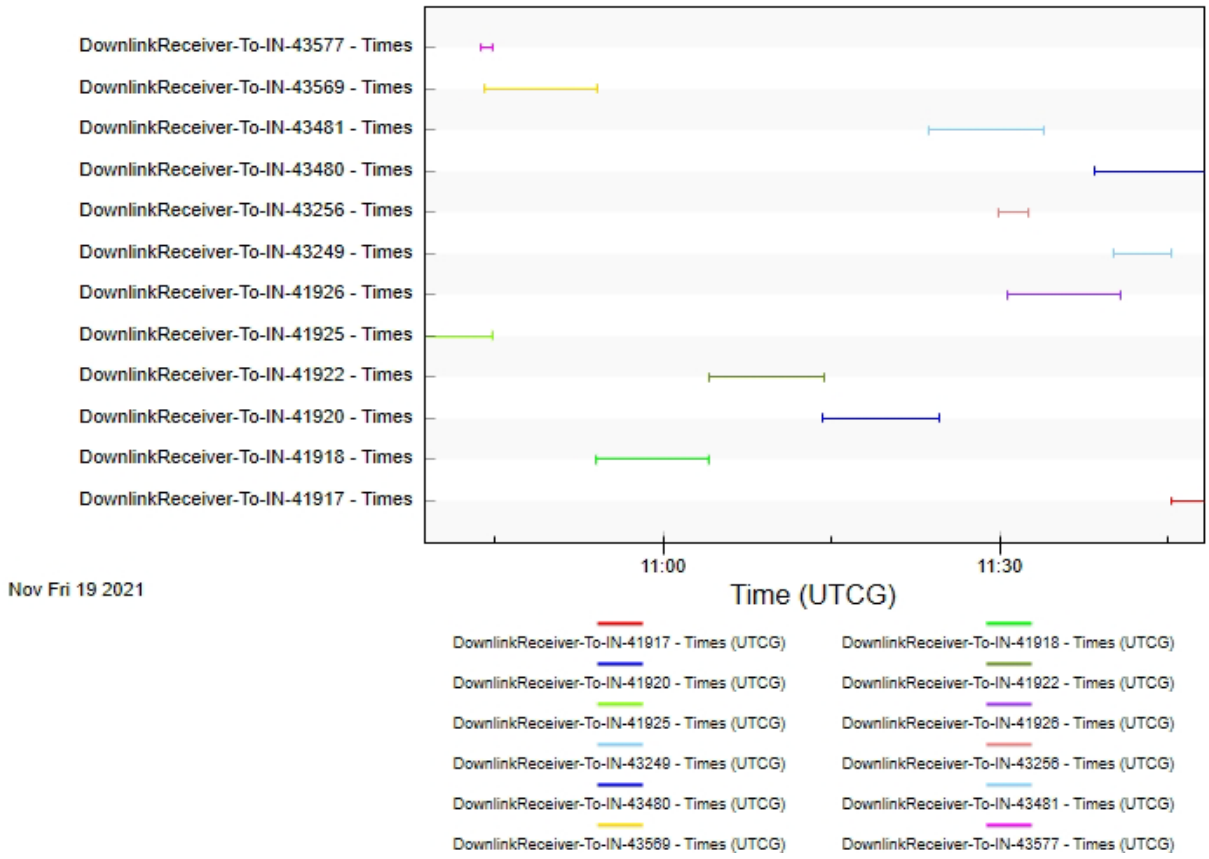

Figure 65: *Access analysis for the first trajectory.*

To verify, in detail, when the access is guaranteed, it is possible to visualize a revisit diagram. Thanks to this diagram, it is possible to be sure that access is always guaranteed with the constellation. But even if the link is always ensured, it would be necessary to evaluate its quality even in critical situations, such as the handover between one satellite and another. From the previous chart, it is possible to observe that in several points during the mission the handover happens in time instants in which it is not possible to obtain multiple access. That means that if the helicopter slightly varies its speed or its trajectory, could lose communication with the constellation for some period of time. That could be a problem if the vehicle is remotely controlled. To overcome this criticality it could be interesting to study a new trajectory path or elaborate new mission plans to optimize the communication handovers.

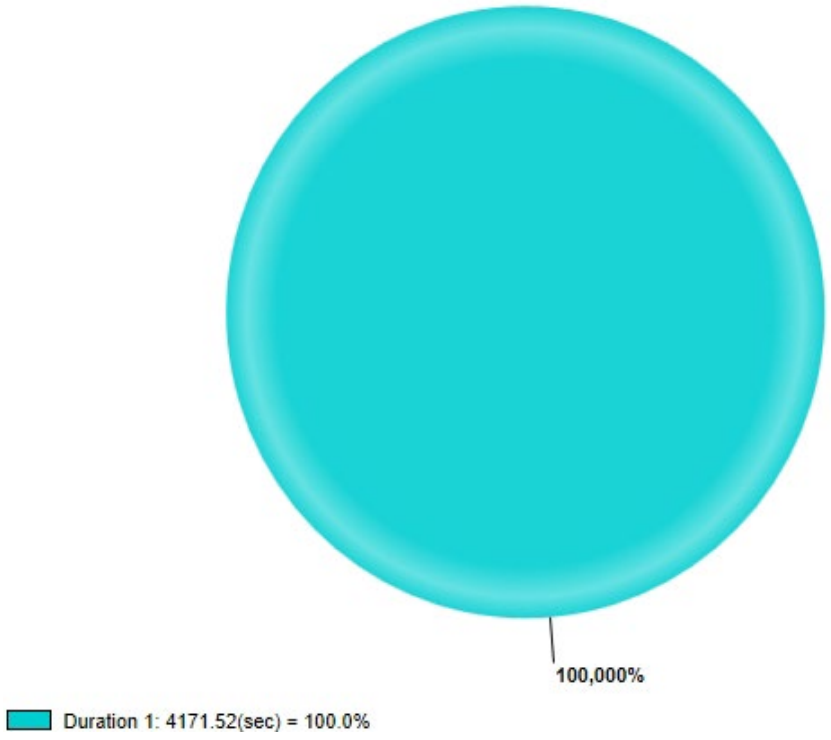

***Figure 66**: Revisit time diagram considering the accesses between Iridium-Next and the helicopter.*

4.5 Link budget analysis

After having verified the coverage offered by the chosen constellation and having determined the available access during the mission time, it is now necessary to evaluate the quality of the exchanged signals through a link budget analysis. STK allows to compute and extract several parameters that represent the signal characteristics, such as the effective isotropic radiated power (EIRP), the received gain over the equivalent noise temperature (g/T), the Carrier-to-Noise density at the receiver input (C/N_0) and so on. But this analysis will focus on the energy per bit at the receiver (E_b/N_0) that depends on the previously listed parameters and can be considered as the performance parameter of the entire communication architecture. This performance parameter is defined by the following formula:

$$\frac{Eb}{N_0} = EIRP + L_{tls} + \frac{g}{T} - 10\log_{10}(k_B) - 10\log_{10}(R) \quad (4.\ 3)$$

where k_B represents the Boltzmann constant (1.38·10-23), R is the datarate and Ltls includes all the attenuation that the signal undergoes between the transmitter and the receiver (atmospheric, pointing, path loss…). The datarate is a fundamental parameter in the evaluation of the link budget. It indicates the speed of the transmission of a data stream. To transmit a higher datarate, it is necessary to increase the energy of the signal, represented by the E_b/N_0.

To evaluate how good the modeled system is for the transmission of a signal, it is necessary to compare the computed E_B/N_0 (or system E_B/N_0) with a "required" E_B/N_0, that represents the energy required to send a bit for a chosen modulation, coding, and bit error rate (BER). The BER indicates the probability that in a stream of a certain number of bits, there is one that is wrong. A small bit error rate indicates a high precision and better accuracy of the signal but, of course, requires a higher energy per bit. The figure below allows visualizing how the probability of BER varies according to the required Eb/N_0 and different modulations. By consulting the chart, it is possible to say that to have a BER probability of 10^{-8} for the chosen QPSK modulation, it is required an $\frac{E_b}{N_0} = 12\ dB$.

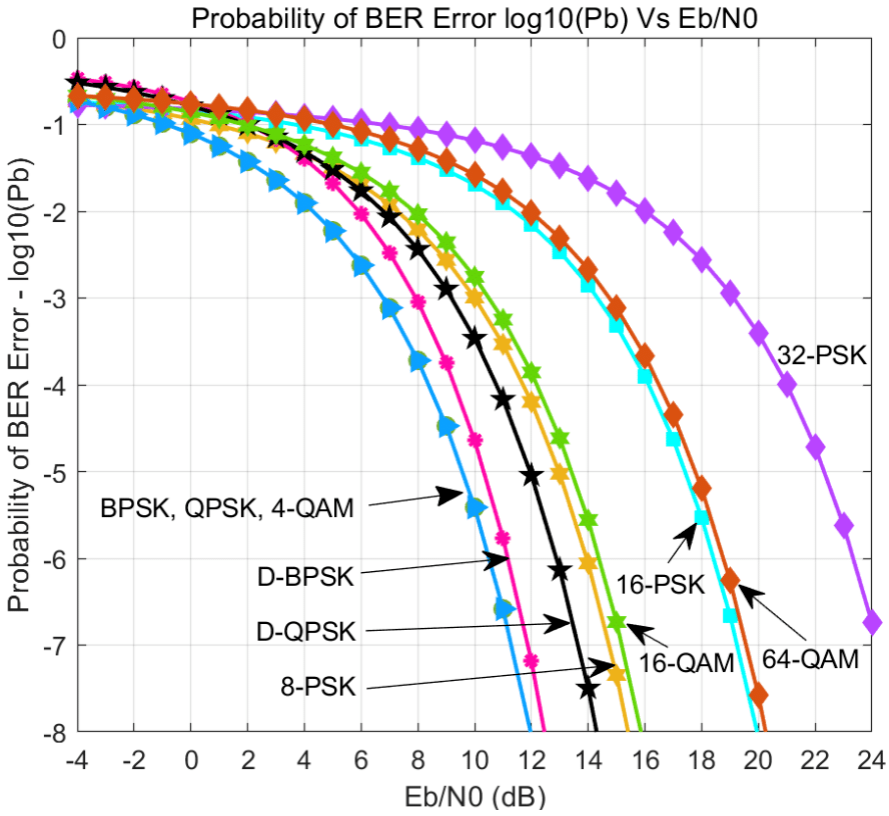

Figure 67: *BER as a function of modulation and required Signal-to-Noise ratio [22].*

The difference between the system and the required E_b/N_0 is called Link Margin (LM) and represents the effective capability of the communication system. If the LM<0, it means that it's not possible to create a link between the transmitter and the receiver. If the LM>0, the link is available but the best thing to do is to consider a further margin (that is often about 5 dB) that allows taking into account eventual underestimation of signal losses. So, if the LM>5dB, the link can be considered closed and the communication is guaranteed but if the 0dB<LM<5dB the link is "marginal".

When the analysis ends, all the parameters are sent to Matlab and stored in a structure to make it possible to visualize the link budget for each Satellite that has access to the helicopter. These parameters can be, subsequently, plotted to visualize their variation for all the mission time.

4.5.1 Downlink analysis

This analysis is automatically run from Matlab and consists of the evaluation of the quality of the signal captured by the helicopter receiver antenna. The first simulation doesn't include the algorithm for the blade blockage losses and allows visualizing the power of the received signal and if the link is closed. Moreover, this first analysis allows to verify if all the losses, previously discussed, are successfully integrated into the analysis. In particular, the chart below shows the trend of the atmospheric absorption with the variation of the mission time. The reason for this variation of the absorption value is connected with the variation, in time, of the signal elevation angle. It is possible to observe as the attenuation tends to decrease as the elevation angle increases. The lower value of the absorption is registered when the elevation angle reaches its peak, that is when the satellite is directly above the helicopter.

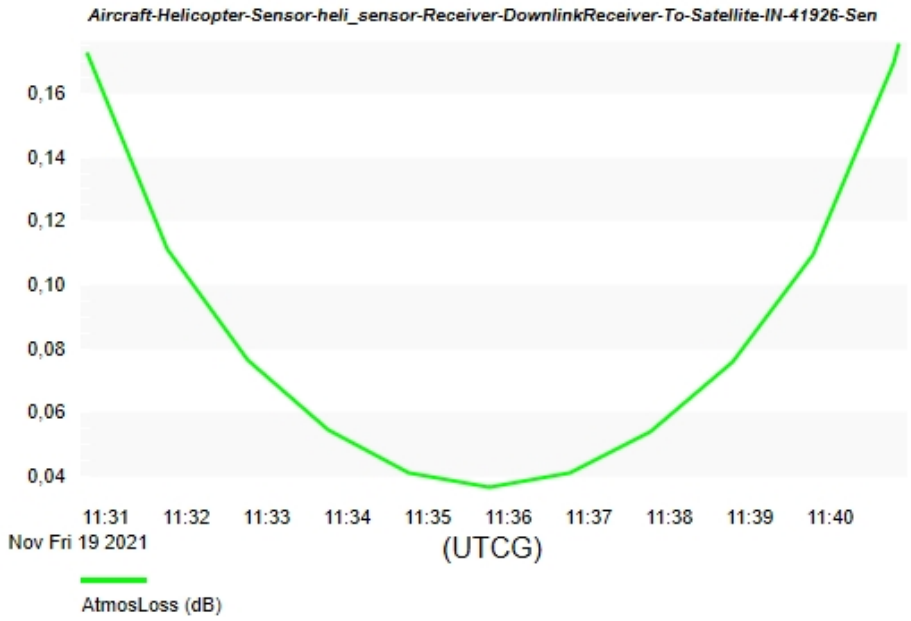

Figure 68: *Absorption loss [dB] trend in time in the access with IN-41926.*

The time interval coincides with the instant in which access to this specific satellite is available.

Verified that the propagation losses are correctly integrated into the analysis, it's now possible to proceed with the link budget analysis.

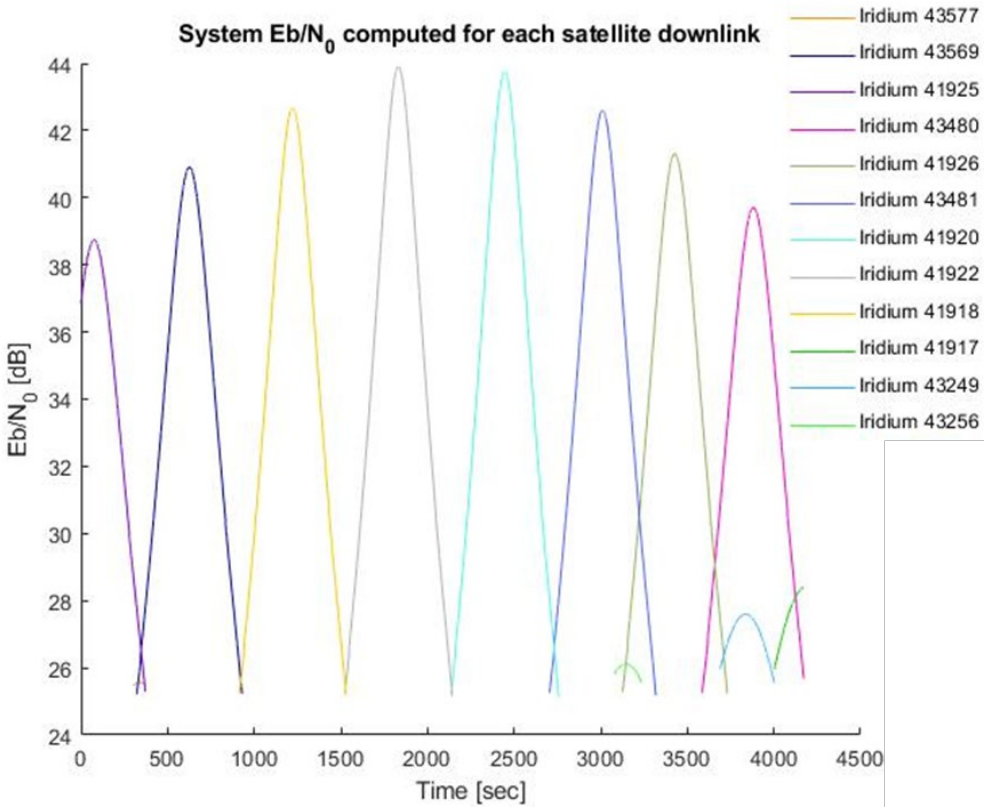

Figure 69: *Downlink system E_b/N_0 time variation for each access.*

As mentioned before, the link is interrupted when the elevation angle required becomes lower than 10°. From the chart above, it is possible to observe that the energy of the signal tends to be low when the link is just established or is going to interrupt. That is strictly related to the lower elevation angles that the signal has in these situations. For smaller elevation angles, the losses due to the propagation tend to be higher. The E_b/N_0 reaches its peak for every access, when the involved satellite is in its nearest position to the vehicle (in this case the elevation angle is equal to or about 90°). It's also interesting to observe that when multiple accesses are available it is possible to exploit a signal with a lower energy per bit for a smaller amount of time. To better explain this phenomenon it is necessary to imagine that all the E_b/N_0 trends with the higher peaks are related to links established with satellites sharing the same orbital plane that, for convenience, can be named "principal satellites". All the links with $25dB < \frac{E_b}{N_0} < 28dB$ are established with satellites in different orbital planes ("secondary satellites") in which FOV cone intercepts the helicopter. Since these signals can guarantee a good Signal-to-Noise per bit ratio at the same point, it could be possible to modify the trajectory of the vehicle to ensure a "backup" link while there's a handover between two principal satellites. A perfect example can be found at the end of the mission. Here, even if the helicopter can maintain a link with the principal satellite IN-43480, a link with the secondary satellite IN-41917 is available moreover allowing a better link margin. Assuming to extend the mission duration, that secondary link available would be useful to improve a handover. The figure below shows

the described situation. As can be noticed, the FOV cone colors have been adapted to the legend used in figure 69.

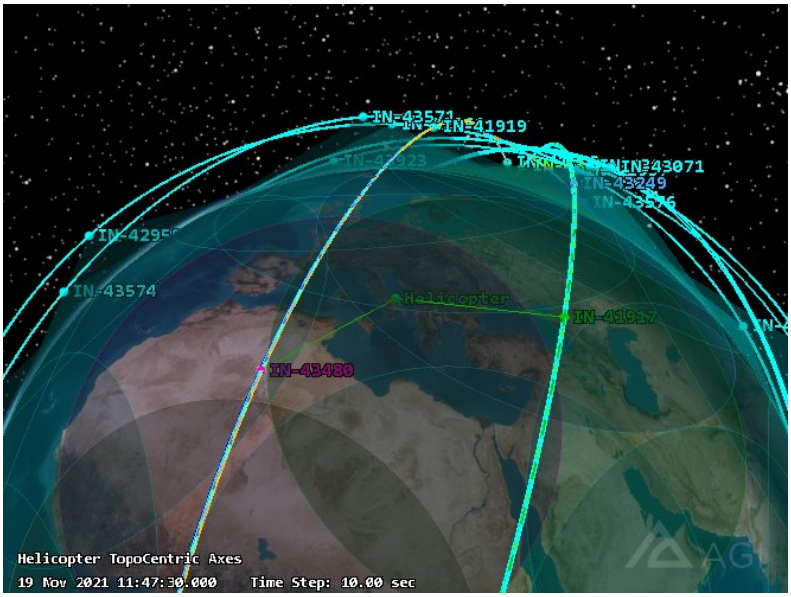

Figure 70: *Multiple access available in the last part of the mission.*

To try to explain why there is a higher E_b/N_0 for IN-41917 it would be useful to consult the azimuth, elevation, range (AER) charts.

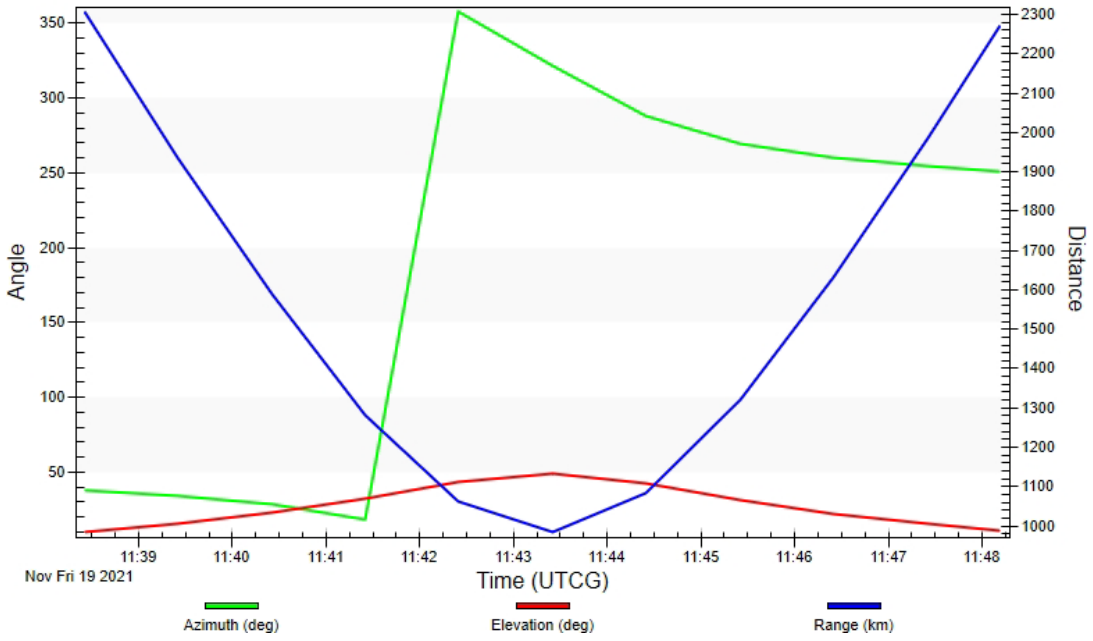

Figure 71: *AER chart for the link between the helicopter and the IN-43480 satellite.*

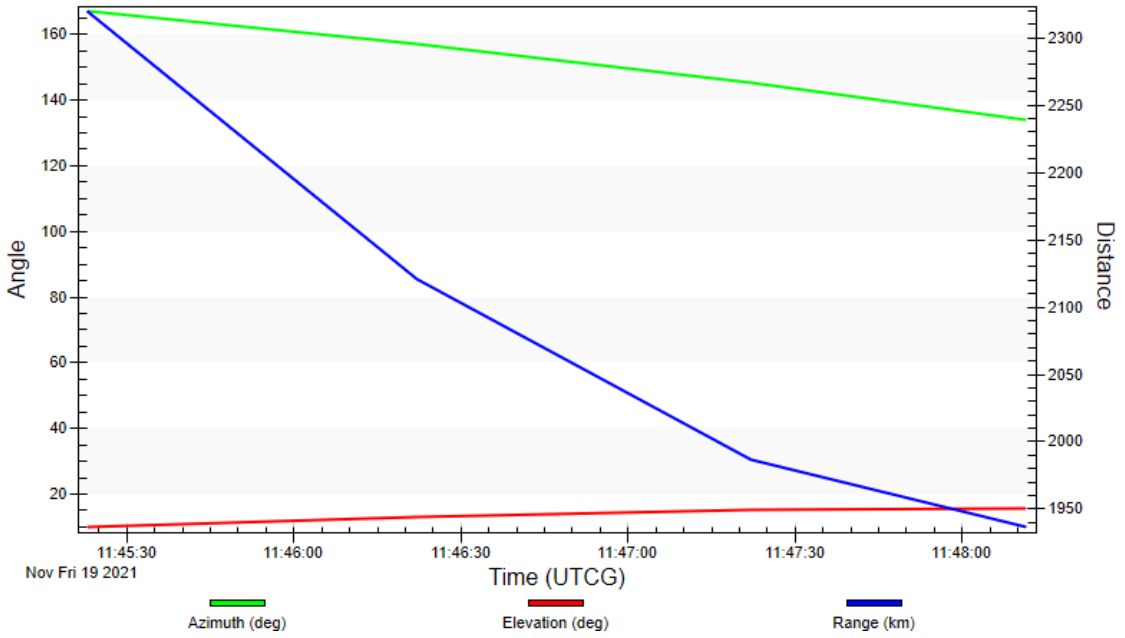

72: AER chart for the link between the helicopter and the IN-41917 satellite.

Since the access with IN-41917 starts, the range value of this link tends to decrease, differently from the range of the link between IN-43480 and the vehicle. The direct consequence of this trend is that the path loss for the first link mentioned tends to become smaller, guaranteeing a better signal quality. The AER data, moreover, will be fundamental for introducing the rotor blade losses in the next part of these analyses.

Now that the system E_b/N_0 for each satellite link are collected, it is possible to obtain the corresponding Link Margin chart by subtracting from the energy per bit the required $\frac{E_b}{N_0} = 12\ dB$. It is possible to observe that the link margin is widely above the safety margin line and that is a sign of the good quality of the communications during the helicopter mission. These results can be a starting point for the improvement of the satellite channel in future iterations.

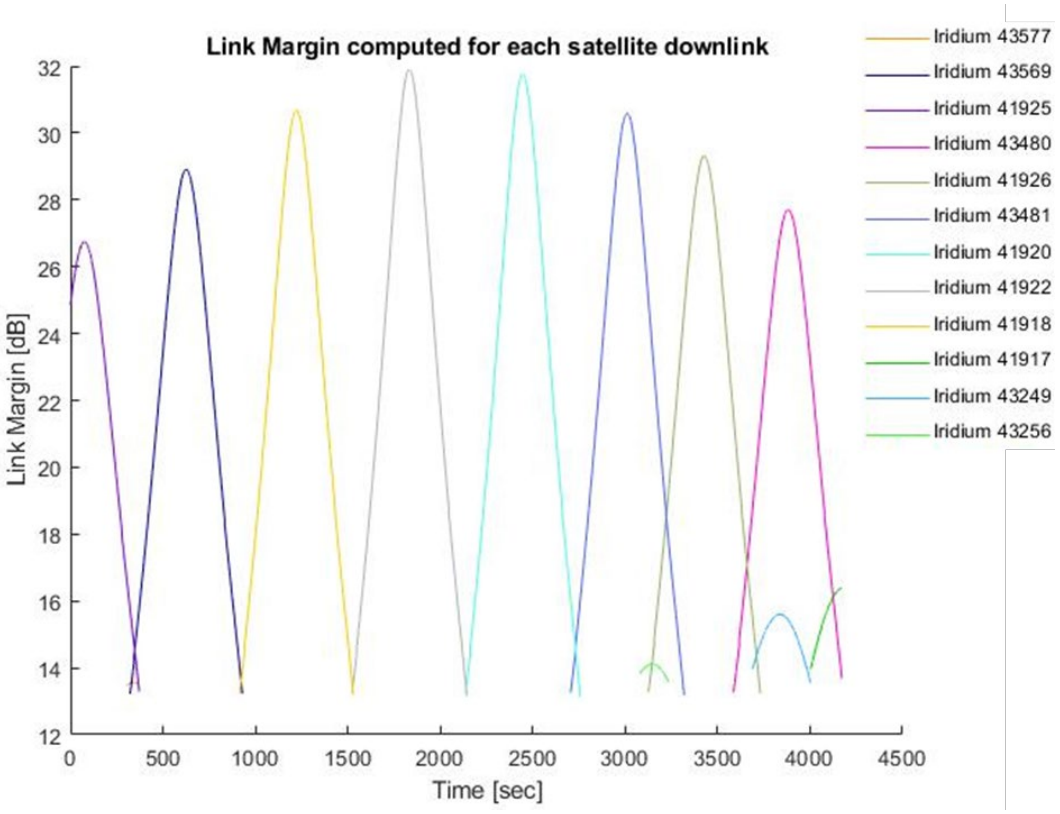

***Figure 73**: Downlink link margin computed for each access considering the E_b/N_0 required equal to 12dB.*

4.5.2 Downlink analysis introducing rotor blades disturbances

As mentioned before, the first run simulation is useful for collecting data on the signal unfazed by the blade rotation and on its orientation in terms of azimuth, elevation, range, and time of the simulation. While these data are transferred from STK to Matlab, the rotor blockage algorithm computes the blockage duration for each instant of the mission. All the AER and time data are saved in a matrix in which the last column contains a 0 dB when the blade is not passing over the signal, and -10 dB when the attenuation is afflicting the link. Then the "Loss Matrix" is saved in a .txt file that can be read from the script plugin while the next analysis is running. The script plugin will check, between the "Loss Matrix" rows, the range value equal to the one that the simulation is measuring at a certain instant and, then, will take the loss value from the column corresponding to that row. That will allow the introduction of a time variable loss in the link budget computation that can be a good representation of the periodic signal disturbance produced by the helicopter blades.

To have a general vision of how all the communication links will be affected by this phenomenon, it is possible to simulate with a high step time (1 second). This step time is chosen to lighten the simulation, reducing the amount of data that has to be collected, and allowing to see the periodical attenuations (white stripes) on a large scale. The figure below shows the results obtained for every link.

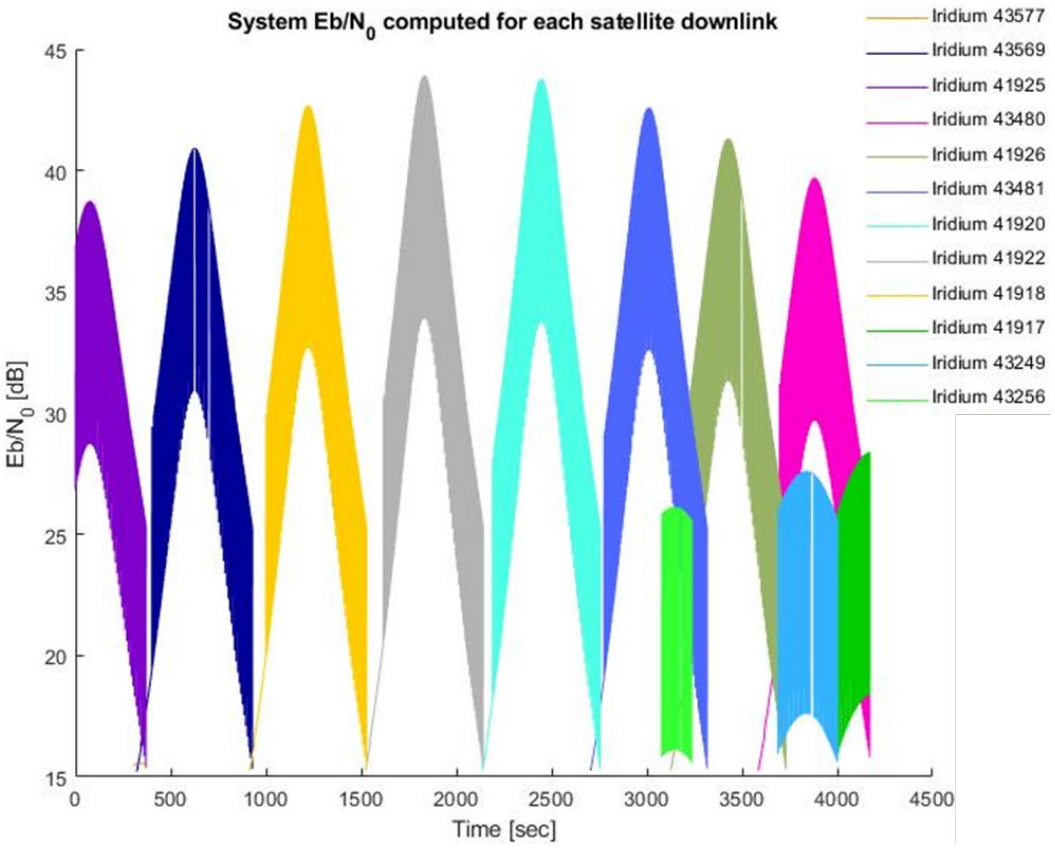

Figure 74: *Downlink E_b/N_0 for each access periodically reduced by blade rotation.*

To better visualize the attenuation phenomenon and to verify that the attenuation algorithm is correctly applied to the signal, it could be useful to run another analysis, with a smaller step time (0.07s), focused on a single signal. Then the signal trend will be compared with the elevation and azimuth angles expecting to have a shorter signal attenuation for high elevation angles (and short ranges) and a more persistent disturbance when the link has just been established or is going to end. The figure below shows how the helicopter-IN-41922 E_b/N_0 looks on a 0.07s step time scale.

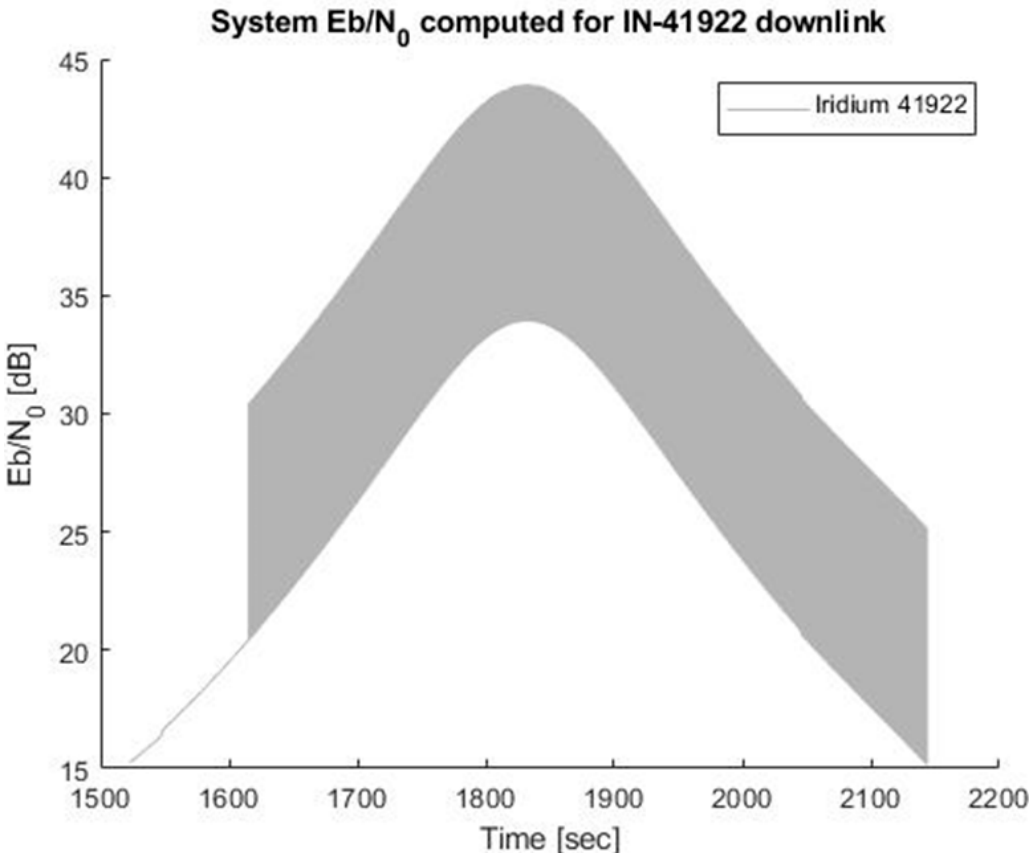

***Figure 75**: Downlink E_b/N_0 for IN-41922 link with blade attenuation.*

This temporal scale doesn't allow us to visualize the periodic attenuation produced by the blade rotation. However, at the start of the link connection, it is possible to observe that the energy per bit of the signal is always reduced. This, probably, depends on the fact that, as mentioned in the second chapter of this study, for very small elevation and azimuth angles, the blockage ratio (γ) could be equal to 1, meaning that the signal power is constantly reduced. To verify if this assumption is correct, it is necessary to consult the AER chart corresponding to this link and analyze the signal in specific time intervals of interest.

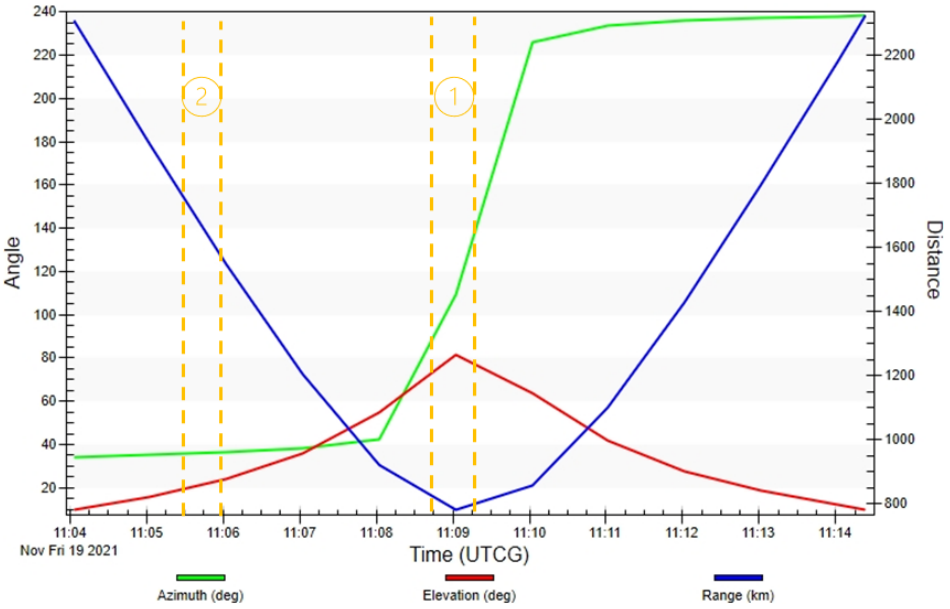

Figure 76: *Azimuth, elevation, and range variation for the link with IN-41922.*

The two highlighted time intervals are chosen because they represent two situations in which the blockage phenomenon has a different impact on the signal and its link budget. In particular, the first time interval refers to a phase of the mission in which the satellite is above the helicopter and the signal, consequently, is characterized by a high elevation angle and a rapidly changing azimuth angle. For these reasons, it is expected that the attenuations produced by the blades have a shorter duration letting the signal with a higher E_b/N_0 for longer periods.

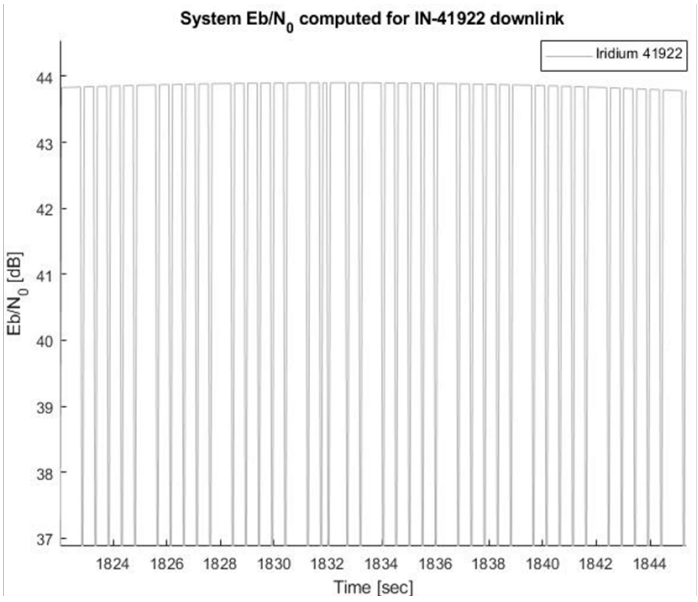

Figure 77: *Downlink E_b/N_0 for IN-41922 with blade attenuation at the maximum elevation angle.*

The second time interval represents the switching from a constant attenuation of the signal to a situation in which the signal is still heavily attenuated because of the small elevation angle. Different from the chart above, in this case, the blockage duration is visibly longer.

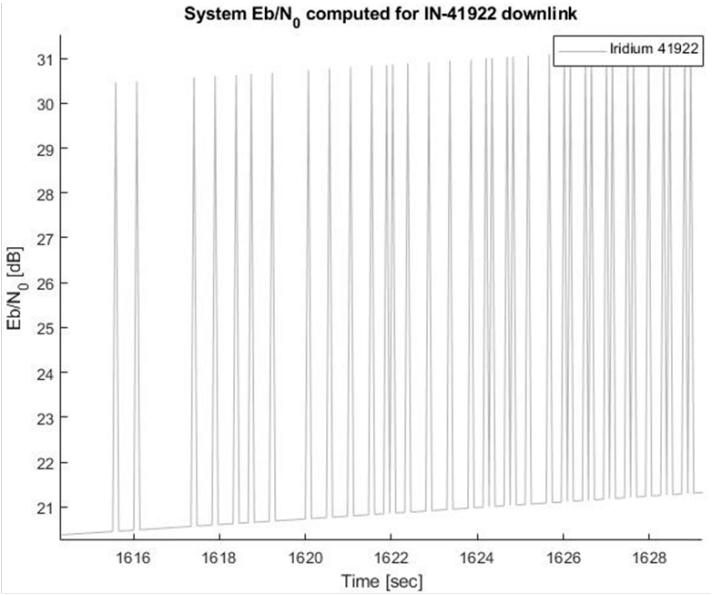

***Figure 78**: Downlink E_b/N_0 for IN-41922 with blade attenuation at the minimum elevation angle.*

Now it can be interesting to observe how the rotor blade blockage affects the Link margin of the communications.

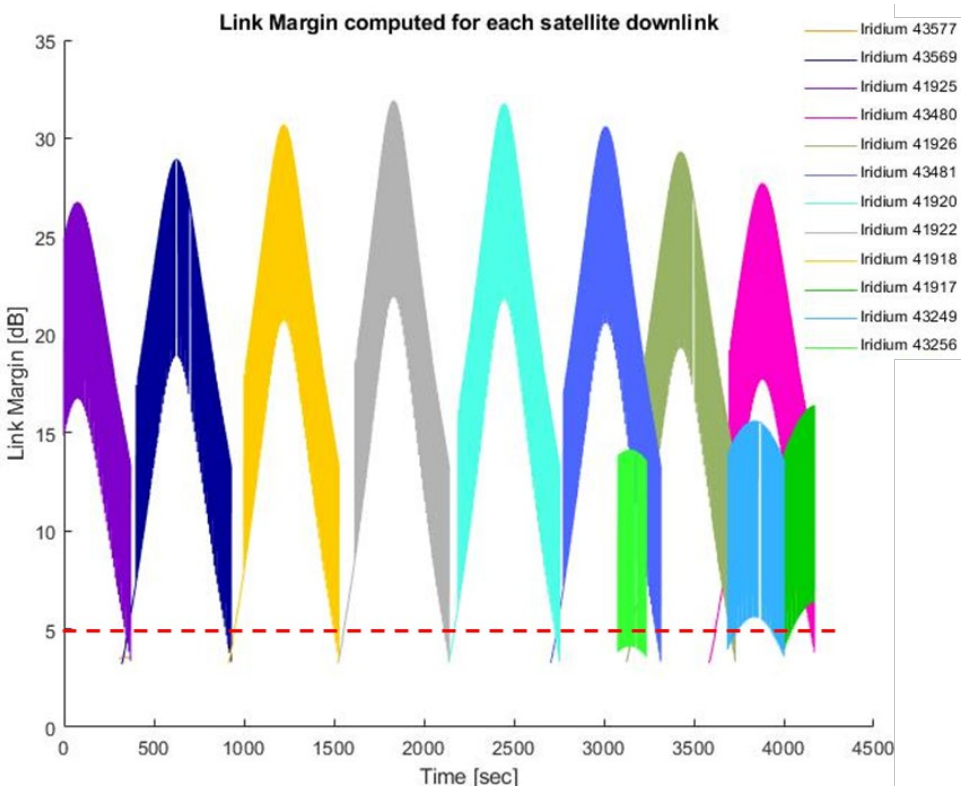

***Figure 79:** Downlink link margin for each access periodically reduced by blade rotation.*

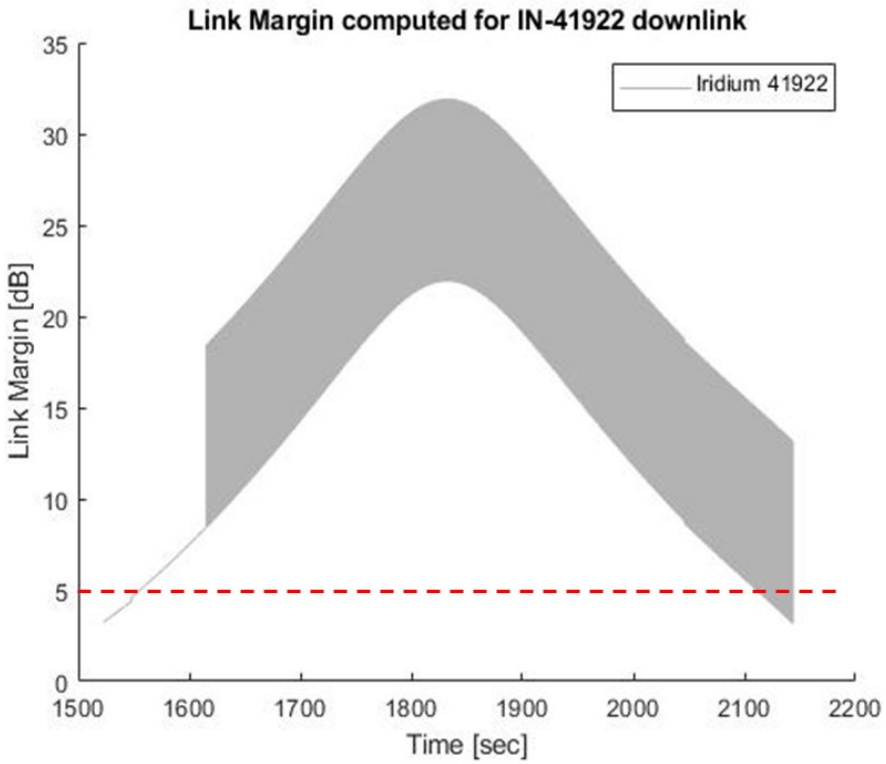

Figure 80: *Downlink link margin for IN-41922 link with blade attenuation.*

As it can be observed in the two charts below, the attenuation caused by rotor blades makes the link margin lower than 5dB at the start and at the end of the access (when the elevation angle is particularly small). This happens for very short periods during the mission (less than a minute). However, for these instants, the link is marginal and can create an even more critical switch between two consecutive satellite channels. This problem could be easily overcome by increasing the transmitter power of the satellite but, as mentioned before, another strategy could be the definition of a better trajectory plan for the helicopter, to guarantee the opportunity to establish a link (with a higher link margin) with a consecutive satellite before the connection with the current satellite becomes marginal.

Asking why during the handover phases the signal becomes so weak, it could be possible to check which kind of losses have the highest impact on it. Of course, having smaller elevation angles during these phases, the path losses are higher. But the highest losses are caused by the atmosphere layers and, in particular, by the ionosphere that, due to its electron content, causes a polarization rotation that produces significant losses for the signal, especially when the elevation angles are small. According to the "Iono Fading model" exploited from STK and already mentioned in section 4.1.4, the losses produced by this layer of the atmosphere for the link with IN-14922 are reported in the chart below.

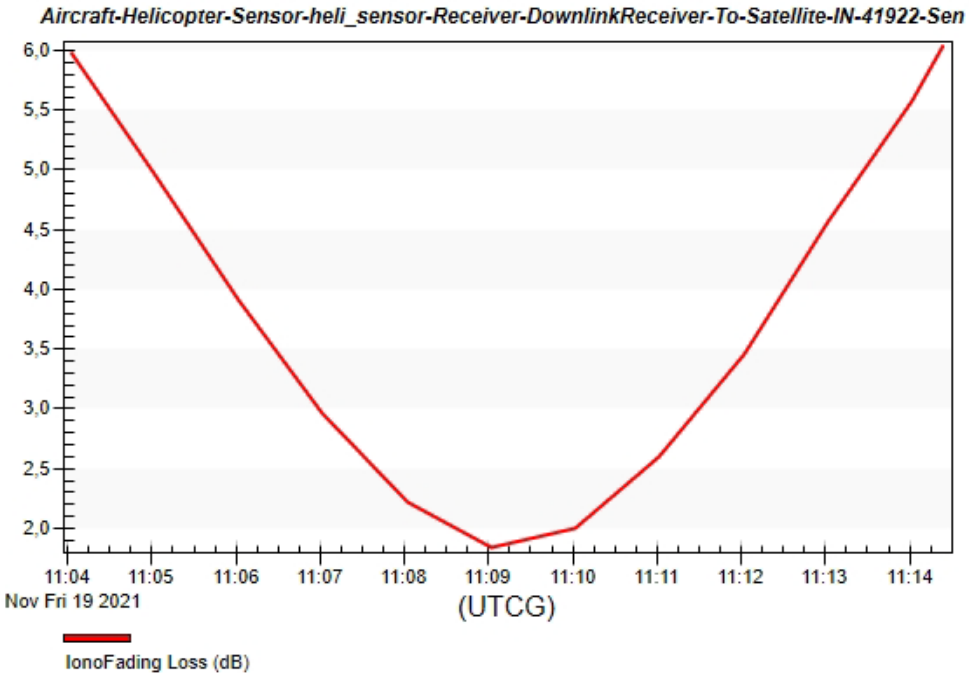

Figure 81: *Ionospheric Propagation Loss [dB] time variation in the link with IN-41922*

4.5.3 Uplink Analysis

As for the downlink, this analysis has the purpose to evaluate the quality of the signal transmitted by the helicopter and if there's an adequate link margin that makes the satellite link always closed. The first simulation is run without the rotor blade disturbances and shows very similar results to the downlink one. In the Eb/N0 chart it is possible to observe a reduction of the average value of the energy per bit of each link. That is determined by the different types of antennas used for the transmission. Consulting the "Link Budget (detailed)" report provided by STK it can be verified that the average EIRP of the signals transmitted by the satellites is higher than the one transmitted by the vehicle. In particular, this is caused by the higher gain that the phased-array antennas can obtain while they are in downlink. Nevertheless, the link margins guaranteed for the uplink transmissions are always above the 5dB safety value. So, even in this case, the link is always closed even if, it is possible to predict that during the satellite switch phases, adding the blade attenuations, the link will become marginal with lower values than the previous analysis. Even in this case, the handover phases are critical, as expected.

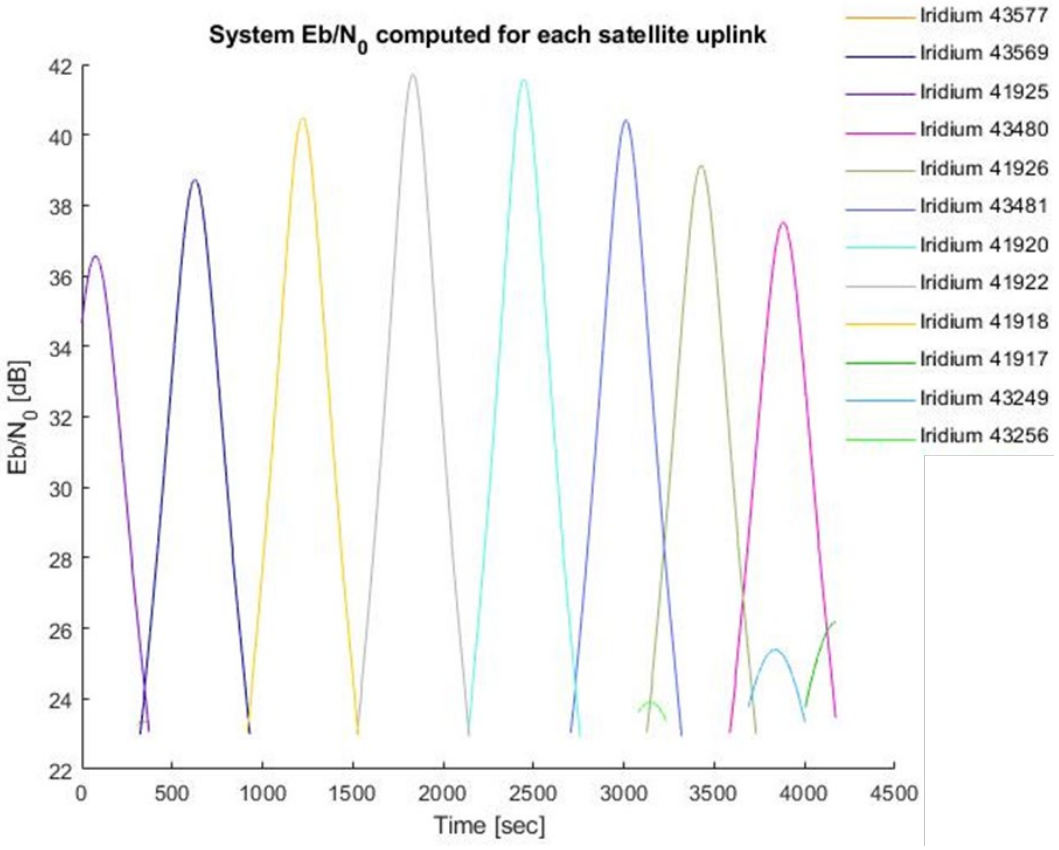

Figure 82: *Uplink system E_b/N_0 time variation for each access.*

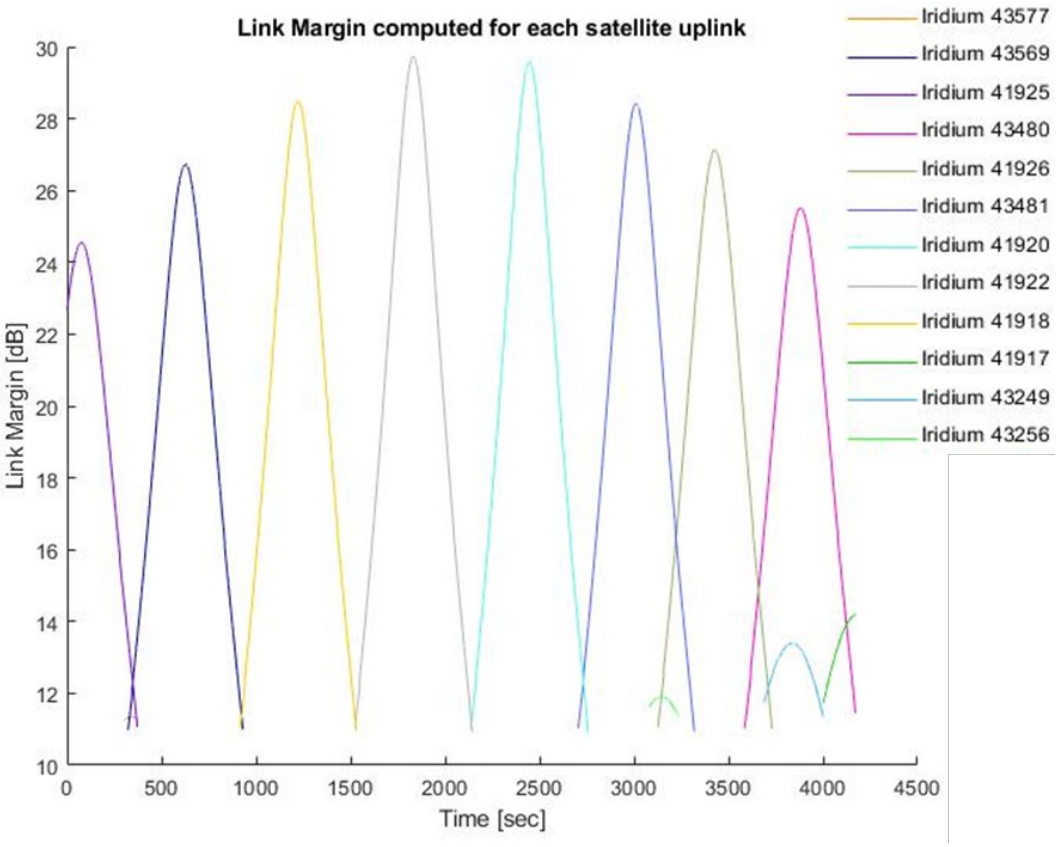

***Figure 83**: Uplink margin computed for each access considering the E_b/N_0 required equal to 12dB.*

4.5.4 Uplink analysis introducing rotor blades disturbances

The charts below allow visualizing the effects of the rotation of the blades on the signal transmitted by the helicopter. As mentioned before, even if for most of the mission the link margin guaranteed is above 5dB, it is possible to observe a strong deterioration of the signal quality during the transition from one link to another. In particular, the link margin reaches almost 1dB and that represents a deterioration of the connection quality compared to the downlink case. Moreover, that could be an unacceptable risk for the success of the mission. So, for safety reasons, it might be necessary to increase the power of the transmitted signal to raise its energy per bit and, consequently, its link margin. The 10dB transmitter power is an assumption because, for the GEO communication study, the transmitter power of the vehicle was equal to 16dB. So, establishing a good quality link with LEO satellites will require lower transmission power. However, nothing prevents increasing this parameter if the situation requires it. So in the following pages it will be demonstrated both the results obtained using a 10dB transmission power and the ones obtained using a 13dB power to better visualize how it could be possible to improve the link quality.

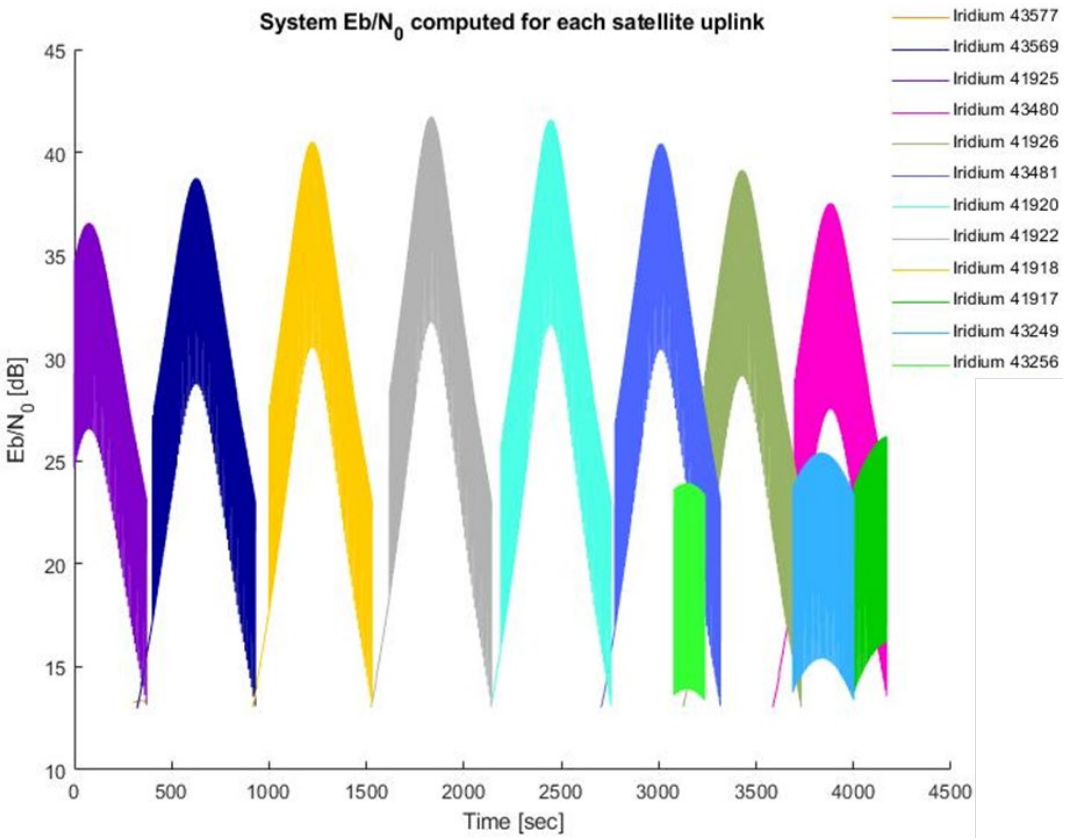

Figure 84: *Uplink E_b/N_0 for each access periodically reduced by the blade rotation (for 10dB transmission power).*

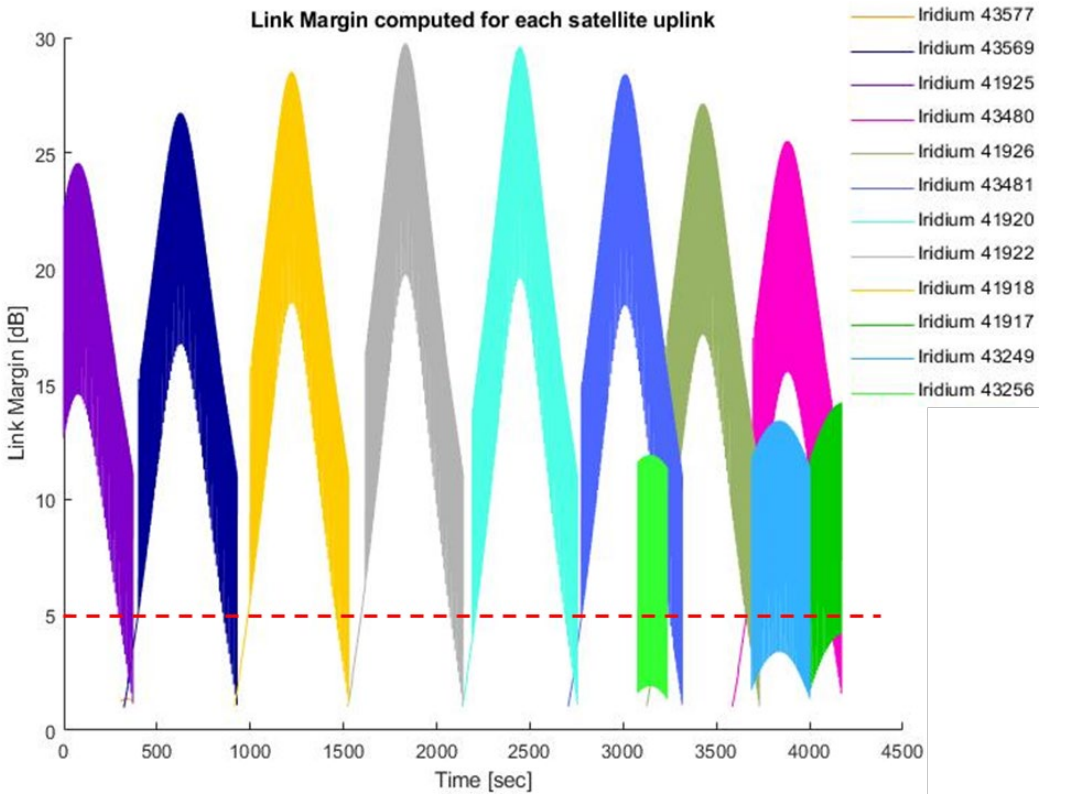

Figure 85: *Uplink link margin for each access periodically reduced by the blade rotation (for 10 dB transmission power).*

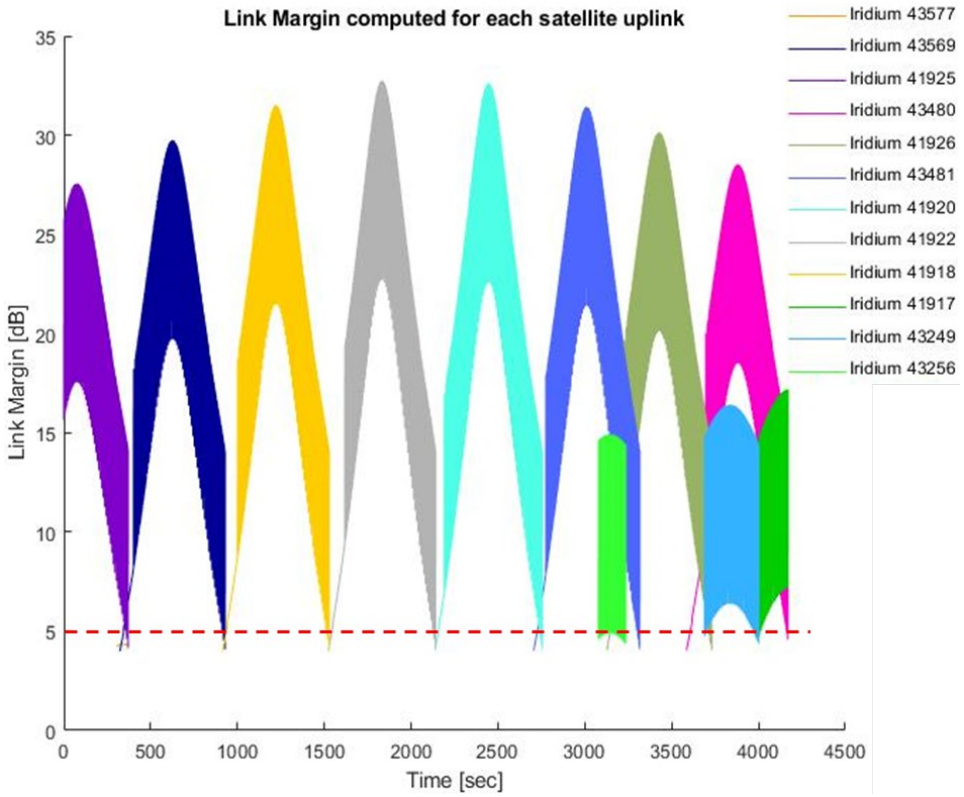

Figure 86: *Uplink link margin for each access periodically reduced by the blade rotation (for 13 dB transmission power).*

This last chart shows, for sure, a better link margin during the handover phases. So, this demonstrates that the problem has been overcome by the increase in transmission power.

4.6 Ship-Landing scenario

This part of the study has the purpose of verifying if the link connection is acceptable even if the helicopter follows another trajectory compared to the previous one and of exploiting the STK automatization to rapidly create a new mission scenario. In particular, in this mission context, the helicopter take-off from the shore, its approach to a ship anchored offshore, and, in the end, its landing on the ship is simulated. Differently from the previous mission scenario, the helicopter is now moving in a transversal path concerning the satellite direction. That may show different combinations of azimuth and elevation angles and could reveal if the attenuation produced by the blade rotation is more or less severe than the one observed in the previous section. This section contains a rapid overview of the new scenario and the results obtained by the link budget analysis.

4.6.1 Scenario Overview

As for the satellites and the helicopter, through the MatLab script it is possible to add a "ship object" to the scenario. STK doesn't allow the implementation of a stationary object just giving the software a single couple of coordinates (i.e latitude and longitude) for all the duration of the simulation. Therefore, to simulate an anchored offshore ship, it is necessary to give to the object a couple of coordinates that differ by very small degrees and a speed that tends to 0 km/s.

The helicopter's new trajectory has been preliminarily set in STK by the "Object edit" tool, choosing a starting point and considering the ship coordinates as an arrival point. Then, all the waypoints coordinates were extracted and saved in a .txt file to make the editing phase easier. The editing is necessary to set the helicopter speed in each phase of the flight and to adjust all the waypoints to have a smoother trajectory. In the last part of the flight, the speed of the aircraft is drastically reduced to simulate a more realistic landing phase. The helicopter starts from the shore with an average speed of 90km/h rising from 100m to 350m (i.e the cruise altitude). Then the helicopter proceeds towards the ship position maintaining an average speed of 170 km/h. When the helicopter is near 300m next to the ship, it starts to decrease its speed and reduce its altitude. At 100m above the ship, its speed is around 20km/h and continues to decrease until 5m of altitude. The helicopter flies at a speed of 5km/h just before landing. The flight duration is around 20 minutes. During the trajectory, it is possible to change the attitude of the vehicle dividing the mission into temporal segments and setting the pitch, yaw, and roll angles of the helicopter for each segment. Unfortunately, it is not possible to exploit Matlab to automatically set the attitude of the vehicle so, in this case, all the angles have to be set manually by the user. All the elements used for the trajectory implementation are resumed in the table below.

Latitude [deg]	Longitude [deg]	Altitude [km]	Speed [km/sec]	Trurn Radius [km]
40.970	17.247	0.100000	0.025000	11.685800
40.995	17.241	0.258915	0.025000	11.685800
41.007	17.239	0.336403	0.025000	11.685800
41.023	17.237	0.350000	0.047222	11.685800
41.048	17.237	0.350000	0.047222	11.685800
41.092	17.239	0.350000	0.047222	11.685800
41.117	17.236	0.350000	0.047222	11.685800
41.21993	17.23746	0.350000	0.047222	11.685800
41.249	17.241	0.344400	0.047222	11.685800
41.287	17.242	0.269657	0.035056	11.685800
41.291	17.242	0.210142	0.027778	11.685800
41.292	17.242	0.180278	0.017700	11.685800
41.29681	17.24270	0.103761	0.005556	11.685800
41.299	17.243	0.035000	0.001389	11.685800
41.29938	17.243	0.005000	0.000001	11.685800
40.970	17.247	0.100000	0.025000	11.685800
40.995	17.241	0.258915	0.025000	11.685800
41.007	17.239	0.336403	0.025000	11.685800
41.023	17.237	0.350000	0.047222	11.685800
41.048	17.237	0.350000	0.047222	11.685800
41.092	17.239	0.350000	0.047222	11.685800
41.117	17.236	0.350000	0.047222	11.685800
41.21993	17.23746	0.350000	0.047222	11.685800
41.249	17.241	0.344400	0.047222	11.685800
41.287	17.242	0.269657	0.035056	11.685800
41.291	17.242	0.210142	0.027778	11.685800
41.292	17.242	0.180278	0.017700	11.685800
41.29681	17.24270	0.103761	0.005556	11.685800
41.299	17.243	0.035000	0.001389	11.685800
41.29938	17.243	0.005000	0.000001	11.685800

Table 4.12: *Ship landing scenario, helicopter trajectory parameters.*

The next figures show, respectively, a view from above of the trajectory of the vehicle and the visualization of the landing phase.

***Figure 87**: Vision from above of the helicopter trajectory in the ship-landing scenario.*

***Figure 88:** Helicopter landing phase.*

4.6.2 Link budget analysis results

The link budget analyses show that the results are compliant with the ones obtained in the previous case of study. Even for this new mission profile, the link is always closed with link margins highly above the safety value of 5dB. It is also possible to observe that the handover phases present fewer criticalities allowing to establish access with two consecutive satellites, at the same time, during the channel switching for the entire mission duration. In this scenario, it is very important to keep a good signal quality while the helicopter is approaching the ship and is going to land on it. Without the blade disturbances, this requirement is guaranteed. In general, the signal energy per bit, compared to the previous mission scenario, is equal for each access. Let's have a look at the results obtained for the downlink case without the implementation of the blade attenuations.

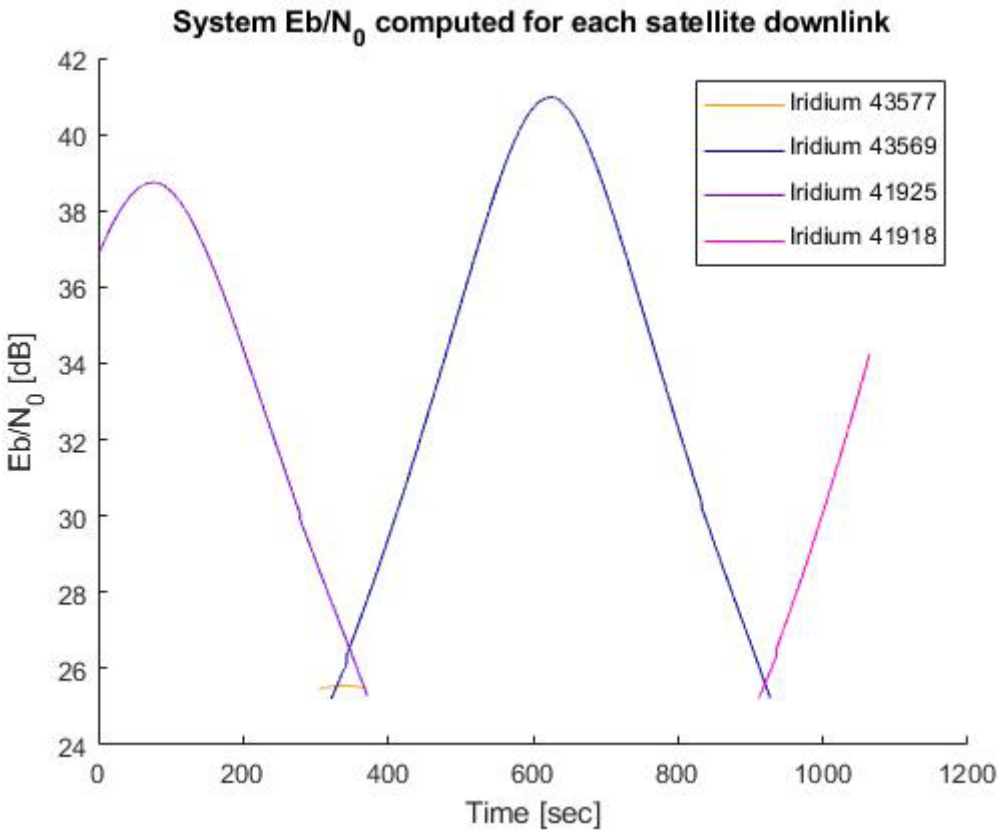

Figure 89: *Downlink system E_b/N_0 time variation for each access in the Ship-Landing scenario.*

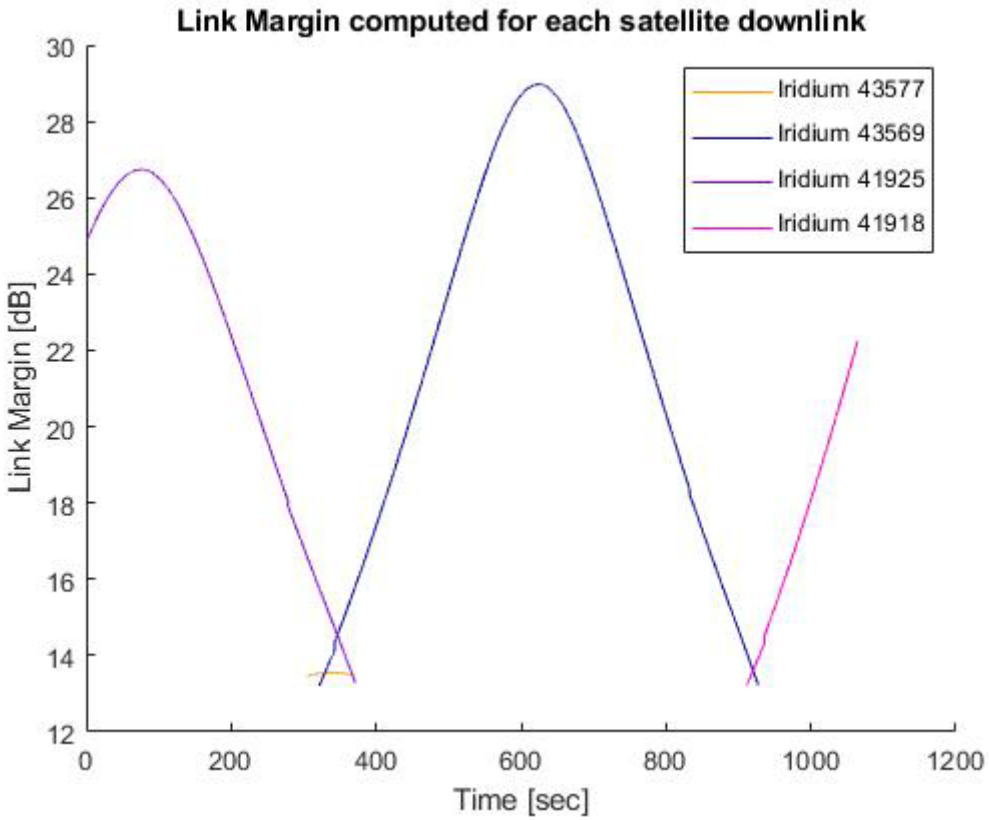

Figure 90: *Downlink link margin computed for each access in the Ship-Landing scenario.*

In the charts below are reported the same link budget results, considering the attenuation produced by the blade rotation. The observations that can be made are very similar to the previous ones. Having a less number of accesses, on a temporal scale of 1 second, it is possible to better appreciate the periodic attenuation of the signal and the variation of the signal blockage duration while the helicopter is changing its relative position to the satellite. When the white stripes are more visible, it means that the signal is less attenuated and the link quality is on average higher. That can happen for high elevation angles and small azimuth angles and vice versa. Even in this case, the presumed attenuation caused by the blades would bring the link margin under 5dB making the link marginal. As mentioned before this problem could be overcome by adjusting some parameters of the satellite transmitters.

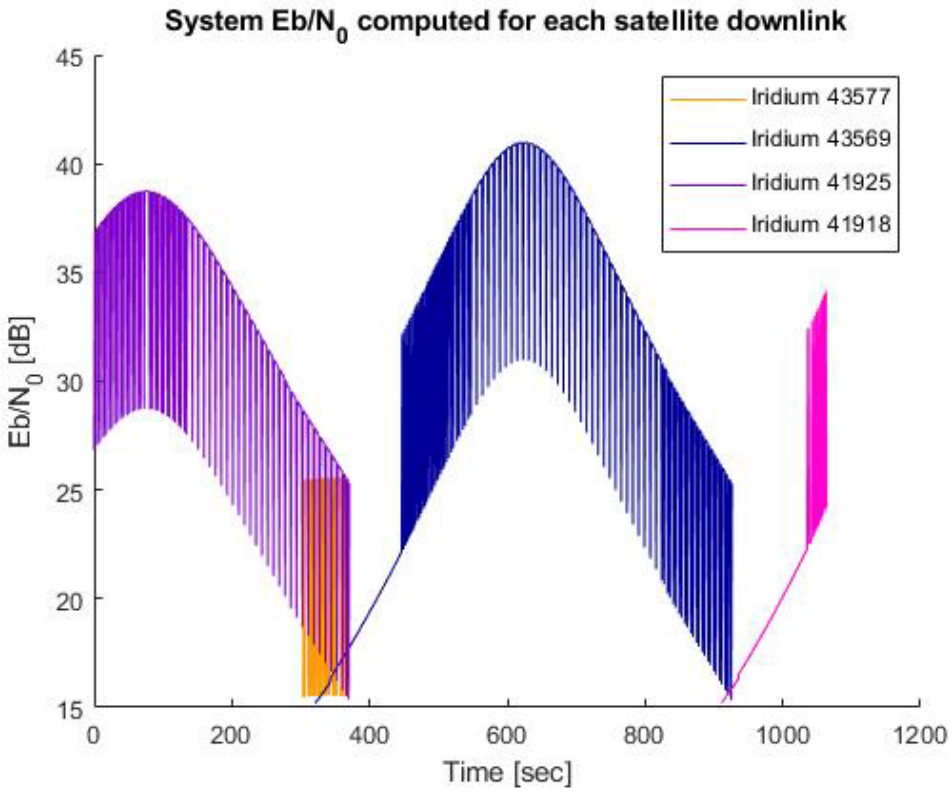

Figure 91: *Downlink E_b/N_0 for each access periodically reduced by blade rotation in the Ship-Landing scenario.*

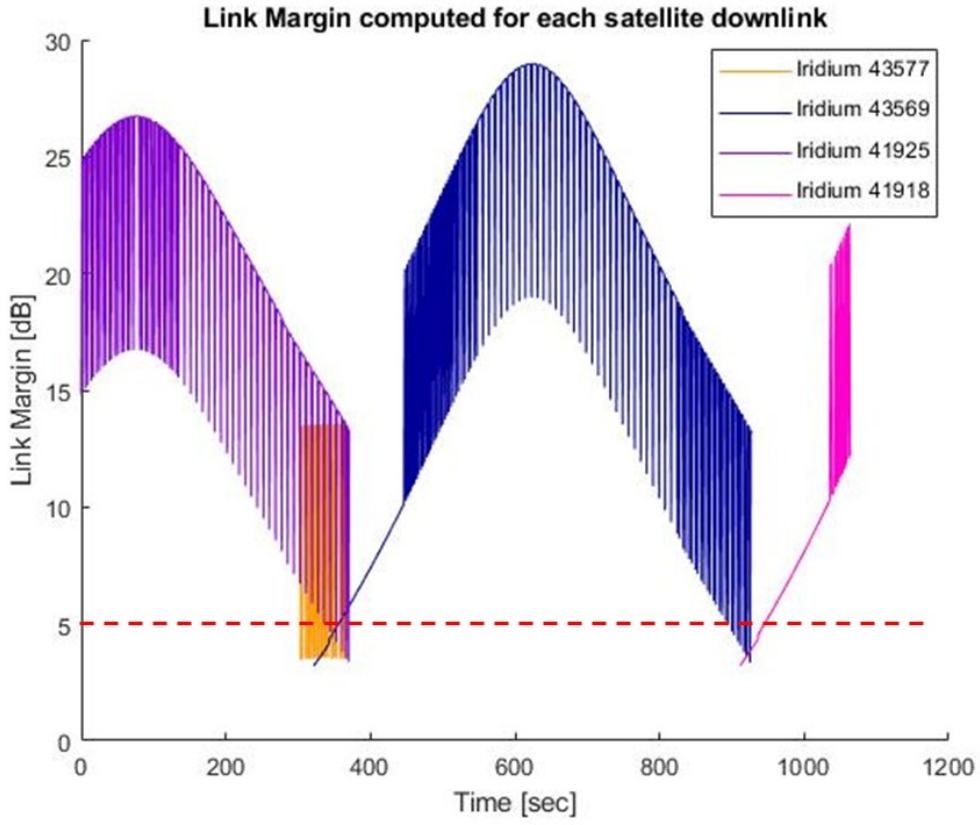

Figure 92: *Downlink link margin for each access periodically reduced by blade rotation in the Ship-Landing scenario.*

5. Conclusions and future works

The main purpose of this study was to model a satellite communication channel for rotary-wing vehicles starting from the proposal of the implementation of an antenna for satellite communications under the rotor blades of a remotely piloted helicopter. On the assumption to control the vehicle through a satellite communication channel, it was essential to verify the quality of the links in various scenarios and try to introduce as many disturbances and interferences as possible. So, in the first instance, the attention was focused on the attempt to reproduce the periodical attenuation caused by the rotation of the blades. Literature is full of dissertations in which this phenomenon is analyzed and characterized through complex analytic and mathematical formulations but, for the purpose of this study and to further implement these disturbances on real signals, it was chosen to rely on papers in which the attenuation is modeled as a rectangular window fading. The attempt to reproduce the results found in the consulted documentation was successful and allowed to innovate the formulation of this phenomenon by replacing the antenna dimension with the signal beamwidth in the blockage ratio (γ) formula. This change increases the bonding between the signal frequency and the attenuation phenomenon. First of all, it was possible to obtain, even with some differences, a γ trend very similar to the one (found in literature) used as the starting point. That comparison was necessary to verify if the new results were compliant with the original ones. Moreover, the new model of disturbance allowed us to verify that, for the same used antenna, a lower frequency signal tends to be more attenuated by the rotation of the blades. The new disturbance algorithm was first tested in MatLab then was introduced in Simulink, in an attempt to recreate a Ka-band communication channel between the chosen helicopter and a GEO satellite. In this phase of the project, the "Spectrum analyzer" made available by Simulink was fundamental to analyze the power spectrum of the received and transmitted signal by the helicopter. Moreover, Simulink was chosen as software for testing the disturbance algorithm because it allows running simulations for, potentially, an infinite time and changing variables while the analysis is running. These features were exploited to verify if the algorithm still worked changing the orientation angles of the signal during the simulation. The results reported in section 3 refer to a scenario in which the helicopter is moving in the satellite direction and the only parameter that changes is the elevation angle. However, in addition to the scenario simulated and reported in this study, other combinations of azimuth and elevation angles variations have been tested, verifying that the algorithm worked and the obtained results were compliant with the expectations given by the blockage ratio diagram presented in section 2.

In this first part of the study, the attention was focused on the signal analysis but, verified that the communication channel can be recreated in a "semi-static" environment, the new purpose was to extend the signal analysis into a mission scenario context. STK was a fundamental instrument since it provides all the elements and tools to achieve this purpose. Moreover, the use of this software was the perfect occasion to test how deep the automation of STK through Matlab scripts can go and the limitations of this feature. An additional value of this study, can, indeed, be considered the attempt to automate and parameterize as much as possible the

mission scenarios that can be created in STK. Especially for simulations in which a lot of elements and objects are involved, using the Matlab algorithm it was possible to simplify and run all the analysis and data collections faster as well as the customization of the scenario itself. That would make it easier, for future iterations, to change the mission profile, the transmitter and receivers parameters, the propagation disturbances, and so on.

In the first implemented mission scenario, the helicopter follows a simple trajectory, communicating with the satellites of the LEO constellation "Iridium-NEXT". In this case, the communications have been tested in downlink and uplink exploiting L-band frequencies signals. The purpose was to verify the quality of the signals exchanged with each satellite of the constellation that has access to the vehicle during its mission and to check if, for the chosen communication constraints, the switches between a satellite channel to another allow to have a constant coverage for the communications. This is a very important aspect to take into account if there is the will to remotely pilot the vehicle for all the mission duration. The analyses carried out for the downlink and uplink cases showed good results in terms of signal quality. For the modulation used by the Iridium-NEXT satellites (QPSK), it is possible to always obtain a link margin (LM) above the fixed safety value of 5dB (when the blade rotation disturbances are not implemented). Introducing the rotor blade blockage attenuation, it was possible to observe that, for the chosen trajectory, during the handover between one satellite and another, the new link is constantly attenuated due to its orientation and, subsequently, the attenuation starts to become increasingly periodic and the blockage duration becomes smaller with the increase of the elevation angle. The minimum blockage duration is reached when the elevation angle is at its minimum and the azimuth angle is around 180°. Therefore, the handover phase, from the analysis, results as the most critical because the LM can reach values under the safety value making the link "marginal" for less than a minute for each access. This becomes worse in the uplink because of the smaller E_b/N_0 of the signals. To overcome this criticality it could be possible, in future iterations, to adjust some parameters (such as the transmitter power, the datarate..) to improve the link margin in these phases. However, these can be considered good results for the first iteration. Another cue for possible future studies could be to verify if there's a way to optimize the handover phases through the elaboration of particular flight strategies. In the switching between a satellite communication channel and another, the signal energy could rapidly drop and the connection could be lost for some instants. It could be interesting to adapt a mission plan to guarantee a high quality of the signal for most critical phases (i.e landings, hovering on an area of interest…).

In the end, a new mission scenario, which provides for helicopter landing on an offshore anchored ship, was created. This was a way to test to see if the modeled communication channel (including the blade attenuations), still works for a more elaborate trajectory in terms of speed, attitude, and path variations. Even in this case, the obtained results are promising as a starting point for future adjustments and iterations.

So, summing up, the main purposes of this study were achieved. In the next iterations, it will be interesting to further explore how the blade materials impact the attenuation of the signal,

possibly having responses from tests carried out on real helicopters. Moreover, the already implemented missions could be analyzed in different weather conditions to have a better look at the degradation that the rain or clouds could produce on the signal. The high level of customization of the used Matlab script could be exploited to create new scenarios or to implement and test new constellations for satellite links. Lastly, this work could be useful for preliminary feasibility studies in the selection of possible satellite constellations and onboard antenna models for communication with rotary-wing vehicles.

References

[1] R. Daşbaşı and B. Polat, “An analytical approach to rotor blade modulation,” *Elsevier,* pp. 1-2, 2021.

[2] I. Tardy, G. P. Piau, P. Chabrat and J. Rouch, “Computational and Experimental analysis of the scattering by rotating fans,” *IEEE,* vol. 44, no. 10, pp. 1-6, 1996.

[3] A. C. Polycarpou, C. A. Balanis and A. Stefanov, “Helicopter Rotor-Blade Modulation of Antenna Radiation Characteristics,” *IEEE,* vol. 49, pp. 1-2, 2001.

[4] C. Cerasoli, “KA-BAND SATCOM IN A2C2S,” *IEEE,* pp. 1-5, 2004.

[5] P. Wang, L. Yin and J. Lu, “Efficient Helicopter−Satellite Communication Scheme Based on Check-Hybrid LDPC Coding,” *TUP,* vol. 23, no. 3, pp. 1-3, 2018.

[6] “QPSK Modulator Baseband,” MathWorks, 1994-2022. [Online]. Available: https://www.mathworks.com/help/comm/ref/qpskmodulatorbaseband.html.

[7] “Raised-cosine filter,” Wikipedia, 1 February 2022. [Online]. Available: https://en.wikipedia.org/wiki/Raised-cosine_filter. [Accessed December 2021].

[8] InternalTelecommunicationUnion, “Recommendation ITU-R P.618-13: Propagation data and prediction methods required for the design of Earth-space telecommunication systems,” ITU-R, 2017.

[9] InternationalTelecommunicationUnion, “Recommendation ITU-R P.840-7: Attenuation due to clouds and fog,” ITU, 2017.

[10] InternationalTelecommunicationUnion, “Recommendation ITU-R P.676-9: Attenuation by atmospheric gases,” ITU, 2012.

[11] InternationalTelecommunicationUnion, “Reccomandation ITU-R P.372-15: Radio Noise,” ITU, 2021.

[12] InternationalTelecommunicationUnion, “Recommendation ITU-R P.531-12: Ionospheric propagation data and prediction methods required for the design of satellite services and systems,” ITU, 2013.

[13] eo, “eoPortal Directory,” ESA, 2000-2022. [Online]. Available: https://earth.esa.int/web/eoportal/satellite-missions/i/iridium-next. [Accessed December 2021].

[14] Spaceflight101, “Spaceflight101: Iridium-Next,” Spaceflight101(SpacecraftLibrary), [Online]. Available: https://spaceflight101.com/spacecraft/iridium-next/. [Accessed December 2021].

[15] SignalIdentificationGuide, “SigidWiki: Iridium,” 14 April 2021. [Online]. Available: https://www.sigidwiki.com/wiki/Iridium. [Accessed December 2021].

[16] F. Buntschuh, “IRIDIUM NEXT ENGINEERING STATEMENT,” 2013.

[17] S. Dey, D. K. Mohapatra e S. D. . R. P. Archana, «An Approach to calculate the Performance and Link Budget of LEO Satellite (Iridium) For Communication Operated at frequency Range (1650-1550) MHz,» *ULTET,* vol. 4, pp. 1-8, 2014.

[18] C. M. Shahriar, “MITIGATION OF INTERFERENCE FROM IRIDIUM SATELLITES BY PARAMETRIC ESTIMATION AND SUBTRACTION,” BLACKSBURG, VIRGINIA, 2006.

[19] ICAO, “TECHNICAL SPECIFICATION FOR AERONAUTICAL MOBILE SATELLITE (ROUTE) SERVICE (AMS(R)S) PROVIDED BY IRIDIUM SATELLITE SYSTEM”.

[20] A. Ketsdever, “Communications and Data Handling,” [Online]. Available: https://www.slideserve.com/dea/communications-and-data-handling. [Accessed 1 2022].

[21] S. Cakaj, B. Kamo, I. Enesi and O. Shurdi, “Antenna Noise Temperature for Low Earth Orbiting Satellite Ground Stations at L and S Band,” *SPACOMM 2011 : The Third International Conference on Advances in Satellite and Space Communications,* pp. 1-6, 2011.

[22] V. Mathuranathan, "Performance comparison of Digital Modulation techniques," GaussianWaves: Signal Processing for Communication Systems, 14 April 2012. [Online]. Available: https://www.gaussianwaves.com/2010/04/performance-comparison-of-digital-modulation-techniques-2/. [Accessed 1 2022].

[23] V. Kharchenko, A. Grekhov and W. Bo, “COMPUTER MODELING OF RADIO FREQUENCY SATELLITE TRANSPONDER FOR TRANSMISSION OF ADS-B MESSAGES SATELLITE COMMUNICATION CHANNEL,” *Researchgate,* vol. 61, no. 4, pp. 1-8, 2014.

[24] E. L. Cid, M. G. Sánchez, A. V. Alejos and S. G. Fernández, “Measurement, Characterization, and Modeling of the Helicopter Satellite Communication Radio Channel,” *IEEE,* vol. 62, no. 7, pp. 1-10, 2014.

Acknowledgement

I would like to express my special thanks of gratitude to my teacher Sabrina Corpino who accepted to be my academic tutor and follow me in the development of this case study. I also want to thank my company tutor Engineer Giuseppe Tomasicicchio and Engineer Marco Brancati for this opportunity that they offered me and for all the inputs, the support, and the instruments that were made available to me over these months allowing me to accomplish the objectives of this study.

My gratitude also goes to AGI and GMSpazio SRL for providing me with an STK educational license which was indispensable for the simulations that are reported in this thesis.

I want to thank Abby Jo Sax Palermo for helping me with the grammatical and syntactic correction of this document.

I would like to thank all my relatives and all my friends who believed in me during this very intense course of study and that have been such great emotional support while I have been struggling during these years.

Last, but not least, I would like to thank my parents. I had years full of joys, sorrows, successes, and failures, but, despite the extensive physical distance between us, I've always felt like I was facing all of it with you here at my side. Even when I was too tired, too angry, or too discouraged to ask for your help, you were always here at my side ready to cheer me up at every moment. I hope, one day, to give back to you all that you have given to me.